Automated Rugosity Values from High Frequency Multibeam Sonar Data for Benthic Habitat Classification

A THESIS SUBMITTED TO THE GRADUATE DIVISION OF THE
UNIVERSITY OF HAWAI'I IN PARTIAL FULFILLMENT
OF THE REQUIREMENTS FOR THE DEGREE OF

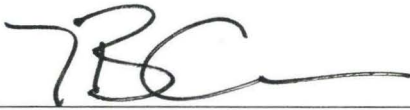MASTER OF SCIENCE

IN

GEOLOGY AND GEOPHYSICS

MAY 2007

By
Erin S. Diurba

Thesis Committee:
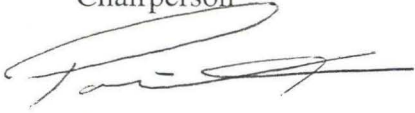
Bruce Appelgate, Chairperson
Paul Wessel
John Rooney

We certify that we have read this thesis and that, in our opinion, it is satisfactory in scope and quality as a thesis for the degree of Master of Science in Geology and Geophysics.

THESIS COMMITTEE

_____
Chairperson

_____

_____

ACKNOWLEDGEMENTS

"Acknowledge yourself for how far you have come, instead of how far you think you have to go."

I recited that quote every time I felt overwhelmed and thought I was going to break. It forced me to take a deep breath, take small steps forward and realize how many great things I have already accomplished in my life. The quote also made me realize that none of this would have been possible if it wasn't for the sacrifices of my friends and family who pushed me to succeed and were there to hold me up when I believed I had failed.

To Mom and Dad- Thanks for paying the phone bill and always being there.
To Landon –Thank you for bringing love, friendship and Monkey into my life.
To all the friends I have made along the way – Thanks for putting up with me and always giving me good advice whether or not I wanted to hear it.

I would like to thank Bruce Appelgate, for funding a girl from Mars, and my committee for their support and collaboration. I am also grateful to NOAA and CRED for helping me to gain research experience, and utilize their extensive data collection for my thesis.

Finally, I would like to thank all the amazing teachers I have had in the past who have shaped who I am today and who I hope are proud of me now.

.

ABSTRACT

Rugosity literally means wrinkled, or marked with folds and ridges. When applied to seafloor texture, rugosity is one piece of the puzzle that is necessary in order to understand benthic habitats. Traditionally, rugosity was calculated by draping a chain of known length over the seafloor and comparing the total chain length with the horizontal distance the chain covered. The equation Rugosity=100*(horizontal length of chain/ actual length of chain) was then applied to get a percent rugosity. However, the process is subjective, time consuming, depth limited and is capable of only small scale coverage. My objective was to develop an automated algorithm that would calculate rugosity from clean, un-gridded, multibeam data using the manual rugosity method. This method rapidly produces objective, reproducible rugosity data for any multibeam data set that is comparable with manual rugosity data. The final product is an objectively derived, quantitative map that can be used for benthic habitat mapping.

TABLE OF CONTENTS

LIST OF TABLES

LIST OF FIGURES

ix

CHAPTER 1: INTRODUCTION

1.1 Introduction

In the past 20 years sonar technology, including multibeam sonar, has improved faster than the techniques used to process the data these systems produce. As a result data are being collected faster than they can be interpreted, causing much of the data to be neglected. Automated tools are necessary to quickly and objectively classify the data to allow for quicker interpretation and use of the data.

Coral reef habitats represent one marine ecosystem where rapid seafloor mapping and interpretation is vital. These fragile benthic habitats sustain life for millions of marine species but are susceptible to environmental and anthropogenic changes. In order to protect marine ecosystems before irreparable damage is done resource management policies need to be put in place that take into account small and large scale environmental factors affecting coral reef health (CRTF, 2004). Benthic habitat maps, which integrate, analyze, and interpret several different types of data including substrate type, topography, and biological species, are used to delineate these marine protected areas. These maps set the foundation for management plans, guide future protection, and provide a means to monitor and detect change within a coral ecosystem (CTRF, 2004). In order to understand what makes a coral reef healthy a comprehensive benthic habitat map is required that incorporates multidisciplinary data from multiple surveys. Some environmental factors that effect coral reef health are beyond the control of local or regional management efforts such as global warming and changes in global storm patterns. However, some global practices can be regulated in order to promote healthy reef systems. One example is to stop the over fishing of reef fish which have been shown

1

to be indicative of a healthy coral reef ecosystem (CRTF, 2004). It is also important to study the factors that affect coral reef fish distribution such benthic complexity, or rugosity, which has been shown to be a critical component (Friedlander et al., 1998). Therefore, in order to enhance conservation efforts and promote coral reef health, it is important to develop methods that characterize factors affecting reef fish populations, such as rugosity.

Rugosity which literally means wrinkled or marked with folds and ridges. When applied to bottom texture, rugosity is one piece of the puzzle that is necessary in order to understand benthic habitats. Friedlander (1998) looked at how habitat characteristics influence fish assemblages and suggested a model that used four variables to predict species density. These variables were distance to the reef edge, distance to a river mouth, depth, and hole size. It was suggested that hole size and rugosity values could be interchangeable as both are ecologically similar measures of primary habitat complexity and both explain some of the variability in population numbers and biomass. Therefore, rugosity can be used to make basic predictions of fish assemblages and biomass (Friedlander and Parish, 1998). In another study it was found that areas with high rugosity exhibited the greatest mean species richness and species abundance out of the 12 reef sites studied (Kuffner et al., 2007). This is because when the seafloor is "rough", with holes and crevasses for fish and other fauna to hide, there is a balance between predators and prey. Conversely, when there is a flat bottom, such as a sand field, there is less likely to be suitable substrate for coral to attach to or adequate shelter for fish to hide causing a predator-dominated environment with less diversity.

2

Seafloor rugosity can help classify the texture of the seafloor. Traditionally, rugosity was measured by divers using a chain of known length and a tape measure. The chain was draped along a transect making sure that it followed the bottom topography as closely as possible. The smaller the chain link size, the more detailed the rugosity measurement since the smaller chain can fall into tighter areas. Because the chain is following an irregular bottom its total horizontal extent "shortens" and that new length is measured (Figure 1). Rugosity is expressed as a simple ratio shown in equation 1.

(Equation 1)
Rugosity=100*(horizontal extent of chain/ actual length of chain) (Frost et al., 2005)

Because manually collecting rugosity data is time intensive, subjective, depth limited, and only covers small areas, the usefulness of rugosity data is negated. By developing an algorithm that can calculate rugosity from a remotely sensed multibeam data set, rather than manually collecting data, rugosity can be calculated objectively, at quicker rates, deeper depths, and over larger areas with denser data concentrations. This is because multibeam data cover larger areas and deeper depths than divers can go and have depth and horizontal position information that can be used to mathematically determine seafloor rugosity. An automated rugosity tool also needs to be easy to use, conceptually descriptive, and able to be used at varying scales in order to be useful (Hobson, 1972). The purpose of this study is to develop a new acoustic method for measuring rugosity, analyze manual rugosity measurements to determine the algorithm's accuracy and use this method in conjunction with other types of data to characterize the seafloor of a coral reef environment as a first step in assessing the status of the benthic habitats there.

3
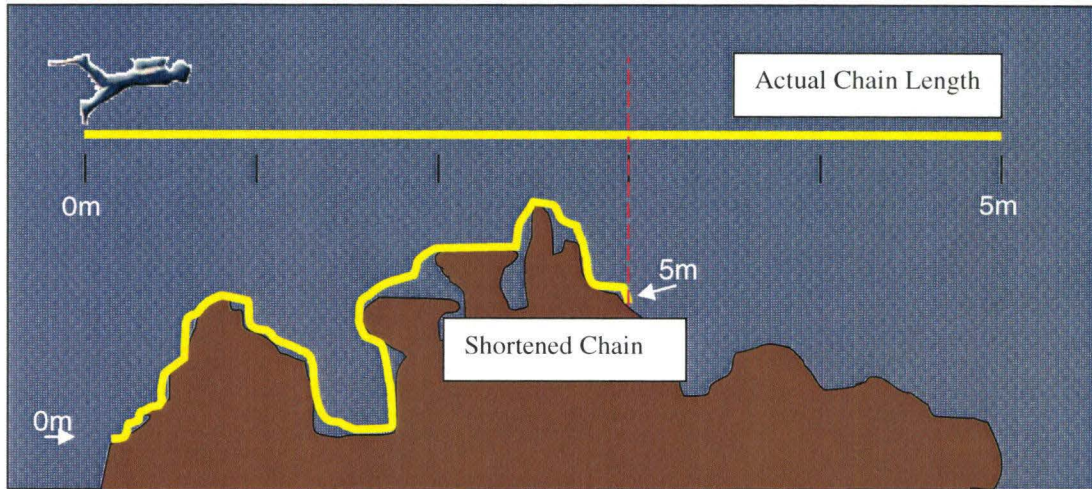
Figure 1: Calculating rugosity using the chain method. This figure shows how the chain (actual chain length) shortens in length as it is draped over the seafloor making sure it follow the contours of the seafloor as closely as possible. After the chain is laid the horizontal distance is measured from the start of the chain (0m) to where it stops (3m).

CHAPTER 2: BACKGROUND

2.1 Coral Reefs

Coral reefs are home to nearly one million species of fish, invertebrates, and algae even though they only cover 0.2 percent of the ocean floor (Weier, 2001). Over 4,000 species of fish and tens of thousands of invertebrate species are known to depend on some 800 types of known coral. It is estimated that there are still hundreds to thousands of reef organisms yet unidentified (Bryant et al., 1998). Coral reef systems are important to humans because their coralline structures act as barriers against erosive wave action for islands and coastal areas. They also provide economic benefit through commercial and recreational fishing, ecotourism, and as sources of medicine such as vitamins, histamines, pain killers, and antibiotics (CRTF, 2004)

Coral reefs are usually composed of multiple types of carbonate-secreting organisms, including both scleractinian corals and coralline algae. Coralline algae often acts as the cement that holds the coral framework together and also provide the preferred substrate upon which coral larvae will settle and grow (Birkeland, 1997). In order for coralline algae to find space to flourish, and to promote coral recruitment, herbivorous fish and sea urchins need to clean the reef of competing turf and macroalgae (Houk, 2001). Reef systems are fairly sensitive and can become stressed when changes in water temperature, nutrient levels, pH, dissolved oxygen and turbidity occur. Biological changes, such as a decline in reef fish my also affect the health of a reef which make coral ecosystems especially sensitive to over fishing, pollution, and land-based activity such as development (Houk, 2001). Most scleractinian corals host symbiotic algae that provide them with an additional food source through photosynthesis. When corals are

5

stressed, they expel these algal symbionts through a process known as coral bleaching. Once the symbionts are expelled the coral is likely to die and leave behind a "bleached" white coral skeleton (NOAA, 2006). According to the National Oceanic and Atmospheric Administration's (NOAA) Coral Reef Task Force (CRTF) ten percent of all coral reefs are already damaged beyond repair and thirty percent are in critical condition and may die in the next ten to twenty years(CRTF, 2004). Sixty percent of the world's reefs could die by 2050 if current pressures are allowed to continue (CRTF, 2004).

To help decrease some of the stress put on reef environments President Bill Clinton signed executive order 13089, on June 11, 1998, which stated that all Federal agencies whose actions may affect U.S. coral reef ecosystems shall identify which actions affect coral reef environments, take measures necessary to reduce and mitigate coral reef ecosystem degradation and restore damaged coral reefs (Hoegh-Guldberg, 1999). This meant that all Federal agencies, including the Department of Defense, must determine their impact on the reef system and develop a strategy to minimize the impacts on coral reef ecosystems which include all the species, habitats and natural resources associated with coral reefs.

2.2 Area of study

The data presented in this study was collected by NOAA's CRED and was utilized by the Department of Defense (DoD) to satisfy environmental impact study requirements stated in executive order 13089. The DoD and CRED's goal was to identify areas of dense coral growth before additional military vessels were brought to Saipan. This way new anchor circles could be chosen that would minimize the effect of the ships anchors on coral rich environments.

6

2.2.1 Saipan

Saipan is a small (124 km^2) island located on the southern end of the 644 km-long Mariana volcanic arc in the Commonwealth of the Northern Mariana Islands (CNMI) (Figure 2). The island, with a maximum altitude of 474 m, consists of an Eocene volcanic core enveloped by younger limestone (Cloud et al., 1959). There is a barrier reef on the western side of the island that shelters the Saipan Lagoon from the Philippine Sea (Cloud et al., 1959).

Saipan is characterized by a tropical oceanic climate with an average temperature of 27° C (Carruth, 2003). Precipitation varies across the land from 206 cm in the southwestern lowlands to 231 cm in the central ridge area, and can reach upwards of 330 cm a year. Across the island of Saipan over 276 million m^3 of rain falls in an average year (Cloud et al., 1956). Most freshwater on the island occurs as groundwater and is found in aquifers composed mainly of fragmental limestone (Carruth, 2003).
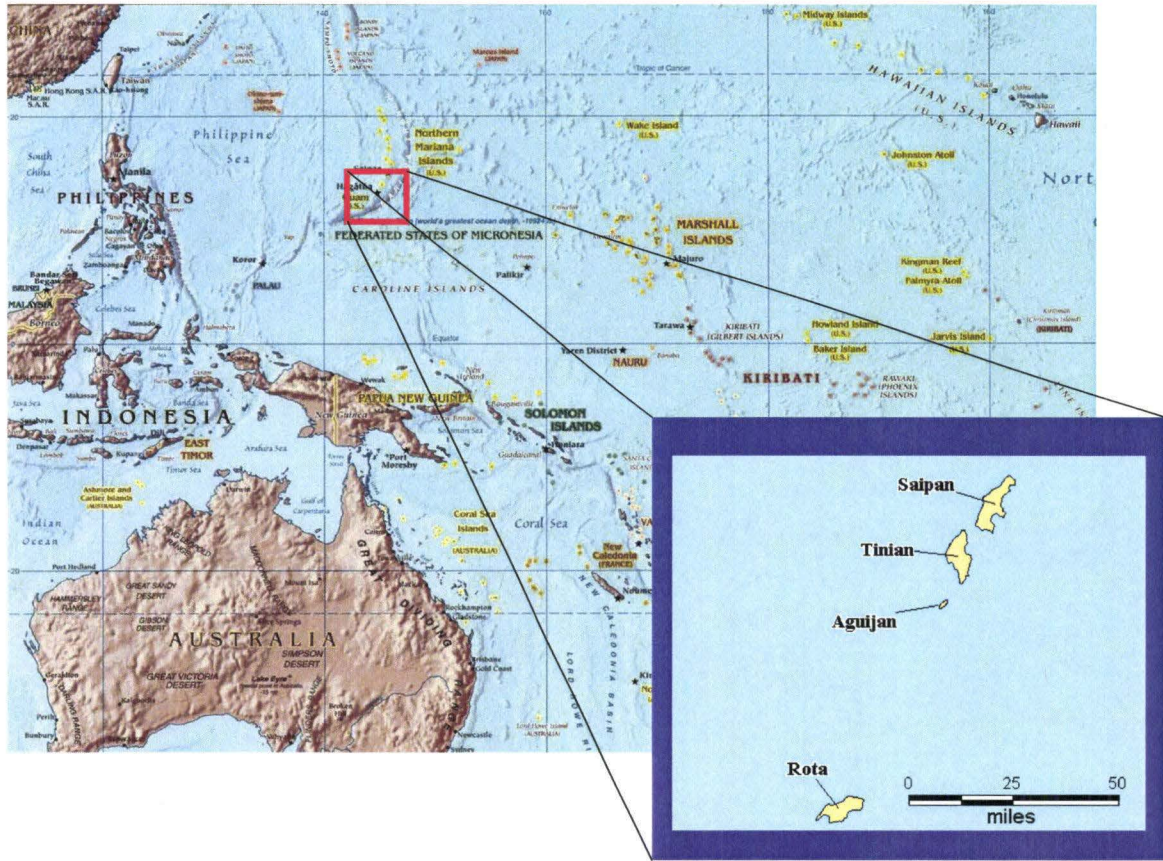
Figure 2: Oceania map. This figure shows an overview of Oceania to show the location of The Commonwealth of the Northern Mariana Islands (The World Fact Book, 2002). Some of the main inhabited islands are shown in the inset including Saipan which is the area of study (FEMA, 2005).

On the northwest side of the island the lagoon opens up and a dredged channel is the entrance to Puetton Tanapag, or Tanapag harbor (Figure 3). Outside of the lagoon is a large reef system which is split into two sections, inner and outer reef, by a deep sand channel. The large ships that cannot anchor in Puetton Tanapag anchor in both the inner and outer reef of Garapan Anchorage. However, the inner reef of the Garapan Anchorage site is less exposed to storm surges and strong currents which make anchorage locations there more desirable. This is also an area of dense coral growth (Rooney et al., 2005). Because of the dense coral growth the Garapan Anchorage is of interest to the Coral Reef

Conservation Program (CRCP) who has a mission to map all coral reef environments in the U.S.-related Pacific Islands by 2009. This shallow marine mapping project began in 2002 and CRED, working with the CRCP, has surveyed coastal marine environments around American Samoa, the Northwestern Hawaiian Islands and CNMI. In 2003, CRED conducted a multibeam survey of the Garapan Anchorage as a regular part of their coral reef mapping and monitoring program as part of the CRCP. Over the course of a month the anchorage area was acoustically mapped using the NOAA R/V AHI. This 8 m coastal research vessel is equipped with a hull-mounted 240kHz RESON SeaBat 8101 multibeam sonar, which was used to produce a bathymetry map of the Saipan Anchorage area (Figure 4).

The CRCP is not the only organization interested in the Garapan Anchorage. Because of the storm surges and strong currents found around Saipan the Navy uses the sheltered inner reef of the Garapan Anchorage to anchor a fleet of Maritime Preposition Ships (MPS). These ships transport ammunition, equipment, fuel and supplies to sustain U.S. forces worldwide during peacetime and in war and each MPS has enough supplies to support 15,000 troops for a month (Rooney et al., 2005). Currently there are 8 MPS within CNMI. In response to Department of Defense Global Forces Program Strategy initiatives the U.S. Navy wants to bring 5 more ships into the area (Rooney et al., 2005). There are no moorings around the inner reef that the ships can tie off on. To prevent drifting, each MPS uses large anchors that tend to drag along the ocean floor. To minimize damage to the reef each ship has a designated area in which they may anchor. However, if new ships are to be brought to Saipan, new anchorage areas need to be identified. Because executive order 13089 requires environmental impact assessments to

9

identify coral-rich areas within Garapan Anchorage, the U.S. Military Sealift Command (MSC) needed to complete benthic mapping and habitat studies. When the Naval Facilities Engineering Command, Pacific (NAVPAC), and the MSC saw that CRED had already completed comprehensive bathymetric mapping for the Garapan anchorage they contacted CRED to ask for use of their data and to discuss further benthic habitat surveys. In 2004, the navy funded CRED to return to Saipan and conduct additional optical characterization of coral reef communities in the Garapan Anchorage area. Optical assessment was necessary to identify coral rich environments so that they would not be chosen as potential anchorage sites. A total of 123 linear kilometers of video of benthic habitats was completed. The video data were analyzed using CRED's standard optical classification protocol (http://www.soest.hawaii.edu/pibhmc/pibhmc_cnmi_saipan.htm).

Manual rugosity measurements were also collected at six dive sites. A map was produced showing the percentage of the seafloor inhabited by coral communities along each video survey line. Coral community percentages were interpolated using ordinary kriging to estimate coral community cover across the entire Garapan Anchorage. These data were presented to the MSC to help them avoid coral-rich areas when selecting additional anchorages.
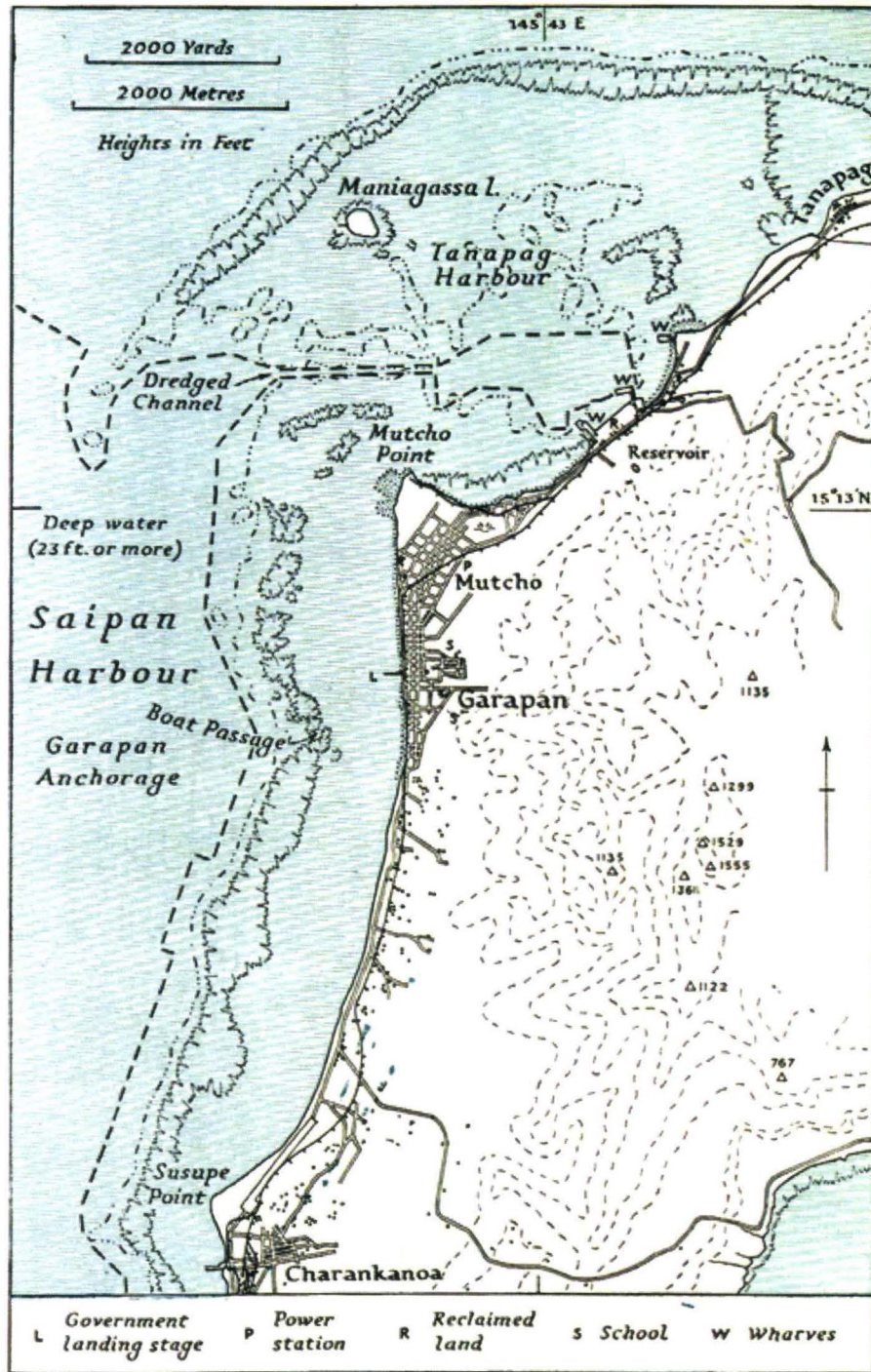
Figure 3: Saipan Harbor Map. This figure shows Garapan Anchorage and
Tanapag Harbor to the north west of Saipan (Naval Intelligence Division, 1945).
Garapan Anchorage is the site CRED surveyed in 2003 and 2004.
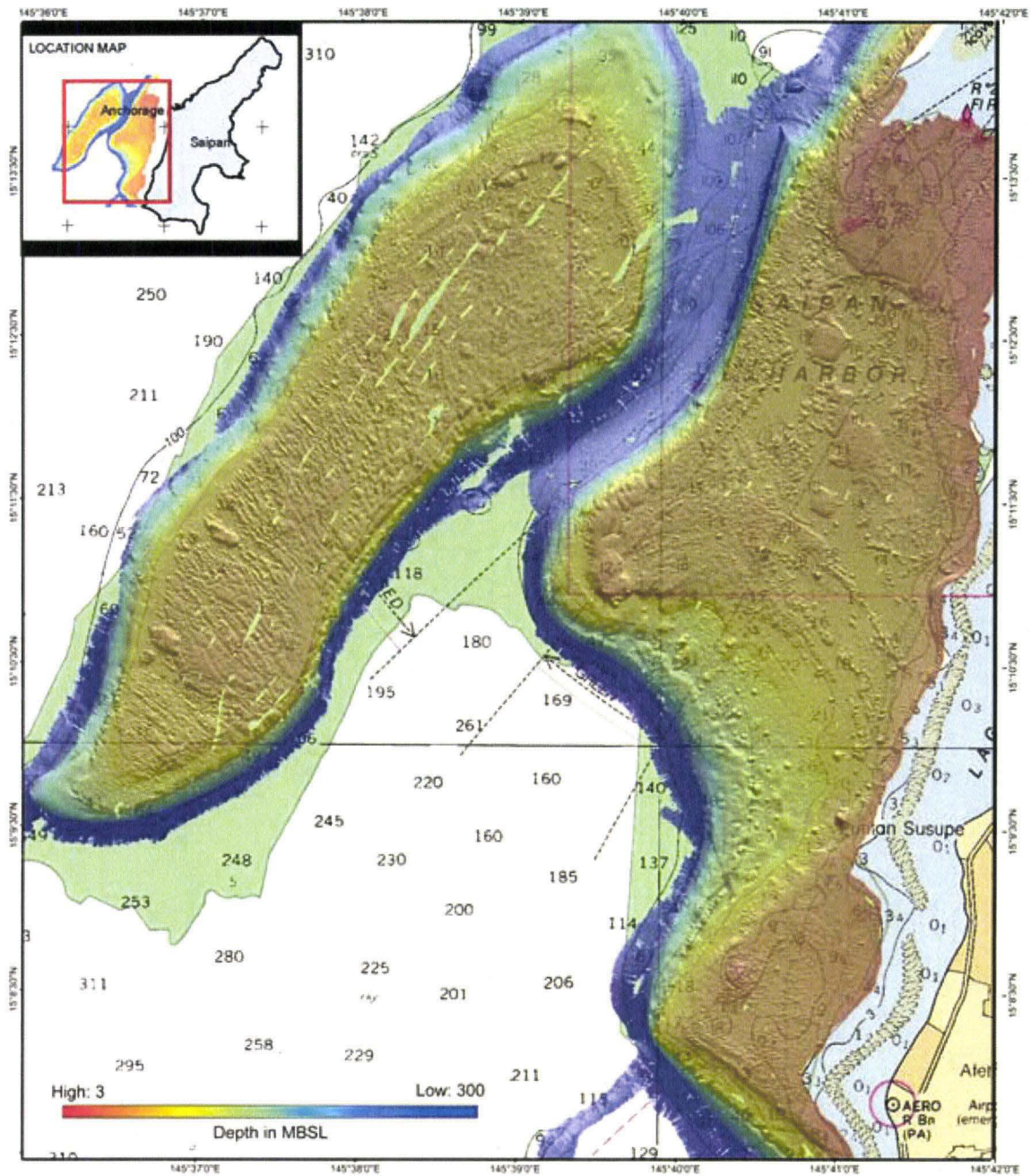
Figure 4: Multibeam Bathymetry Map of the Saipan Anchorage- (Rooney et al., 2005). The multibeam bathymetry map is of Garapan Anchorage, Saipan. The scale bar shows water depth in meters below sea level with the deepest depths in blue. The inset map in the upper left corner shows the location of the Garapan Anchorage off the NW side of Saipan.

2.3 Tools for Habitat Mapping

The data that were collected in the Garapan anchorage will be used to develop a benthic habitat map which is an important tool for monitoring reef health, delineating marine protected areas (MPA's), regulating commercial fishing, and, for this study, determine the areas of densest coral growth. Prior to the development of remote sensing tools scientists used qualitative visual observation of flora and fauna to create benthic habitat maps (Cloud et al., 1959). Scientists sometimes used boats with Plexiglas bottoms for dry observations and employed a combination of swimming or towing using a face mask, air hose, and weights. Direct observations over a given area were depth limited (Cloud et al., 1959).

Because worldwide reef monitoring and mapping efforts only started around 1990 there is little information available about complex reef systems (Weier, 2001). Without comprehensive maps of the world's reefs scientists and resource managers are ill-equipped to monitor changes in reef systems, let alone develop solutions to prevent further degradation (Weier, 2001). Complete maps of the world's reefs would allow scientists to identify large-scale threats and locate reefs in the most danger.

Many different remote sensing tools have been developed to study and map the bathymetry of the ocean. Some of these tools include satellite imagery, side-scan sonar, multibeam sonar, and video data. Each sensor has benefits and limitations determined by its resolution, coverage range, and depth range. Tools are chosen based on the depth and spatial scale of the subject to be studied. For example, warm water coral generally flourish in warm waters at depths between 5 and 30 m with some deep water corals living down to 200 m. To resolve coral colonies at depths between 20 m-100 m CRED typically

13

uses high frequency sonar and towed video since those remote sensing tool operate across

the full range of coral growth (Figure 5).
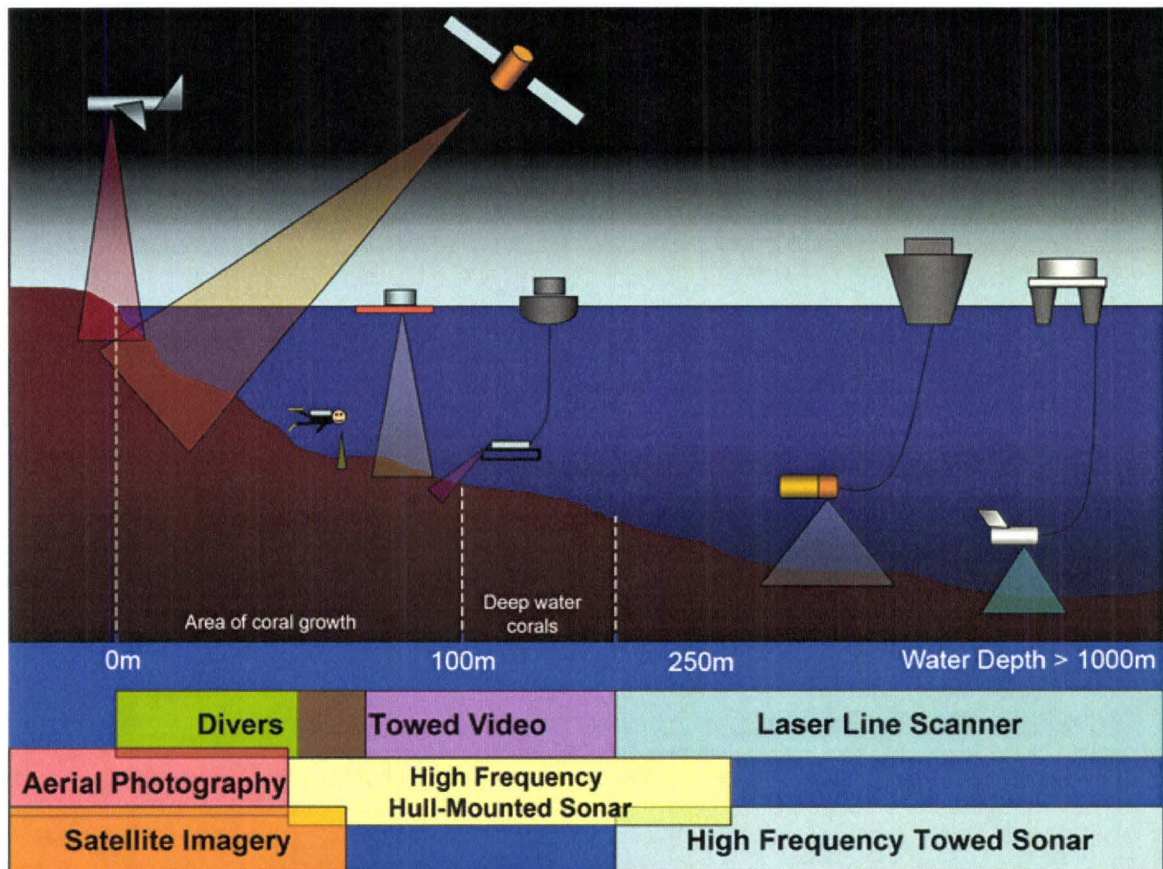
Figure 5: Remote Sensing Tools and Their Capabilities. The colored rectangles show the depth range (m) of each remote sensing tool. The tools most useful for mapping coral reef areas are towed video and high frequency mounted sonar because the give the most direct coverage across the entire region of coral growth.

2.3.1 Satellite Imagery

The remote sensing tools that operate furthest from the earth's surface are

satellites. There are several different types of satellites but the most commonly used types

include IKONOS, Landsat (Thematic mapper (TM) and Multispectral scanner (MSS)

imagery) and SPOT (Multispectral (XS) and Panchromatic (Pan) imagery). Each type of

14

satellite has different spatial and spectral resolutions. Spatial resolutions can vary from 1 to 80^2 meters (Mumby et al., 1997).

Satellite imagery is useful when mapping coral reef systems because of its ability to provide consistent coverage over large areas for extended periods of time. Satellite data also have the ability to distinguish between healthy and bleached coral (Holden and Ledrew, 1999). Other types of remote sensing data, such as multibeam and side-scan sonar data, are not able to quickly map reef systems at the same scale as satellite imagery nor are they yet able to distinguish between healthy and dead coral heads (Holden and Ledrew, 1999). However, there are many disadvantages to satellite data. Some of the disadvantages are attenuation and scattering of electromagnetic energy due to depth, quality of water and brightness of the substrate. Bright substrate will work to augment the spectral signal from the effects of multiple scattering and potentially cause misclassification. The morphology of reef features also affects spectral reflectance characteristics and many features in the coral reef environment are optically similar which give a similar spectral response and contributes to misclassification errors (Holden and Ledrew, 1999). There is also error associated with a loss of radiance contrast due to atmospheric Rayleigh scattering (Mumby and Edwards, 2002). In order to perceive subtle differences in spectral response, high spectral resolution sensors are required. Spectral resolution increases as the width of the spectral bands decrease. However, the higher the spectral resolution the lower the spatial resolution, which means there is a decrease in the image's ability to accurately show the location of features (Holden and Ledrew, 1999). Overall accuracy, defined as the number of correctly identified test sites divided by the total number of test sites, is also decreased the more finely each habitat is classified. For

example, if the imagery is 73% accurate using a coarse (4 habitats) classification it will

be around 37% accurate using a fine (13 habitats) classification scheme (Mumby et al.,

1997). Another drawback of satellite data is that they cannot be used to measure rugosity,

or surface cover, since only two-dimensional data are provided (Mumby et al., 1997).

One type of satellite, Landsat 7, which was launched in 1999, has a resolution of

30 by 30 meters. This means that nothing smaller than something the size of an office

building can be monitored (Weier, 2001). Satellite imagery is not yet well-suited to

accurately map the fine scale biology within a coral reef habitat (Mumby et al., 1997) but

it is capable of mapping al the worlds large scale (greater than 30m by 30m) coral reefs,

such as atolls, in one year using 1,000 Landsat 7 images. Another two years would be

needed for analyzing the data, publishing, and distributing the information to the public

(Weier, 2001). To have a comprehensive map of the worlds reefs could be very import

for delineation of marine protected areas and implementation of reef protection policy.

However, these maps would lack fine scale detail and would not be able to distinguish

between the species of coral or its inhabitants.

In 1999 the IKONOS2 satellite was launched (Mumby and Edwards, 2002) and is

operated by Space Imaging (SI) (Andrefouet et al., 2003). This 11 bit commercial sensor

is equipped with four wide spectral bands and has a spatial resolution of 4 m (Andrefouet

et al., 2003). IKONOS data become less accurate due to dust, clouds, and sea surface

effects such as wave patterns and sun glint. Some of the data need to undergo sea surface

roughness correction before they can be used. Although IKONOS imagery has been

shown to be almost 20% more accurate than Landsat TM with 64% user accuracy, it is

still not as accurate as CASI which boasts 81% user accuracy (Mumby and Edwards,

16

2002). User accuracy is the probability that a pixel is classified the same as it would be on the ground (Mumby and Edwards, 2002). Both the Landsat TM and IKONOS sensors demonstrate decreasing accuracy with increasing habitat complexity (Andrefouet et al., 2003). This is because satellites only have a limited number of water-penetrating bands, usually less than 4, and these bands have broad bandwiths (70nm) which reduces resolution (Mumby and Edwards, 2002). As of July 2001 it was found that both CASI and Landsat TM were more cost-effective to operate than IKONOS, even over small areas. This is because IKONOS data need independent field data to increase their accuracy. An additional cost was added for tasking the satellite. It was found that IKONOS data are not able to identify declining corals reef systems due to their inadequate spectral resolution (Mumby and Edwards, 2002).

Satellite systems are extremely useful for large scale, shallow water, reef mapping and monitoring projects. However, because satellite data have a resolution of tens of meters, the data are affected by surface effects such as clouds, sun glint and wave patterns and the systems are not able to collect data across the entire range of coral growth, satellite data are not useful for this study.

2.3.2 Aerial Imaging

Using a spectroradiometer such as a compact airborne spectrographic imager (CASI) is an alternative to satellite imagery. CASI has a 1m spatial resolution (Mumby and Edwards, 2002) and therefore is significantly more accurate (81% using a detailed habitat classification scheme with 13 classes) than Landsat TM or IKONOS and is more consistent in habitat description. Although CASI can penetrate the upper levels of the water column and therefore occasionally appear to be more accurate than aerial

17

photography, it is considered to be equal in accuracy to aerial photography. This is important because CASI is more expensive per Km^2 than either Landsat or IKONOS satellite mapping since costs for CASI include instrument hire, flight time, and preprocessing time (Mumby and Edwards, 2002). Therefore aerial photography is a more economical choice.

Neither aerial photography nor CASI imagery gives depth information about the seafloor. Therefore, calculating rugosity information from this dataset is not possible which renders this type of data unusable for the purposes of this project. Also, since CASI cannot penetrate far into the water column, data is not available across the full range of coral growth. Comprehensive seafloor coverage is necessary for benthic habitat mapping.

2.3.3 Side-scan Sonar

Another type of remote sensing tool that doesn't measure depth is side-scan sonar which reveals information about sea floor composition by taking advantage of the different sound absorbing and reflecting characteristics of different materials. Side-scan sonar systems use a transducer array (or arrays) to produce a pulse in the across-track direction. The pulse, or ping, expands in a spherical wave as it travels through the water column and then returns in a spherical wave after is reflects off the seafloor (L-3 Communication, 2000). The sonar system measures time vs. amplitude of the pulse. The reflected pulse is the bulk of the acoustic energy that is not absorbed by the seafloor and is scattered back into the water. The fraction of the scatter that is directed back at the transducer array is called the backscattering strength of the seafloor (L-3 Communication,

18

2000). The intensity of the backscatter is controlled by the angle of incidence, the roughness of the sea floor, and the facies effect which is how acoustic properties change across the sediment-water interface (Gardner et al., 1991). Sometimes the sonar signal will penetrate into the underlying sediment layer introducing interference due to subsurface inconsistencies (Gardner et al., 1991). Under normal conditions, the greater the mean grain size the greater the backscatter. Backscatter response is dominated by the largest grain sizes even if that size clast is not the dominant size (Goff et al., 2000).

Before the side-scan data can be used the yaw, pitch, roll, and crabbing noise need to be removed (Malinverno et al., 1990). Once the data are clean the intensity of the backscatter data from side-scan sonar can create a spatially correct grayscale image that looks like a photograph but is actually a representation, or map, of how acoustic energy interacts with the seafloor. Depending on the color look-up table, areas of low backscatter (or low signal return) may be mapped to either dark or light shades. The images in this document are shown such that high backscatter is black, and low backscatter is white.

Side-scan sonar can utilize a large range of frequencies, usually between 12 kHz (Hawaii Mapping Research Group's HAWAII MR1) and 900 kHz (Marine Sonic's side-scan on REMUS AUVs). Higher sonar frequencies produce better resolution but have shorter ranges than lower frequency systems. Because hull mounted sonar must sacrifice resolution for information at deeper depths, towed side-scan sonar are used to gather higher resolution data at deeper ocean depths than hull mounted systems are capable of. Also the lower the altitude of the sonar off the seafloor the faster the data acquisition rate can be.

19

Although side-scan data can give detailed information about the shape or texture of the seafloor over large areas and across the full range of coral growth, they can not provide any depth information. For the rugosity algorithm to work there needs to be depth information associated with each data point. Therefore side-scan data are not useful for this project.

2.3.4 Video Data

Analysis of seafloor video data gives the most direct description of the biological cover in coral reef ecosystems and is capable of deep observation beyond the reach of most divers, aerial photography, and satellites. Because video data allows for direct observation, biological cover and substrate type are more likely to be correctly identified than by other remote sensing techniques. Classifications are also available on centimeter spatial scales instead of tens of meters. However the process is slow and cannot easily give 100% coverage over the areas of interest.

Seafloor video data can be used to calculate the percentage of the seafloor inhabited by various organisms using point-sampling methods. However, when analyzing video there are several potential sources of error that can be introduced. The first is related to the ability of the observing scientist to accurately identify the organism on the screen. This error is multiplied with the introduction of multiple video analyzers who might have varying opinions of what the correct identity of the organism is. Although most people, even without training, can accurately identify the difference between hard coral, soft coral and algae, the more detailed the taxonomic classification the greater the opportunity for misclassification. Another source of error stems from the quality of the video images. Grainy images collected under poor light conditions will be more difficult

20

to correctly identify than fine resolution images with adequate illumination. Also the distance of the camera from the substrate plays a large role in how accurately organisms can be identified. The further the camera is from the substrate, the harder it is to accurately identify the bottom cover (Ninio et al., 2003).

Identification of benthic groups, such as hard corals, soft corals, and algae was most accurately identified since it was the coarsest level of identification (Ninio et al., 2003). In one study, the identification of algae introduced more error than the identification of the corals. Ninio (2003) determined that the accuracy with which observers would correctly identify a species increased when the mean cover increased. It was determined that species diversity can be accurately determined from video transects and that observer error will not limit the ability of underwater video to detect changes in cover over time (Ninio et al., 2003). However, observation and interpretation is time intensive. The more finely the towed video data is analyzed the more time or observers are needed.

Towed video data allows for direct observation of biological cover and substrate type over widespread areas. This type of data is extremely useful for benthic habitat mapping. However, the classifications of the data are subjective, intermittent, and time intensive. Also video data do not measure the bathymetry of the sea floor so the data set cannot be used to calculate seafloor rugosity. The data can be useful for comparison against the automated rugosity data set and used to determine if there is a correlation between observed video classifications and rugosity.

21

2.3.5 High Frequency Multibeam Sonar Data

Another type of remote sensing tool is multibeam sonar. The multibeam sonar systems utilized today evolved from the technique of echo sounding that measured water depths by transmitting acoustic pulses from the ocean surface and listening for their reflection from the sea floor. This technique was utilized to collect a series of depth points that could be contoured to create depth charts. In order to increase the spatial resolution of the echo sounder, and create more detailed sea floor maps, the beam diameter was narrowed. Decreasing beam width also decreased the size of the area able to be ensonified. Until 1960 most depth data was collected using single beam echo sounders (L-3 Communication, 2000). Then in 1964 a technique for multiple narrow-beam depth sounding was developed and the first systems, known as Sonar Array Sounding Systems (SASS), employed two separate sonar arrays. The array was set up in a Mill's cross geometry, with the transmit array oriented perpendicular to the receive array. This system was able to produce high-resolution coverage over wide swaths of the ocean bottom in less time than a single-beam echo sounder (L-3 Communication, 2000).

Most sonar systems make depth measurements based on the time it takes a sound pressure wave to travel back to its source after reflecting off a surface. The deeper the survey depth the more time is required for the soundings to go out and return (Hughes Clarke, 1996). The time interval is converted to distance using an estimate of the speed of sound through the water column. However, the speed of sound in water varies with salinity, temperature, and pressure which means that the sonar data need to be corrected for each of these variables using a sound speed profile (L-3 Communication, 2000). The amount of sound reflected from the sea floor varies with the angle of incidence of the

22

sound wave, or its grazing angle, the smoothness and composition of the sea floor, and the frequency of the sound (L-3 Communication, 2000). The depth range of the multibeam sonar is also dependant upon the frequency of ensonification. Like side-scan sonar, the higher the frequency the better the resolution but the shorter the range.

For multibeam sonar systems to accurately map the seafloor information on vessel position, heave and vessel motion are required so that the errors associated with them can be removed. Tide gauge data is used to remove tide error. Multibeam sonar can be used to identify small-scale changes in seafloor amplitude and position which could help map things like sediment transport. This is useful to resolve fine scale roughness and its changes over time (Hughes Clarke, 1996).

Multibeam sonar are now being used to obtain 100 percent coverage of the seafloor. However, having complete coverage does not mean that the technology is of high enough resolution to detect all seafloor features. Because the sounding spacing increases with depth and distance from nadir (the data point directly under the ship) the most detailed data are found in shallow water near nadir if the sonar is hull mounted.

Multibeam sonar are capable of returning dense, comprehensive, multibeam data sets that have inherent depth information. Because of this multibeam sonar data are the most useful remote sensing tool for mapping the bathymetry around Saipan and are used in this study to calculate rugosity values within the Garapan Anchorage.

2.4 Methods for Measuring Rugosity

2.4.1 Manual Measurements

In order to choose a method for measuring the roughness of a seafloor it is important to first determine which physical properties you are most interested in such as vertical relief and substrate rugosity. Although multiple vertical relief measurements can give you rugosity information, manual rugosity measurements cannot give any information about vertical relief since this method does not directly take individual relief measurements. Once you know what physical properties are important to your study a method can be chosen such as the chain method, profile gauge or complexity.

2.4.1.1 Chain method

This early method of quantifying substrate rugosity requires the use of a chain of known length. The chain is draped along the ocean bottom taking care to follow the bathymetry as closely as possible (Figure 1). The horizontal chain distance is measured and compared to the actual chain length. This ratio is said to be its "rugosity" which is simply a measure of how rough, or wrinkled, a surface is along a vertical plane (Luckhurst and Luckhurst, 1978). Using a scale from 0-100%, a perfectly flat bottom will have a ratio value of 0%. The rougher the bottom becomes the closer that value will move to 100%. However, to achieve a rugosity value of 100%, the measured surface would need to be completely vertical.

Although the chain method is considered to be one of the quickest and easiest manual rugosity measurement techniques it still has limitations and presents its own challenges in the field (Frost et al., 2005). This method is completed during SCUBA dives and measurements are limited to the depth/time capabilities of the divers. It was

24

suggested in a study done by Frost et.al. (2005) that due to the extreme variability of the ocean floor surveyors should make as many chain measurements as logistically feasible in order to ascertain the true roughness of the sea floor. However, scientists generally do not have the time to complete the many measurements needed to determine true roughness.

This method is also affected by the chain length and link size used. McCormick (1994) suggests that the substratum variation be measured at a scale that is appropriate for the organism of interest. Small scale features may require smaller chain link sizes since larger link sizes will not conform to smaller depressions. These lower resolution measurements are reflected in the rugosity ratios causing the surface to appear smoother than it actually is. Another problem with using a chain is that links slip. If the links are not touching end to end it may appear as though the surface is rougher than it actually is since the linear distance will appear to be slightly more compressed. To prevent this error Frost et. al. (2005) used a chain with fixed links.

2.4.1.2 Profile Gauge

Another method for measuring seafloor surface complexity is a profile gauge. McCormick (1994) used a profile gauge 1m wide with eleven sliding vertical needles. The gauge is lowered onto the seabed so that all eleven needles made contact with the surface. The horizontal level that encases the eleven needles provided a reference frame from which measurements are made to the bottom of each needle. After each transect is completed the height differences between needles is calculated and squared. Then the squared values are summed and the square root is taken. The remaining value is said to be the measure of topography for a transect (McCormick, 1994). For this method a

25

perfectly flat bottom would have a value of 0, inverse to the chain method. Increasing surface topography would yield higher values with maximum values determined by the difference in height between the needles and the number of needles used in a survey (McCormick, 1994).

The advantage of this method lies in the vertical height information inherent in the raw data. This means the measure of topography from the profile gauge method correlates better with the actual bottom shape unlike other methods, such as the chain method, which are unable to tell the difference between varying bottom textures (McCormick, 1994). However, because the profile gauge method is time consuming it is probably better suited to studies over a smaller area such as the growth of an individual coral.

2.4.1.3 Complexity

A third method of measuring surface roughness is physical complexity. Ardon (2002) suggests that physical complexity data can be used in place of biological data for marine planning and research. This is because areas with varying bottom habitat are usually areas with high species richness (Ardon, 2002). The more crevices or niches available for organisms to reside, the more types of species will exist there. The complexity of a habitat can also affect the predator-prey ratio. Less complex areas offer less shelter and are consequently predator-dominated. More complex areas allow species to co-exist in greater diversity and allow a greater variety of life stages to be supported. Complex habitats may exhibit greater ecosystem resilience (Ardon, 2002).

Rugosity is different from complexity. Complexity values are calculated so that all depth changes are treated equally whereas rugosity values can be strongly influenced

26

by a single large change in depth. Ardon (2002) defines complexity as how often the slope of the sea bottom changes within a defined area. These changes are based on the slope of the slope of the depth (i.e., curvature). Complexity can capture biologically and physically meaningful features such as sills, ledges, and other distinctive habitats that are associated as biological "hot spots" providing upwellings, mixing, and refugia (Ardon, 2002).

In order to perform this benthic complexity analysis, bathymetry line data in raster (grid) format are used. The data are transformed into evenly spaced points and interpolated using a TIN (triangulated irregular network). The sampling density and spacing of the points affect the accuracy of the complexity results. Because this method looks at large-scale features the small scale changes in bathymetry are regarded as inconsequential (Ardon, 2002). However, because a gridding technique is employed and small scale changes in bathymetry are ignored the resolution of this method is less than the direct measurements calculated with the chain method and profile gauge method. Therefore this technique is not appropriate for studying fine scale rugosity.

2.4.2 Other Seafloor Classification Techniques

Because each of the manual rugosity techniques are subjective, time and labor intensive, and depth limited, new techniques need to be developed to replace the manual data collection and interpretation process. Automating the collection of rugosity data will allow reproducible, objective, data to be collected over large areas more quickly than manual methods allow. Remote classification the sea floor requires an acoustic data acquisition system, an algorithm to analyze the data, and a way to relate the data to what is on the actual seafloor (Collins and Galloway, 1998). There are a few methods that

27

attempt to determine the seafloor texture using sound rather than a manual measuring tool.

2.4.2.1 Measuring Return Signals

One way to remotely classify the roughness of the seafloor is to use the signal complexity of a returning echo to determine how convoluted the sea bottom surface is. To do this, multibeam swath sonar were used to gather bathymetry data of a seafloor. Then the Quester Tangent Corporations (QTC) VIEW seabed classification system is used to classify the ocean bottom based on the shape of a returning echo. The QTC VIEW receives the bottom echo and uses the transmission and reception of an echo trace to produce a digital time series. The data are cleaned and filtered to suppress noise and then shape parameters are extracted from each trace. Then using the calibration data, the three most useful shape descriptors are chosen (Q-Values). The shape descriptors refer to the shape of the return signal, such as a short tail, amplitude, or slope of the peaks. The rougher the bottom, the more complex and longer tail the return signal will have. There are many factors that will influence the shape of the returning wave-form. Some of these include the physical properties of the sediment, the type of large scale bed forms, and whether the bottom has biological cover (Collins and Galloway, 1998). The QTC VIEW classifies the bottom based on the similarity of the signal to the calibration signal which is called its "confidence". Depending on the desired confidence level geological layers such as gravel, medium sand, and coarse sand can be resolved. Although the flora and fauna do play a role in the signal return, their presence cannot be resolved (Collins and Galloway, 1998).

2.4.2.2 Local Fourier Histograms

Another method uses Local Fourier Histograms to determine the bottom type based on pixels extracted from grayscale texture images. Zhou et al. (2001) looked at texture represented by the difference in color brightness variation among neighboring pixels. This work is based on the idea that neighborhood properties have a dominant texture in common. By looking at the number of times the same value occurs, and where it occurs within the pixel neighborhood texture features can be developed. The Local Fourier Transform of each texture image is computed and Local Fourier Coefficient maps are made. The texture feature, called a Local Fourier Histogram (LFH), is extracted from the maps and used to classify texture and for texture retrieval (Zhou et al., 2001). The LFH is a histogram that is used to show the distribution of local frequency information of a texture.

Another technique, proposed by Cutter et al. (2003), utilizes the LFH proposed by Zhou et. al. (2001) to create a benthic habitat delineated map that can be used to model distribution of benthic biology using other data sets such as fisheries data or direct sampling. This automated delineation technique utilizes cleaned and gridded bathymetry data. The algorithm works by calculating a LFT for every data point (grid cell, pixel or node) and then using the Fourier coefficients to characterize the signal's roughness. For each gridded cell, the texture features are described for the node and its surrounding points. This creates a 5-20 m (depending on the operator's choice) square block that has multiple nodes within it. A histogram is then created for each magnitude coefficient which in turn classifies the block of nodes with a LFH texture feature vector. Next, seafloor texture classes are constructed using a fuzzy k-means cluster analysis which

29

minimizes the effect of outliers on classification. The textural classes serve as a physical habitat model for the seafloor upon which benthic faunal inhabitants, and their distribution, can be predicted. Representative LFH texture features are then developed and a LFH map is created. In order to make sure that the identified texture features actually exist on the seafloor, the LFH features can be compared with seafloor samples and other data sets.

In a study done by Cutter et al. (2003) it was determined that a radius of 5 m, with a block size of 10 m by 10 m, struck a balance between regional consistency and oversimplification. This was determined by comparison with sediment samples collected from grab samples, diver observations and towed video data. It was also found that the LFH maps correlated with the relative backscatter and substrate map that had been created for that study area. Because we are interested in rugosity data on a finer scale than 10^2 m, and we do not have direct grab samples or diver observations to accurately correct the LFH texture features, the seafloor segmentation method would not be useful for this study.

2.4.2.3 Surface Ratio Grids

Another rugosity tool was developed by Jenness (2003), which allows surface area and surface ratio grids to be generated from an existing elevation grid. Both the surface area and the surface ratio provide information on an area's topographic roughness and convoluted nature and provides more realistic estimates of land area than simply using planimetric area. The Jenness method is intended for subaerial rather than submarine studies and requires an elevation grid in order to work. Surface area is one way to measure topographic roughness and is calculated as the sum of the surface area

cell values from all cells whose cell centers lie within the polygon boundaries. The surface ratio is calculated by dividing the surface area by the planimetric area. By increasing the number of grid cells used to calculate the surface area the accuracy and precision increase. The output is in raster format so precision is lost calculating surface areas from polygons rather than a TIN.

This method can be used at different spatial scales and it set up to allow the surface area to be calculated within a particular range of all the cells in the grid for neighborhood analysis. However, the smallest grid size that Jenness tested his surface ratio tool was 100 m. Because we are interested in roughness information on the scale of a few meters this function is not able to asses small scale rugosity across coral reef systems.

CHAPTER 3: DATA AND METHODS FOR BENTHIC MAPPING OF GARAPAN ANCHORAGE, SAIPAN

3.1 Remote Sensing Tool Selection

As technology continues to improve more remote sensing tools are becoming available. However, many remote sensing tools are developed for unique surveying and are not appropriate for all types of research. Therefore, before any project can begin, it is important to choose the remote sensing tool that best fits the project requirements. Some things to consider include the scale of the study, the depth to which information is needed, and whether the remote sensing tool has a fine enough resolution to map the object of interest. CRED needed to choose tools that would resolve coral reef systems over the entire Saipan anchorage between 10-300m depth (Figure 5). Both high frequency multibeam sonar systems and towed video surveying were selected for the Saipan survey.

A map of the seafloor in Saipan needed to be developed so that there was a base reference for interpreted data to be plotted upon and so that correlations could be made between species density and bathymetry. High frequency multibeam sonar was used to ensure high resolution data with inherent depth information. Because sonar systems cannot distinguish between coral and rock, towed video data were collected for visual interpretation and ground truthing. The video data allow for large areas of seafloor to be covered and analyzed without needing divers in the water. Once the towed video data were classified the data was overlain on the bathymetry map. During the 2004 video survey, manual rugosity measurements were also collected for the classification purposes of this project.

3.2 Towed Video Data

In order to get the most detailed benthic habitat information forty-four towed video surveys were conducted in the Garapan Anchorage, CNMI from December 3-16 2004. These optical tows covered one hundred twenty linear kilometers of the Saipan Anchorage. Each day an underwater camera sled collected video data of the seafloor habitat using a Deep Sea Power & Light Multi SeaCam 2060 color video camera, two 500 watt lights, and a sonar altimeter to detect the height of the camera above the seafloor. Once the sled was in the water, real time video was transmitted along 200 m of umbilical cable to a control console located on board the *Carolinian*. The depth of the sled above the seafloor was monitored using a video display unit. Instructions to raise/lower the sled were relayed to CRED personnel on deck to maintain the minimum possible distance from the seafloor without incurring collisions with the reef habitat. Video data were recorded to digital video cassette and Hypack Max hydrographic survey software was used to record GPS data, water depth, and camera sled information (height, heading, etc.) (Rooney et al., 2005). The navigation was controlled using POS MV 320, resulting in ±13 m of horizontal position accuracy (Rooney et al., 2005).

3.2.1 Video Data Analysis

Video data collected from the Saipan cruise were analyzed to determine the percentage of seafloor inhabited by different organisms (coral, macroalgae, etc.) and the substrate type, or grain size, (sand, rubble, mud, etc.). The dominant variation in relief visible in the imagery and the number of visible cavities that fish or other aquatic life may be able to take shelter in were also recorded (Table 1) (Figure 6). To analyze the

video data, the bottom type was classified every 40m on the outer reef and every 20m on the inner reef. Five stationary dots were placed on the computer screen or monitor (Figure 7). At each 20m or 40m increment the interpreter classified the bottom type (sand, rock, rubble) and cover (macroalgae, coral, coralline algae, etc.) under each of the dots.

Since most video transects were completed without proper lighting, color information was not available. This made it difficult to distinguish between the different types of benthic cover during analysis (Figure 8). Also, due to the rapidly changing seafloor bathymetry the altitude of the camera varied widely. As a result, the camera was often too far from the bottom to be able to discern the cover, or so close it impacted the bottom creating sediment clouds or turning the camera around so that the area of interest was obscured.

These interpretations were used to create a map showing the percent coral and bottom type, such as sand, mud or rock (Figure 10). These data were interpolated to create a continuous map showing sand fields and the areas of densest coral growth (Figure 11).

Percentage of Substrate		Living Cover		Relief		Holes	
Unconsolidated		Seagrass	1	≤0.5 m	1	No Cavities	1
Mud	1	Macroalgae	2	>0.5, ≤1.0m	2	Few Small Cavities	2
Sand	2	Non-Scleractinian Fauna	3	>1.0m, ≤2.0m	3	Many Small Cavities	3
		Scleractinian Fauna	4	>2.0m, ≤3.0m	4	Few Large Cavities	4
Hard bottom		Coralline Algae	5	>3.0m	5	Many Large Cavities	5
Rubble	6	Coral or Coralline Algae	6			Few Small and Large Cavities	6
Boulder	7					Many Small and Large Cavities	7
Rock	8	None	8			Many Small and Few Large Cavities	8
Man-Made	9	Unclassified Algae	9				
Unclassified	20	Unclassified	20	Unclassified	20	Unclassified	20

Table 1: Video Classification Chart. This table shows the classification system CRED employed to classify the towed video data. First the substrate was classified and then the living cover was classified. The relief and number of cavities were determined across the entire screen, not just at specified points. The numbers 1-20 were used to signify the classification selection.
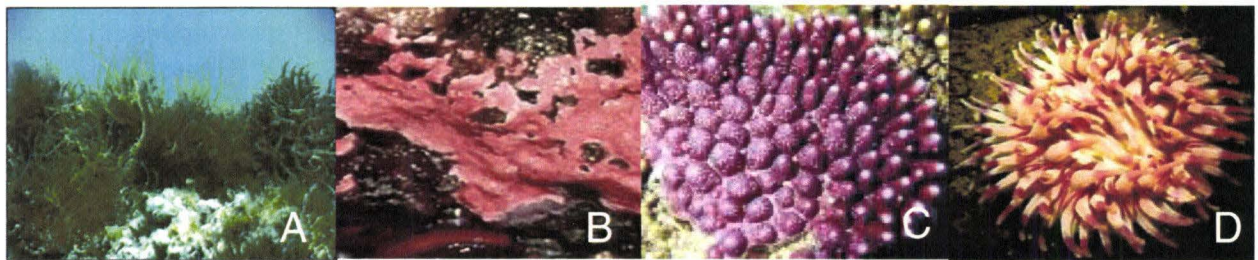
Figure 6: Pictures of benthic cover. This figure shows examples, not from Saipan, of the general types of benthic cover identified during the towed video survey. A is algae, B is coralline algae, C is scleractinian coral and D is non-scleractinian fauna. Pictures B and D are taken from the Coral Reef Information System (NOAA, 2006).
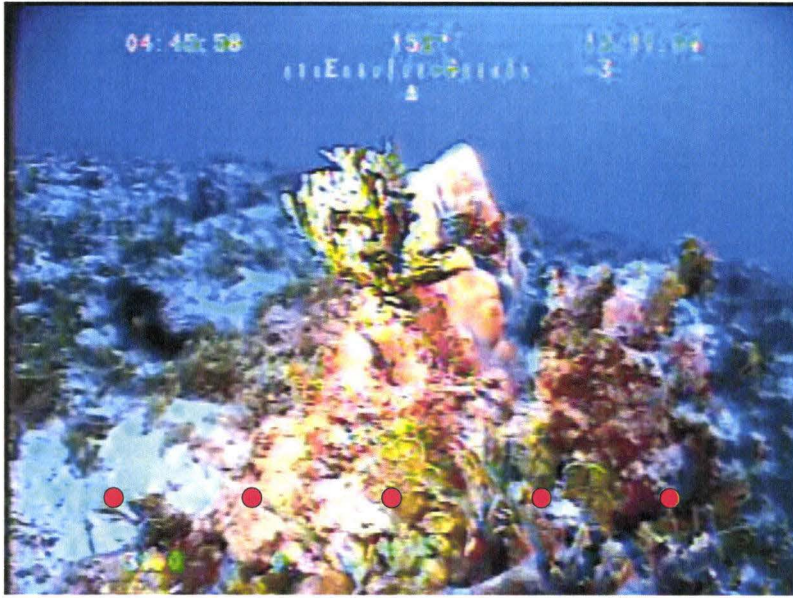
Figure 7: Frame capture from video survey in 2004. This figure is a frame capture from one of the towed video survey lines during the 2004 Saipan survey. The red dots in the lower 1/3 of the monitor delineate areas for substrate and living cover assessment. This survey had working lights and the benthic cover was easily identified (Rooney et al., 2005).
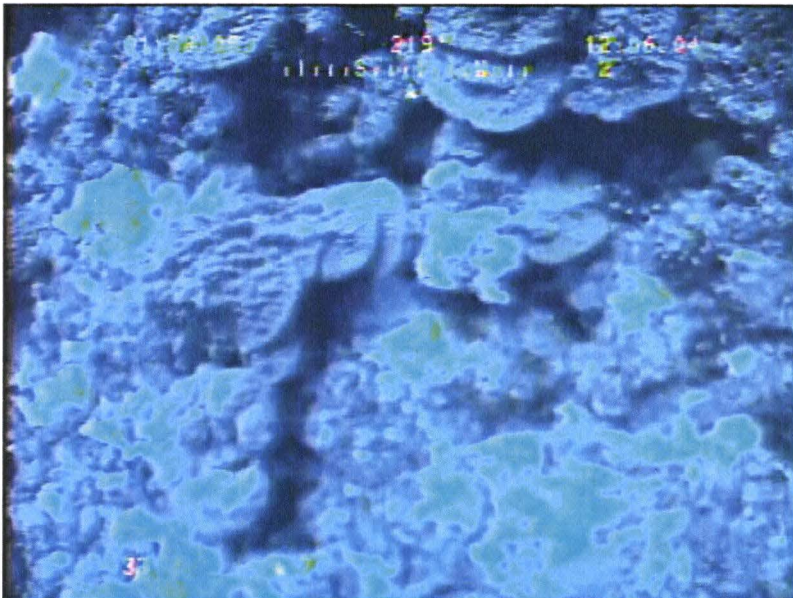
Figure 8: Medium visibility frame capture from 2004 video survey. This frame capture shows an area were the lights on the towfish were not functional making the classification of benthic cover difficult despite the close proximity to the coral head (Rooney et al., 2005).

36
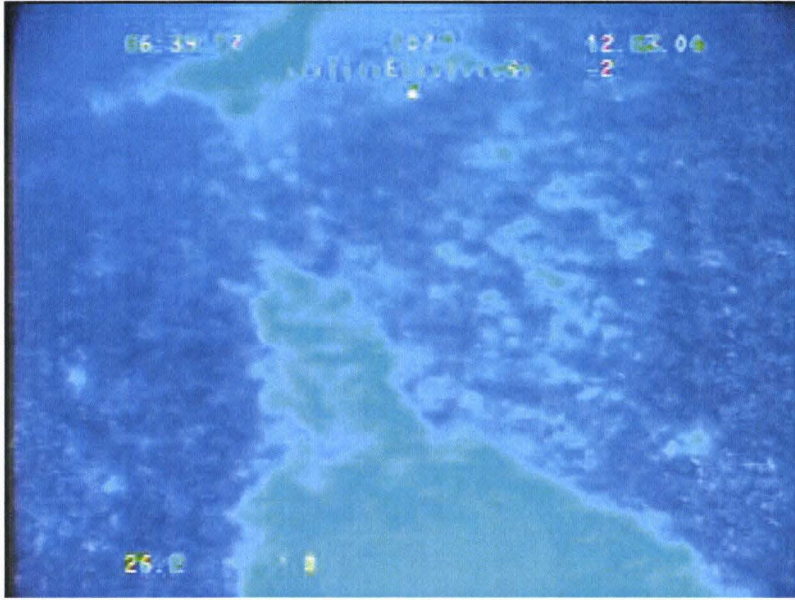
Figure 9: Low visibility frame capture from 2004 video survey. This frame capture shows an area along the survey line where the lights on towfish were not functional and the towfish was too high off the bottom to distinguish benthic cover. No living cover classifications were available for this area (Rooney et al., 2005).
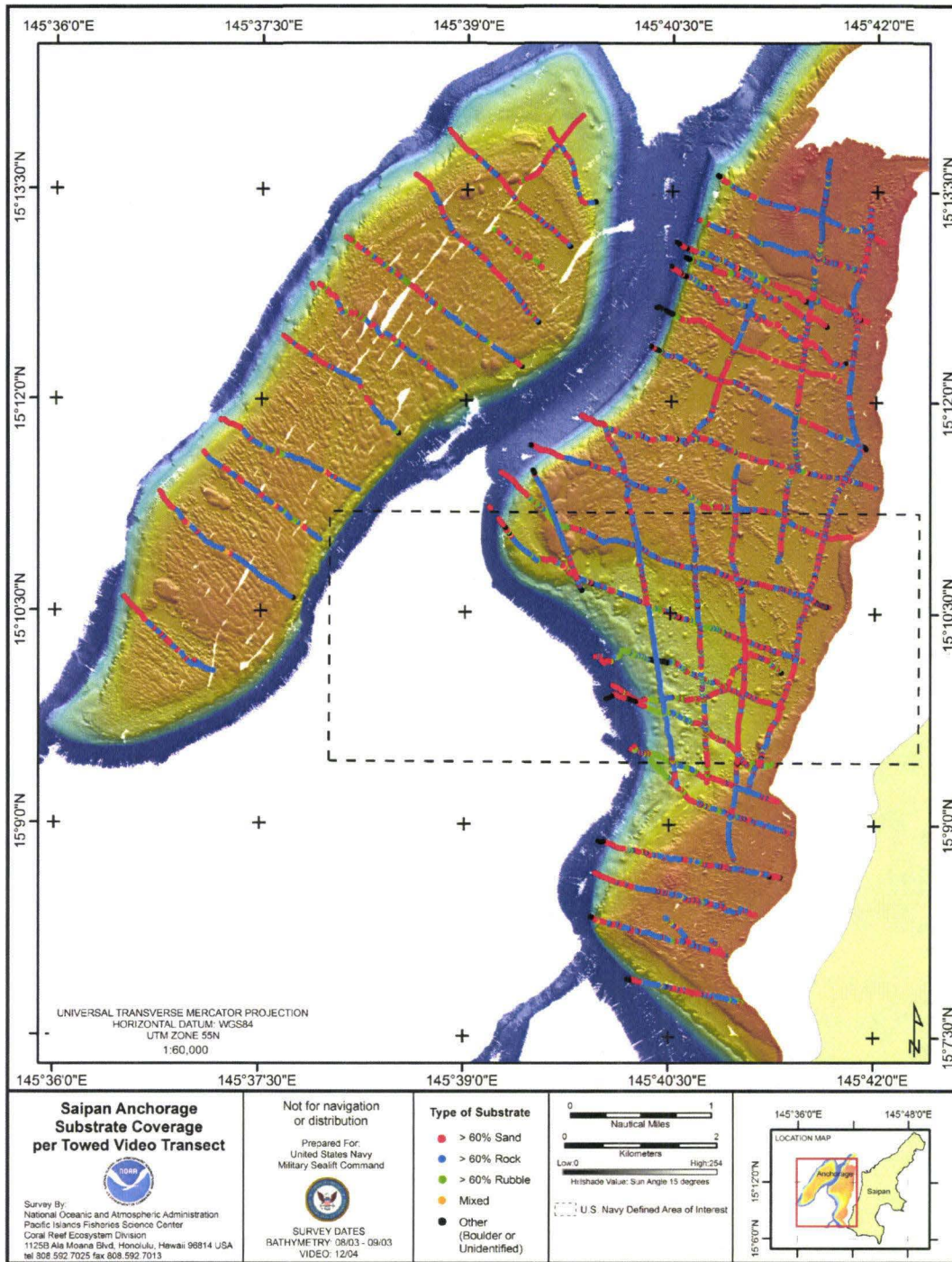
Figure 10: Substrate map. The base image is bathymetry data collected during the 2003 Saipan survey. Plotted on top of the bathymetry data are lines of circles that represent the towed video tracks. The individual circles in each line show the substrate type classified from the video data. The map shows that the two most common substrate types are >60% sand (red) and >60% rock (blue) (Rooney et al., 2005).
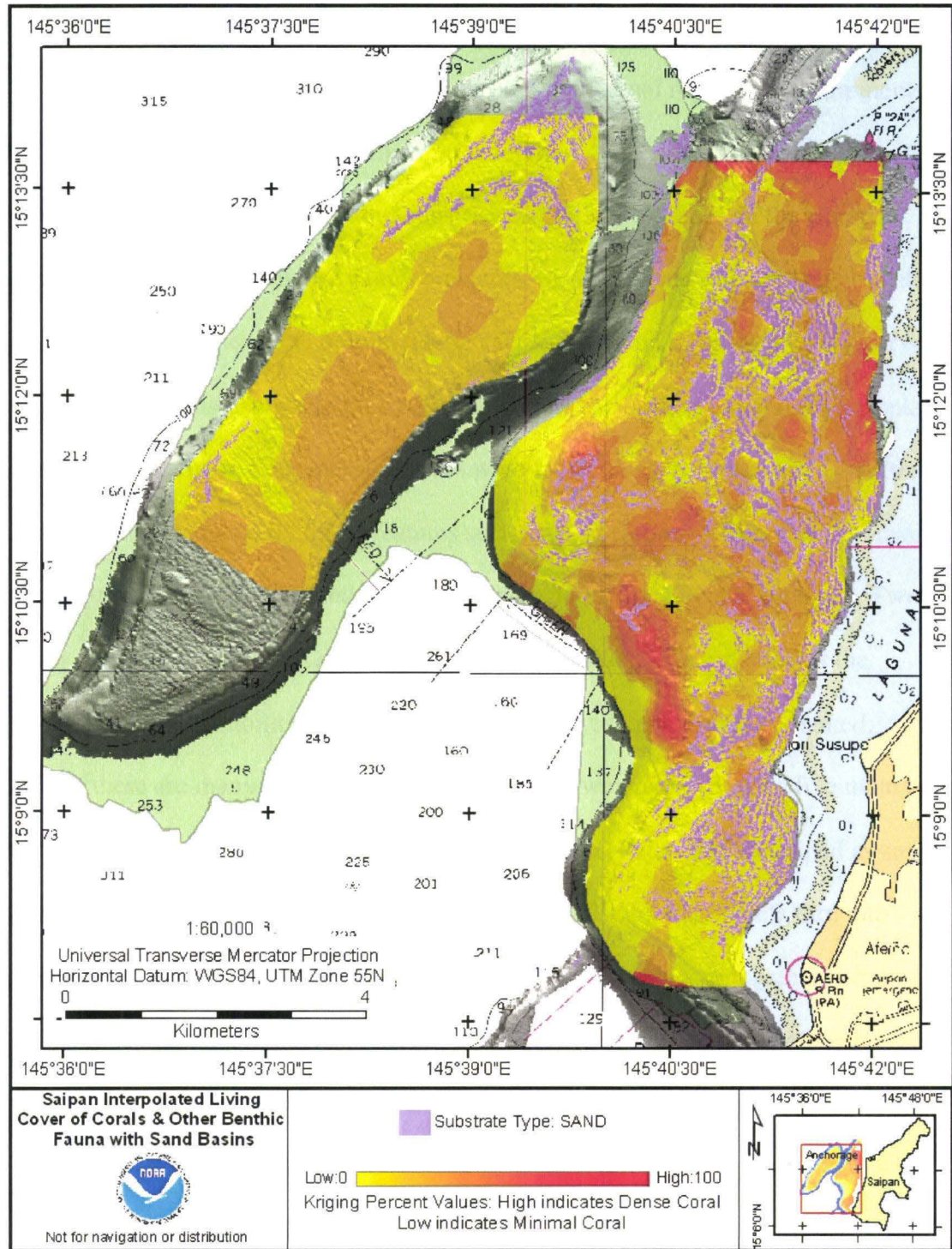
Figure 11: –Interpolated Substrate Map: This figure shows an interpolated substrate map based on data from Figure 10. The map was made using a kriging algorithm and shows sand fields and areas with high and low percentages of coral (Rooney et al., 2005).

3.3 Manual Rugosity Measurements

While in Saipan during the 2004 video survey manual rugosity measurements were collected at six locations to a maximum depth of 40 m (Figure 12). The dive sites were chosen to represent each kind of substrate identification found in the Garapan anchorage. To collect the rugosity measurements, the divers laid out a 5m chain, with 1/2inch links, along the ocean bottom taking care that the chain followed every curve of the bottom. A tape measure was then held taunt along the bottom to get the horizontal shortening of the chain. Four measurements were taken on each dive in an "L" pattern to eliminate bias introduced by linear features such as sand ripples. Video was also taken along the transect line and around the area to characterize the fauna at each site. Two rugosity measurements were taken at each dive site (Table 2). In order to get the maximum bottom variability the bathymetry data and video data were consulted. Although there are many possible bottom types, these were condensed to five main types: sand, pavement, patch reef, aggregate reef and solid reef. Patch reef is defined as small sections of reef unconnected to other patches (NOAA, 2006). Patch reefs turn into aggregate reef when the individual sections of reef start to coalesce together forming large sections of reef, and pavement is defined as low-relief sections of carbonate rock spanning large areas often covered by a thin layer of sand.
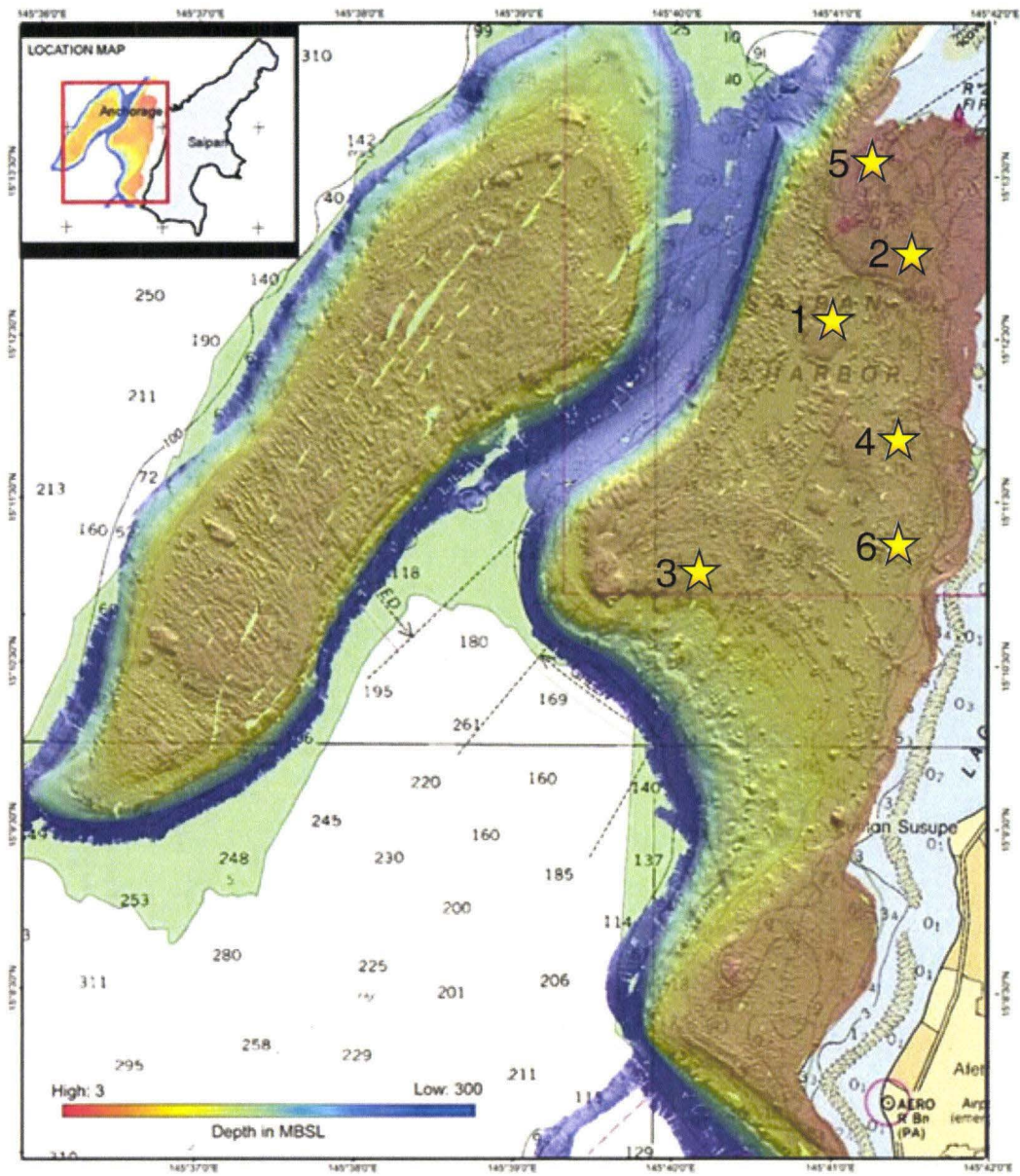
Figure 12: Dive site map. This figure shows the locations of each of the six dive sites (represented by yellow stars) where manual rugosity data were collected. The numbered correspond to the dive site numbers in Table 2.

41

Dive Site	Transect	Latitude	Longitude	Depth	Bottom Type	Rugosity %
1	1	15 12.380	145 41.006	25.15m	Pavement	89
1	2			25.45m	**Figure 13**	63
2	1	15 12.815	145 41.651	26.93m	Sand	98
2	2			26.93m	**Figure 14**	98
3	1	15 11.012	145 40.118	31.08m	Aggregate Reef	62
3	2			31.08m	**Figure 15**	56
4	1	15 11.826	145 41.595	24.38m	Patch Reef	72
4	2			24.07m	**Figure 16**	74
5	1	15 13.399	145 41.305	12.19m	Patch Reef	67
5	2			12.03m	**Figure 17**	80
6	1	15 11.181	145 41.651	24.07m	Reef	57
6	2			23.77	**Figure 18**	54

Table 2: Data from manual rugosity dives. Two transects were completed at each dive site and the coordinates, depths, classifications and percent rugosity values are listed above. The figure names listed below each benthic classification correlate to the pictures in Figures 13 through 18.
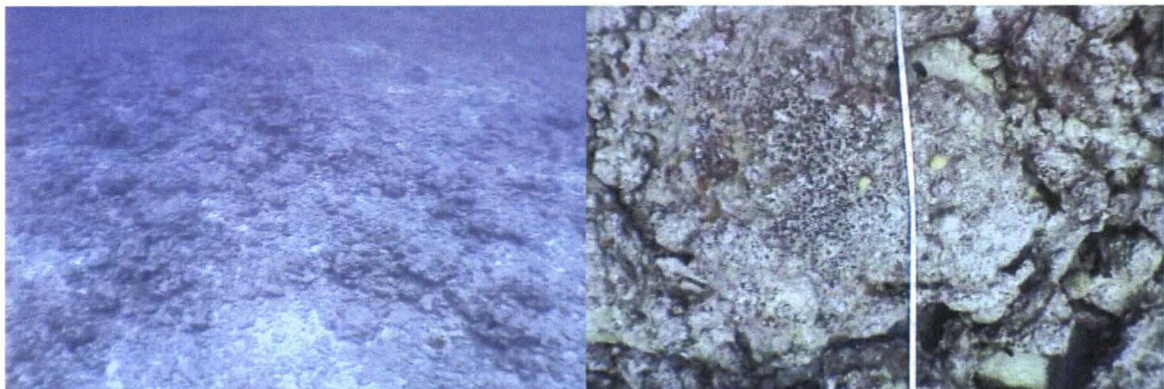
Figure 13: Pavement. This area features rubble from boulder through gravel sizes, with some sand as well. It appears only lightly colonized by hard or soft corals, macroalgae, etc.

42
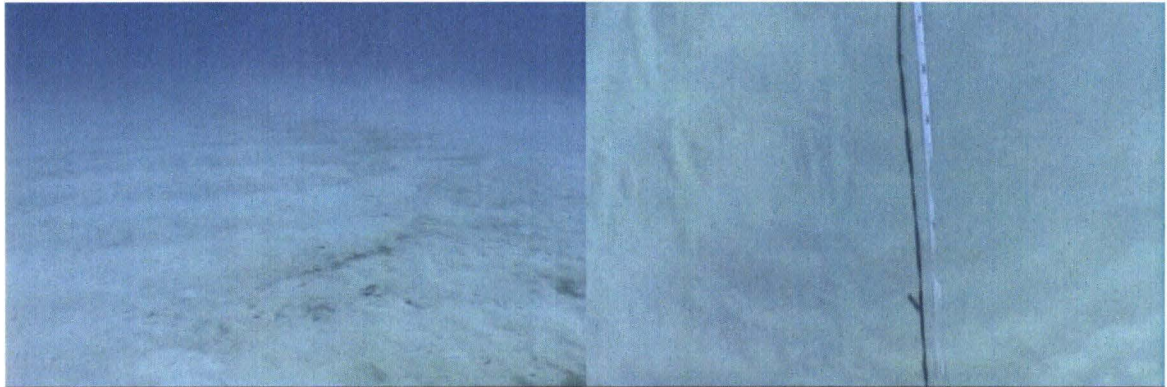
Figure 14: Sand. Area is all sand, with occasional macroalgae, mostly *Halimeda* sp. It has somewhat indistinct ripples with rounded crests ~0.5 - 0.7 m apart and amplitudes of a few cm.
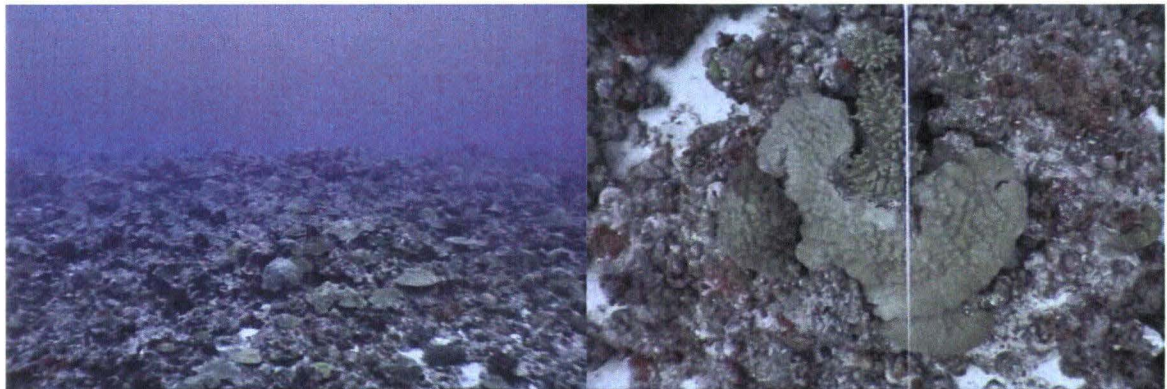
Figure 15: Aggregate Reef. This area is composed of hard substrate with occasional small sand patches and significant coral cover with numerous colonies. The coral colonies provide many holes of small to medium size. The maximum relief is less than 2 m and the average variation in relief is < 1 m.
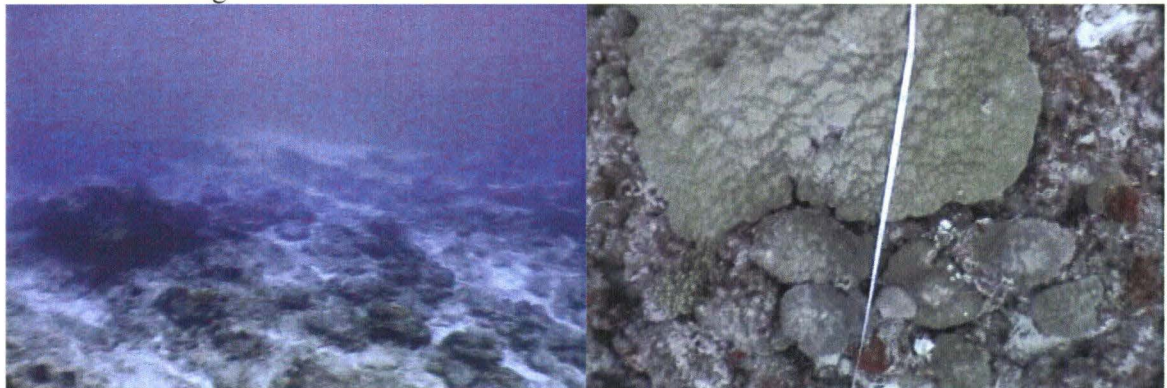
Figure 16: Patch Reef. This area is comprised of low-relief gently rounded hard substrate colonized with corals up to several meters above surrounding sand patches and channels.
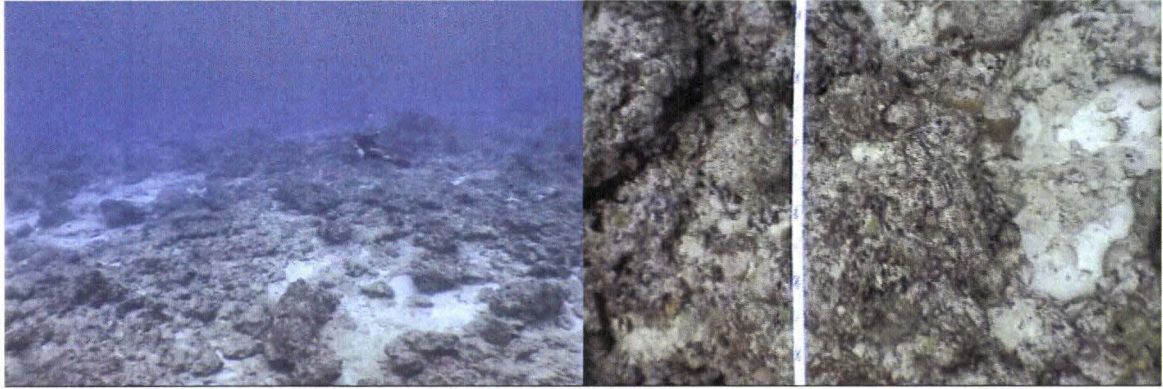
Figure 17: Patch Reef. Substrate is mostly flat and hard with variations in relief of generally 1 m or less but with a few larger boulders and outcrops. There are small channels and sand patches as well.
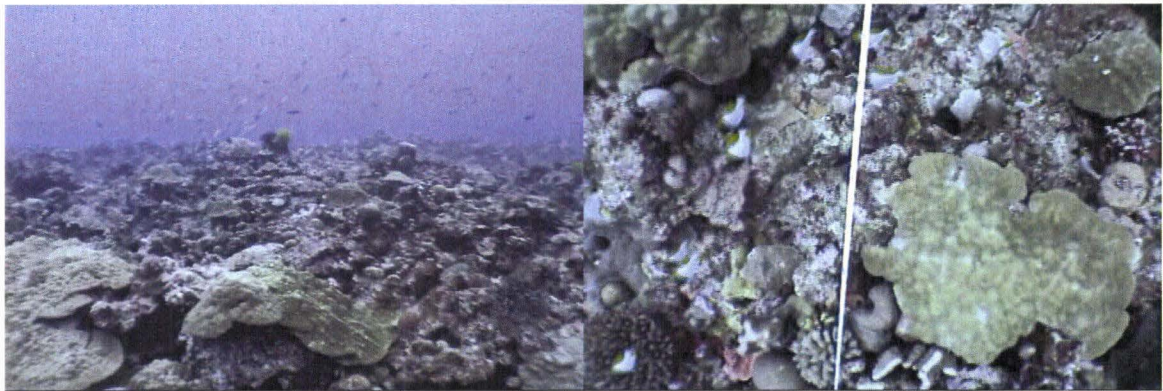
Figure 18: Reef. Mostly hard substrate heavily colonized by coral colonies often larger than 0.5 m in diameter, and a few narrow sand channels. There were a lot of fish, including many longer than ~20 cm.

CHAPTER 4: DATA AND METHODS FOR RUGOSITY ALGORITHM

4.1 Objectives

In order for a tool that measures complexity to be useful it needs to be easy to use, conceptually descriptive, and able to be used at varying scales (Hobson, 1972). My research objectives were to develop a new acoustic method to measure rugosity, analyze the manual rugosity measurements to determine the algorithm's accuracy and to deploy this method in conjunction with other types of data to characterize the seafloor of a coral reef environment as a first step in assessing the status of the benthic habitat there.

We developed an automated algorithm to determine the acoustic rugosity of seafloor surfaces from multibeam sonar data for each line of data or ping. This algorithm can be applied to any multibeam data and objectively quantifies the roughness of the seafloor over any size area where multibeam data are available. The algorithm applies the traditional rugosity equation to multibeam data, so that the results could be compared with historical manual rugosity measurements in Saipan.

This method calculates rugosity in small bins across each ping and is not gridded. This method allows for extremely detailed data sets and quick information about surveyed areas that would otherwise have taken years for divers to manually collect to the same level of resolution. The final product is an objectively derived, quantitative map that is easily comparable to the bathymetry and side-scan data and can be used to help predict population density for benthic habitat mapping.

4.2 Multibeam Overview

The bathymetry data used in this study was collected by a 240 kHz RESON SeaBat 8101 multibeam sonar which measures and records the time for the acoustic

signal (or transmit beams) to travel from the transmit array to the seafloor and back to the receive array. The RESON 8101 can produce 4,000 soundings per second allowing for an extremely dense data set with a vertical resolution of 1.25 cm and a range capability of 300 m. Each $150°$ ping consists of 102 beams that are spaced 1.5 degrees apart (Figure 19) (RESON, 2005).
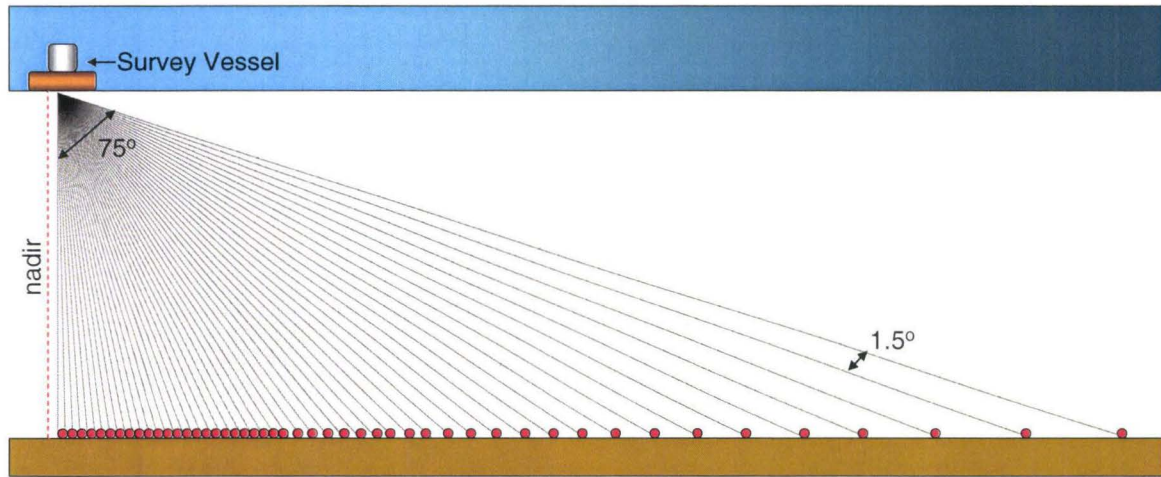
Figure 19: Half of a ping swath showing beam angle. This figure shows a survey vessel as it ensonifies the seafloor. This figure only shows half of the transmit beam or $75°$. Each beam transmits $1.5°$ from the next. Nadir is the center of the ping under the ship. The red dots show the spacing of the soundings when they come in contact with a flat surface.

Because the beams are $1.5°$ apart, beam spacing increases with range on a horizontal surface (Figure 19). Because the size of an object that can be resolved is dependent upon the spacing of soundings smaller features are not able to be resolved at far range. Sounding spacing also increases with altitude. For example, at 20 m altitude the spacing between soundings is 0.52 m at nadir and 7.12 m at the outer edge of the swath. At 100 m depth the spacing between soundings is 2.62 m at nadir and 35.6 m at far range (Figure 20). This continues on with depth until the maximum depth capability of the sonar is reached, at 300 m. This means that if the spatial scale of an object of

46

interest, such as a coral head, is less than 1 m, then the resolution of our sonar system

would only be appropriate to a depth of 30 m and only the information near nadir would

be useful. For sounding spacing computed for across a horizontal seafloor, as a function

of depth over the operational range of the RESON 8101 multibeam sonar, see Appendix

A.

Sounding Spacing at Varying Depth

Distance from Nadir (m)
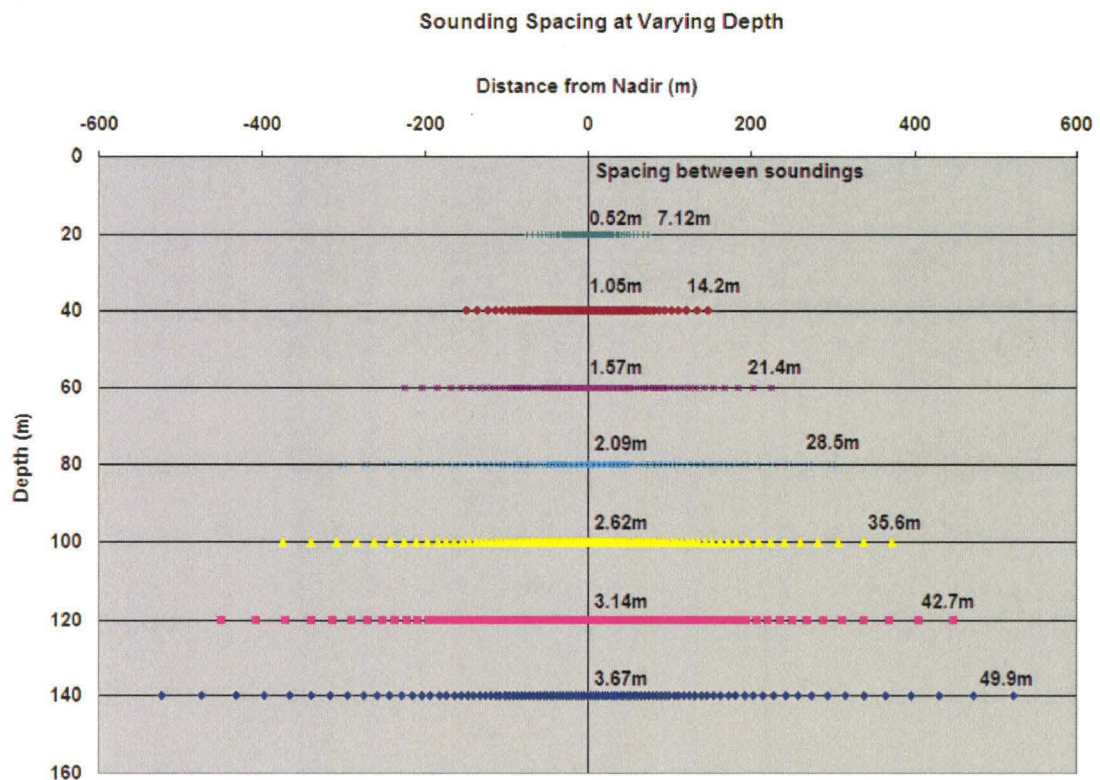
Figure 20: Sounding spacing at varying depths. This figure shows that as depth and distance from nadir increases the spacing between soundings (each symbol on the chart) increases. At 300 m depth, the maximum range of the RESON 8101 sonar, the sounding spacing at nadir is 7.87m and 107m at the edge of the ping. Calculations are shown in Appendix A.

A third was that the sounding spacing changes is with variations in seafloor

morphology. When the transmit beams interact with a flat seafloor the beams will reflect

off the surface and information across the entire ping will be collected by the receive

array. However, if there are features on the seafloor such as holes or mounds, portions of

the features may not be fully resolved because they are in an acoustic "shadow". In

Figure 21 the beams are splaying out at an angle towards the east. The west facing slopes

of objects will be resolved but no information is gathered on the east facing side. The east

facing slopes are said to be in "shadow", or in an area from which no information returns.
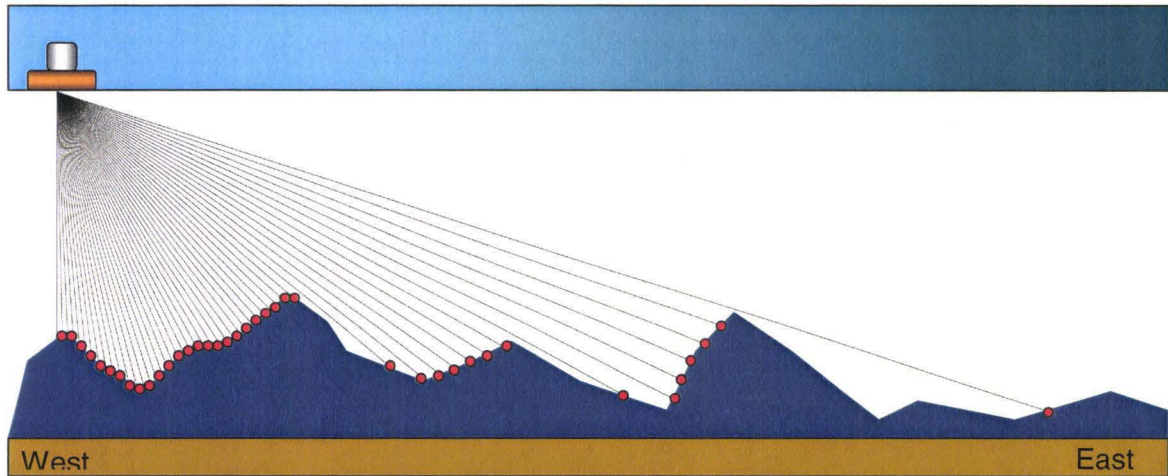
Figure 21: Sounding Coverage on an Uneven Surface. This figure shows half of a transmit array interacting with an uneven seafloor surface. The red dots show where the transmit beams come into contact with the seafloor. Because most of the beams are transmitted at an angle, areas with high relief will block the transmit beams from collecting information on the far side of the object. This is called a data "shadow".

4.3 How the Algorithm Works

We developed an algorithm that takes multibeam data and produces a rugosity

map that can be used for benthic habitat mapping or MPA delineation. This algorithm is

presented in its entirety with explanations in Appendix B.

4.3.1 Algorithm

In general, the rugosity algorithm works by reading a multibeam file and

processing groups of adjacent soundings to produce rugosity values for each group. Each

sounding within a ping has information attached to it including its ping number, x

(distance from nadir), z (depth), and its latitude and longitude coordinates. The x

positions increase positively on the port side and negatively on the starboard side as they

move out from nadir (0). Using the x information the algorithm moves across the ping in

increments controlled by the bin width. If the bin width is set at 10m and the x value is -

79.6 m the algorithm will move across the ping until it reaches an x value less than -69.6

m. All the soundings that fall between -79.6 m and -69.6 m will be placed in a bin file. To

describe a surface there needs to be at least three points. The more data points there are

across a surface, the more accurately that surface will be described. The algorithm allows

a minimum sounding requirement value to be set before processing which allows the user

to specify how many soundings they want in a bin. As each bin file is created the

algorithm checks to see how many soundings are in it and if the minimum sounding

requirement is not met the algorithm does not calculate seafloor rugosity within that bin

(Figure 22).
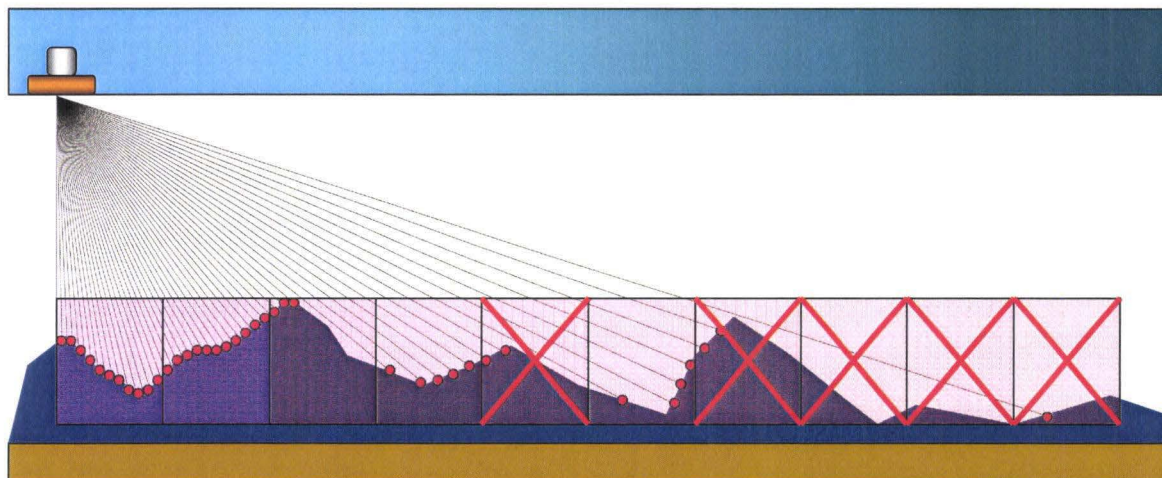
Figure 22: Sounding spacing on an uneven bottom binned. The first step of the automated rugosity algorithm is to bin the data represented by the purple boxes. The bins with less than the minimum sounding requirement (in this example < 4) soundings (red dots) are not used. If there are 5 or more soundings then the data are used to calculate the rugosity value for that bin.

If the number of points per bin exceeds the minimum sounding requirement the data in the bin are used to calculate a rugosity value for that bin. This is done by first determining the data to remove regional slope. Because my study is interested in coral reef environments, which are on the sale of a few meters, small scale rugosity is necessary to give detailed descriptions of these areas. However, in order to get to the small scale rugosity data, the regional slope needs to be removed. To do this, we used the GMT trend1d program to fit a regression model $y = f(x) + e$ by least squares to soundings within the bin (Wessel, 2006). It produces a best fit line and calculates the residual distances between each of the soundings from the trend line. The contoured distance is found by summing up the point to point distances between the soundings that were calculated using the Pythagorean Theorem (Figure 23). Then the x values are taken from the first and last soundings in a bin and subtracted from each other to get the linear distance. These values are then substituted into the manual rugosity equation (Figure 23).
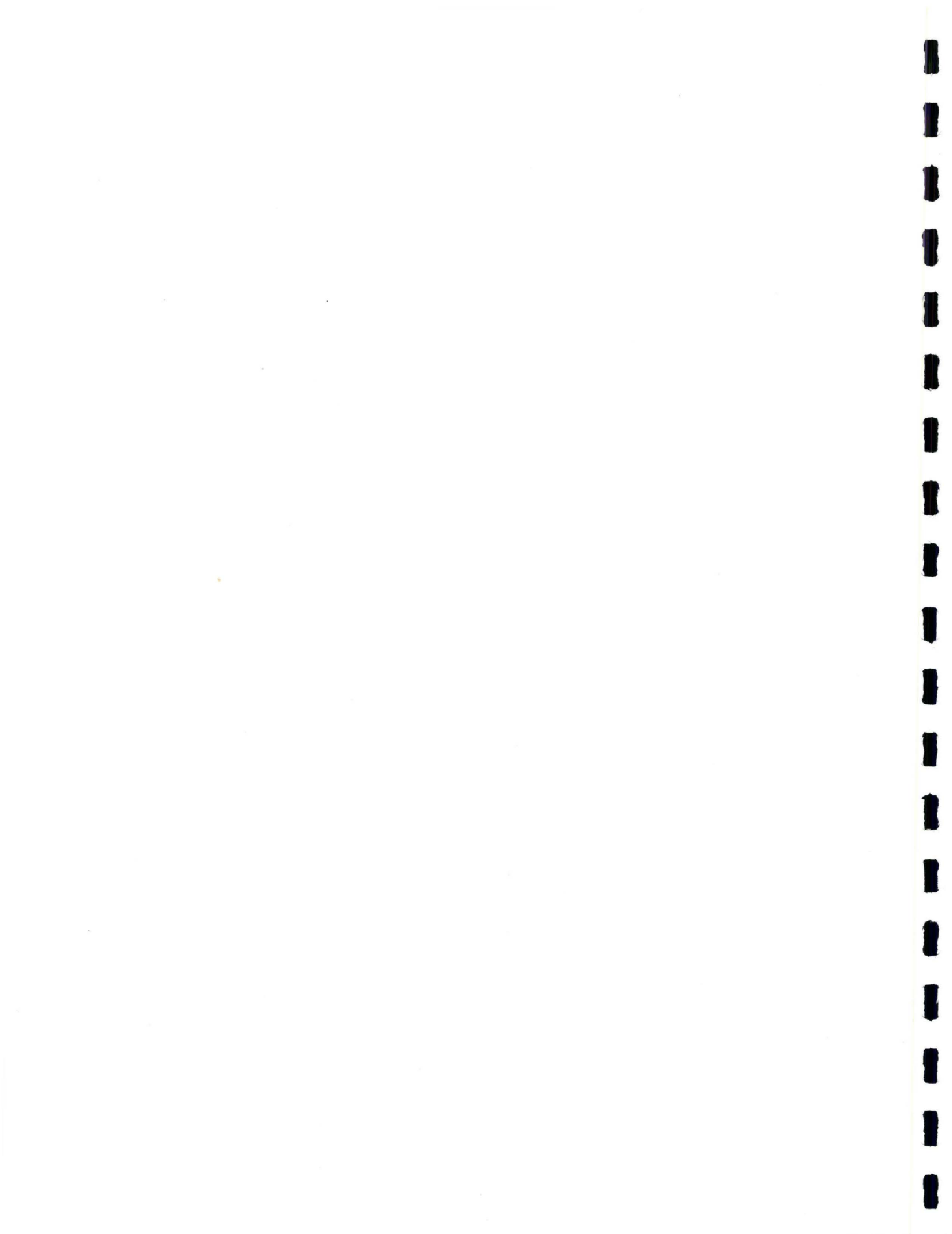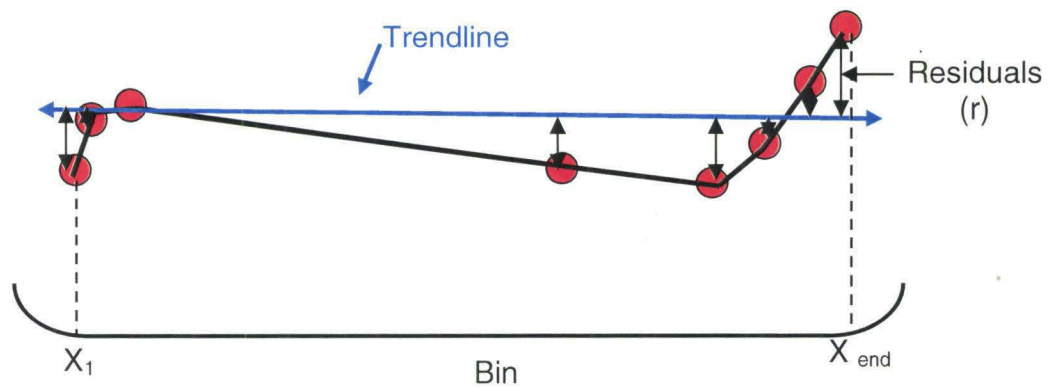
$$\frac{\text{Linear Distance (Across Track)} = |X_1 - X_{end}|}{\text{Contoured Distance} = \text{Summed distance between xr pairs}} = \text{Rugosity (R)}$$

Figure 23: Rugosity equation. This figure is an example of binned data. The soundings are represented by the red dots and the black arrows show the residual distances (r) to the trend line in blue. The solid black line represents the contoured distance which is the summed distance between each of the soundings as calculated using the Pythagorean Theorem.

Rugosity values can range between 0 and 100 percent. The closer the values are to 100 the smother the surface is, with 100 being a perfectly flat bottom. A perfectly vertical surface would yield rugosity values of 0. Intermediate values do not represent unique seafloor morphologies as many different seafloor surfaces can yield the same rugosity values (Figure 24).

The output of the algorithm is a file that contains the latitude, longitude and rugosity values for each completed bin. The completed files are then used to create a rugosity map of the survey area.

| R = 100.000 | R =71.111 | R = 71.111 | R =71.111 | R = 41.667 |
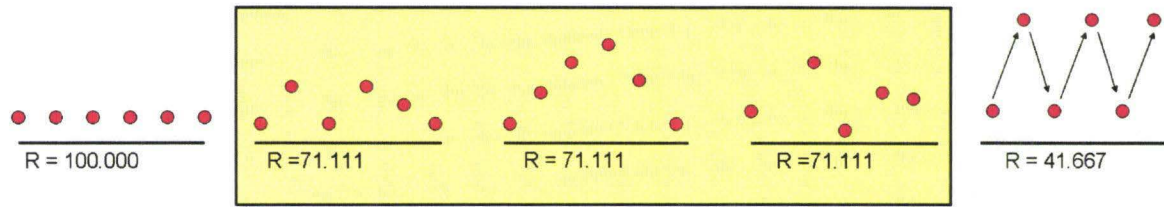
Figure 24: Various arrangements of soundings. This figure shows that the same rugosity values can be produced from multiple seafloor morphologies. This means that intermediate rugosity values are not representative of unique morphologies. A rugosity value of 100% would mean that the surface was perfectly horizontal where a perfectly vertical surface would receive a rugosity value of 0%.

4.3.2 Pre-sets

We set up and tested our rugosity algorithm on a simple model and found that the characteristics of multibeam soundings require that special modifications be made to the algorithm before accurate rugosity data can be calculated. Some of these modifications include cleaning erroneous data and setting up minimum data requirements.

4.3.2.1 Error Factor and Search Radius

The multibeam bathymetry data input into the rugosity algorithm need to be cleaned and free of outliers. However, even after cleaning, some false soundings may still exist in the data making the bottom appear rougher than it actually is (Figure 25). We identify and ignore these outliers by defining an error factor, which is the maximum allowable distance between adjacent soundings that is too large exist in cleaned data. If the algorithm encounters a distance greater than the set "error" that erroneous point is excluded and the program moves on to the next sounding. However, sometimes there are groupings of erroneous data. If the bin width is set at 10 m, the error factor is set at 10 m and the water depth is 100 m the sounding spacing will be 35.6 m at the edges. This means that if we start on the left side of a ping and move across to the second sounding

52

that point will be further away than 10 m and would appear erroneous to the algorithm causing the sounding to be skipped over. Because the sounding spacing increases from nadir, the algorithm will only find seemingly erroneous points till it reaches the end of the ping causing useable information to be skipped over. To prevent this, the search radius is used to tell the algorithm how many "tries" it may go through before moving on to the next sounding and starting over.
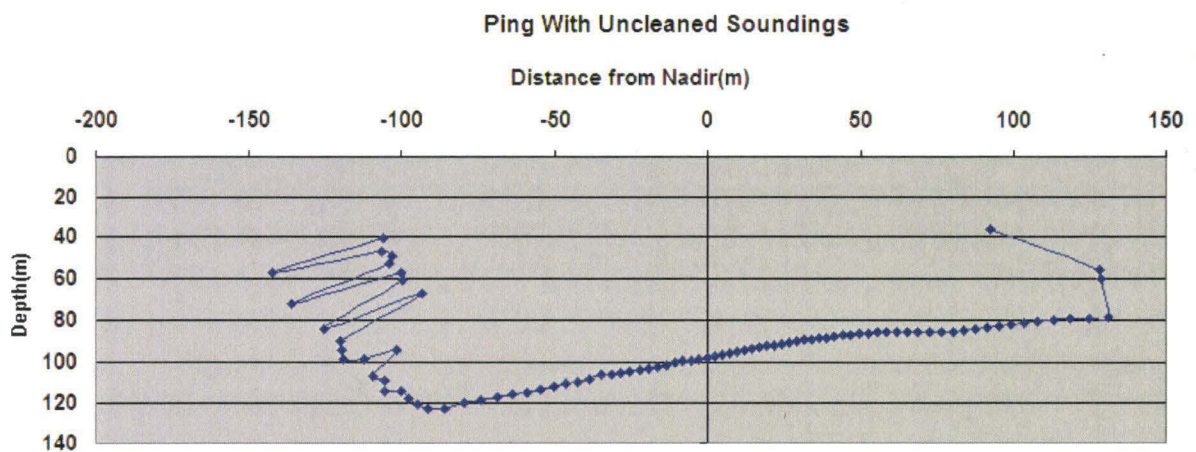
Figure 25: Ping with uncleaned soundings. This figure shows a real data ping with noise located at the left and right edges. The algorithm will start with the sounding on the left side and calculate the distance to the next sounding. If that distance exceeds the error factor, which in this case it does, the algorithm will skip that sounding and move on to the next sounding.

4.3.2.2 Minimum Sounding Requirement

The minimum sounding requirement was put in place to disqualify bins that had too few soundings to adequately describe the roughness of the seafloor. The more soundings in a bin the better the seafloor roughness will be represented. However, if the requirement is set at a value greater than the number of soundings found in most bins than those bins will no longer meet the minimum sounding requirement and the data will be skipped. That means that the information present in those bins will be lost and not

represented on the rugosity map. The depth to which you want to collect rugosity information also needs to be taken into account when choosing a minimum sounding requirement. This is because the deeper the depth the greater the spacing is between soundings. If the minimum sounding requirement was set at 3 soundings per 10m bin, rugosity information could only be gathered to 190 m depth before 100 percent of the bins fail the minimum sounding requirement and were skipped (Figure 26). A higher minimum requirement of 9 would only allow information to be collected to 70m depth before 100 percent of bins failed to meet the minimum requirement. Therefore an intermediate value of soundings between 3 and the maximum number of soundings found in a bin is required to maximize the seafloor description and the depth to which rugosity information can be obtained.
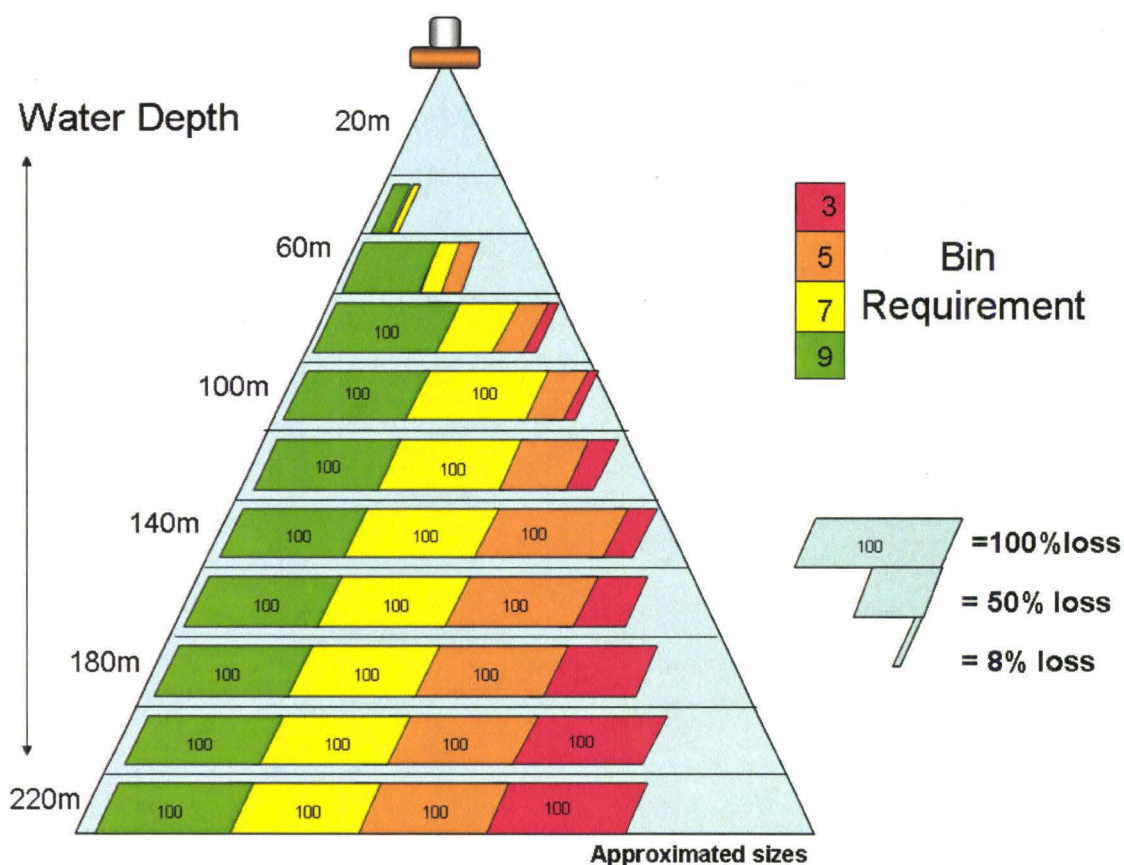
Figure 26: Information Loss at Varying Depths (0-220m) binned at 10m. As depth increases the sounding spread further apart and there are fewer soundings per bin. The minimum sounding requirement isn't met and the bins are eliminated causing 100% of the ping to be unused.

4.3.3 Choosing Bin Size

Bin size is controlled by the resolution of the sonar, the depth of the survey and the minimum sounding requirement. High resolution sonar allow for smaller bin sizes since the soundings are spaced more closely. The higher the sonar resolution the smaller the bin sizes can be and still maintain the minimum sounding requirement. Bin size is also determined by the amount of coverage needed for the area of interest. The larger the bin size is the more bins pass the sounding requirement and more data are used at the

edge of a swath. The smaller the bin size the closer the individual rugosity points will be but fewer bins will pass the sounding requirement on the outside edge of a swath. Out of the three examples presented in Figure 27 the data binned at 10 m provides the most detailed rugosity information around nadir but provides the least amount of coverage. Binning at 20 m provides the widest scan of rugosity values but has the least detailed and lowest resolution rugosity data set. So based on the sonar resolution, sounding requirement and seafloor coverage I choose to map out the rest of the data using a 15m bin size which provides intermediate coverage and resolution (Figure 27).
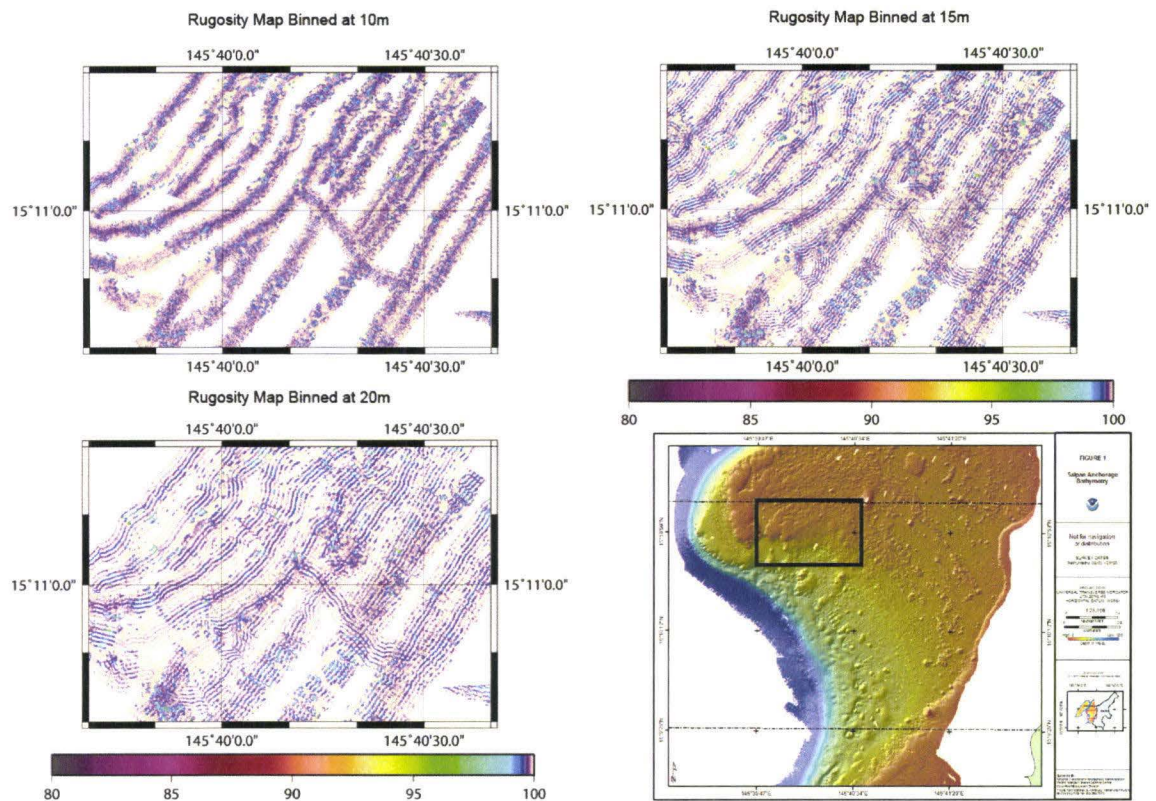
Figure 27: Rugosity maps. These maps are binned at 10, 15, and 20 m with a minimum sounding requirement of 5. The location of these rugosity maps is shown within the black rectangle on the bathymetry map. As the bin size increases the resolution of the rugosity

56

data decreases but the number of bins that pass the minimum sounding requirement increases. Therefore, wider coverage is obtained.

4.3.4 Slope Removal and Contoured Chain Length Calculation

Because we did not use an actual chain to measure rugosity, the actual length of the chain isn't known. The bin size was originally substituted in for the linear chain length and, using the Pythagorean Theorem, the sum of the distances between each sounding in a bin was used as the contoured chain length. However, when there are bathymetric areas of large scale slope the algorithm output is overwhelmed by the large scale features and the small scale rugosity features are overlooked (Figure 28). Therefore to be able to see the small scale rugosity features we removed the slope within each bin.
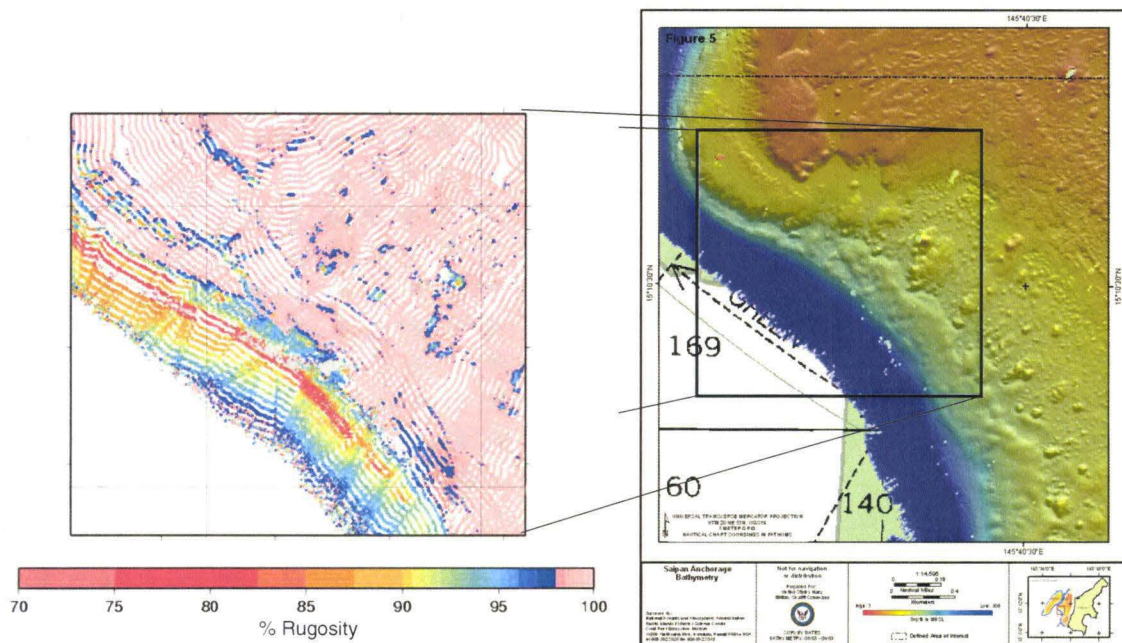
Figure 28: Rugosity map 1 (Binned at 15m). This figure shows the output of the algorithm before slope was removed and a minimum sounding requirement was put in place. The information shown in this rugosity map is dominated by large-scale topographic slope, indicated by the rapid color changes. This means that the rugosity scale is dominated by large features which overpower the small scale rugosity features.

The chain length used in the numerator of the rugosity formula was initially defined as the horizontal width of the bin. However, the position of the first and last soundings may not correspond exactly to the beginning and end of a bin. Therefore, it was found that using bin size as the linear distance introduces a smoothing error because the "length of the chain" appears longer than it actually is. So to correct this problem the rugosity algorithm subtracts the x position of the last sounding in a bin from the first sounding in a bin to get the linear distance. The total distance between each of the soundings in a bin is the contoured chain length.

4.3.5 Striping Effect

When using soundings to describe a surface, the sounding density of the multibeam sonar effects how accurately the bottom surface is described. Fewer soundings result in a too-smooth surface. Because soundings within a ping are more closely spaced at nadir (Figure 19) more bins will have enough points to exceed the minimum sounding requirement and therefore be assigned rugosity values. Also bins near nadir contain more soundings and thus may appear rougher than bins further from nadir (Figure 29 and 30).
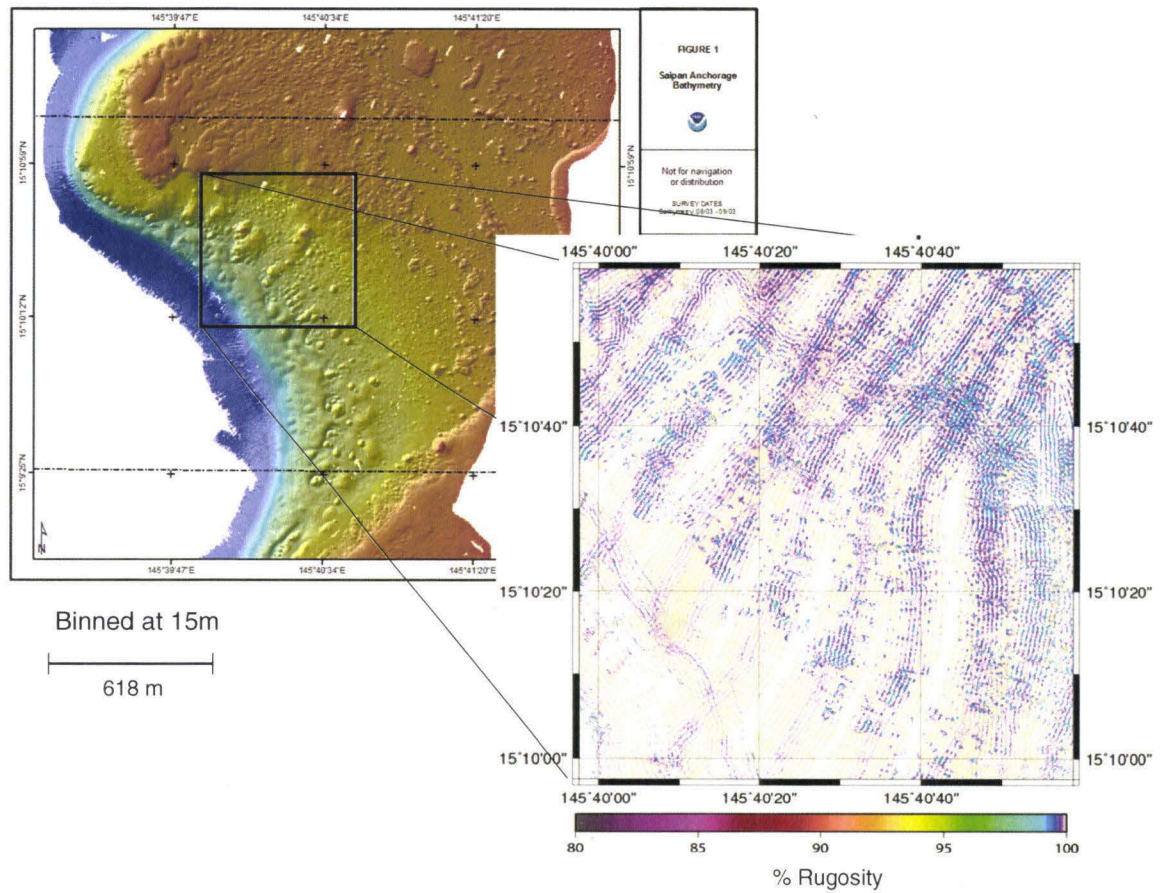
Figure 29: Rugosity map 2. The location of the rugosity map is shown in the black square on the bathymetry map. The rugosity map is binned at 15 m and shows the striping effect caused by uneven sounding spacing. Since there are more soundings at nadir that area will appear rougher that the surrounding edges. In this case the blue color represents the rough areas with the light pink representing a more flat morphology.
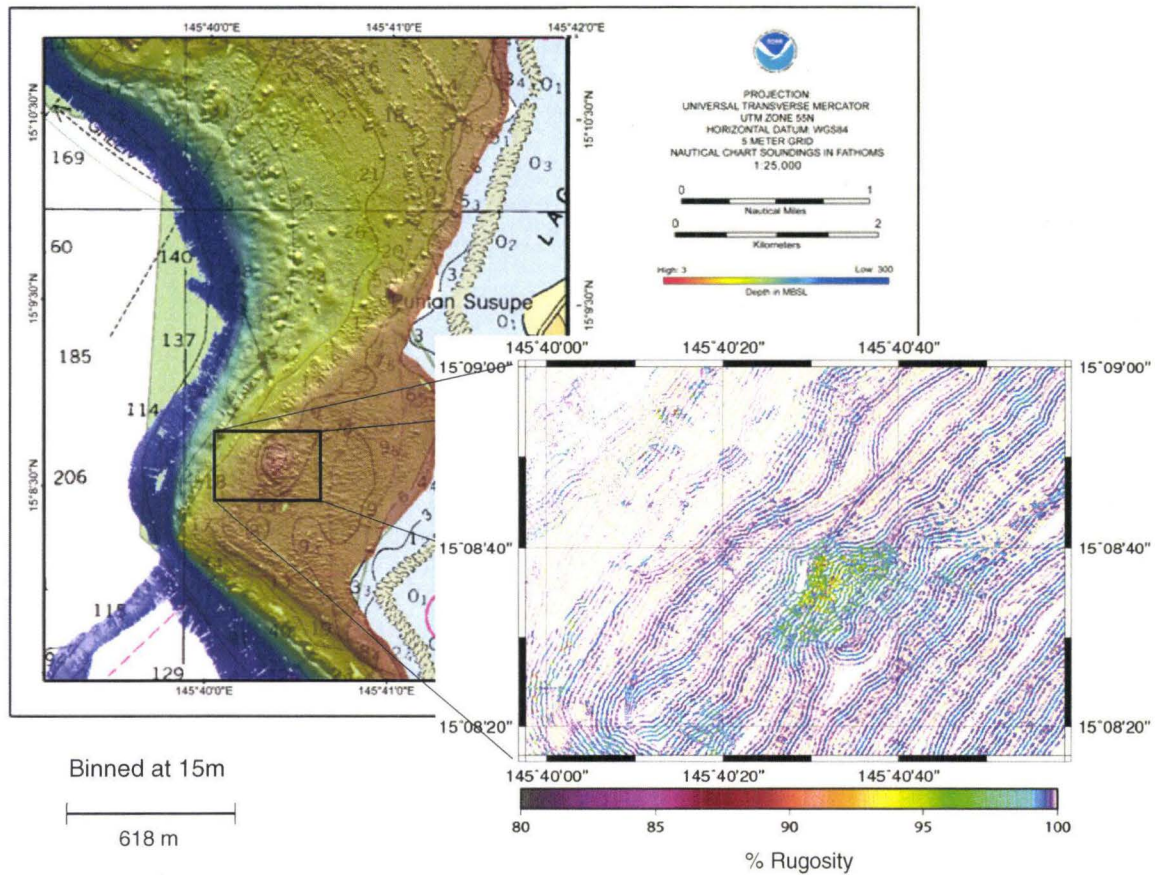
Figure 30: Rugosity Map 3. The location of the rugosity map is shown in the black rectangle on the bathymetry map. The rugosity map is binned at 15 m and shows the striping effect caused by uneven sounding spacing over top of a hill or mound shown in light blue, green and yellow. The stripe pattern is more obvious on this map than Figure 29 but it appears to lessen over top of the mound and in the upper left corner where there is a flat morphology.

We assume that the more soundings there are to describe a surface, the more accurate that description becomes. Because the bins near nadir have the greatest number of soundings, the bins are more likely to return more accurate rugosity values. Therefore, by increasing the minimum sounding requirement the rugosity algorithm will only use the bins with there highest number of soundings and will eliminate the outer bins with too few soundings.

4.4 Understanding the Rugosity Output

4.4.1 Testing

In order to understand the capabilities of the rugosity algorithm, and to determine what rugosity values different seafloor surfaces would elicit, we tested the algorithm on a modeled seafloor. Various seafloor shapes were developed and then the shape of a ping, with the beams spaced 1.5 degrees apart (Figure 31), was overlain to determine where the beams would intersect the surface of the modeled seafloor. Figure 32 shows an example of what the seafloor morphology looked like for the first model and where the beams interacted with it. Where the beams intersected the shape's surface the x and z values were recorded and plotted (Figure 32 and 34). Each modeled data set was run through the rugosity algorithm and the resulting rugosity values were plotted on top of the data from Figures 32 and 34 (Figure 33 and 35).
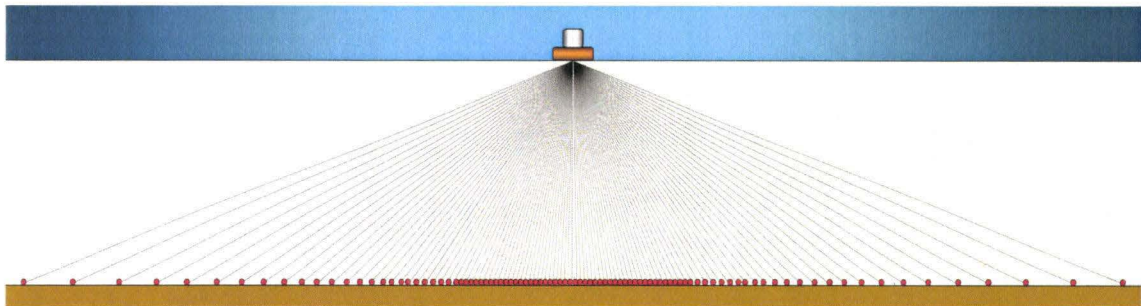
Figure 31: Full ping showing sounding spacing. This figure shows the sounding spacing along a flat surface across an entire ping.

10m/20m Blocks at 40m

Distance from Nadir(m)
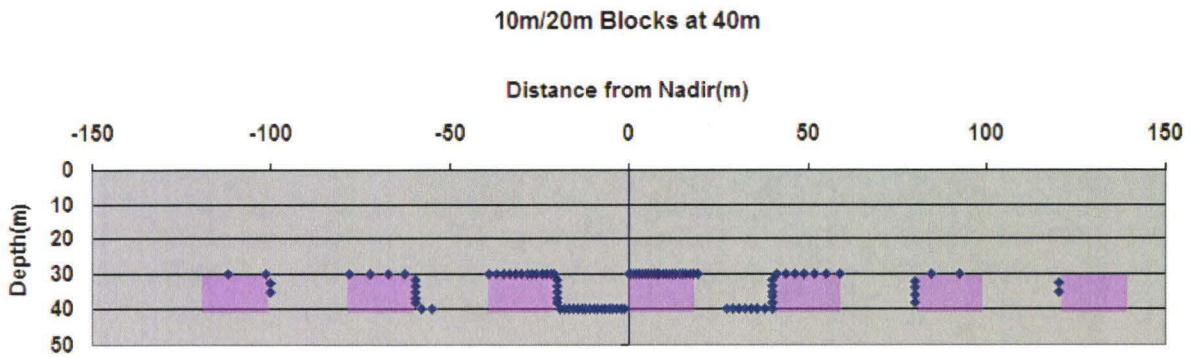
Figure 32: Shape of 10 m/20 m rectangles. The original surface, represented in pink rectangles, is on a flat surface at 40 m. The soundings (blue diamonds) show where they would intersect the seafloor after being ensonified by Reson 8101 multibeam sonar.
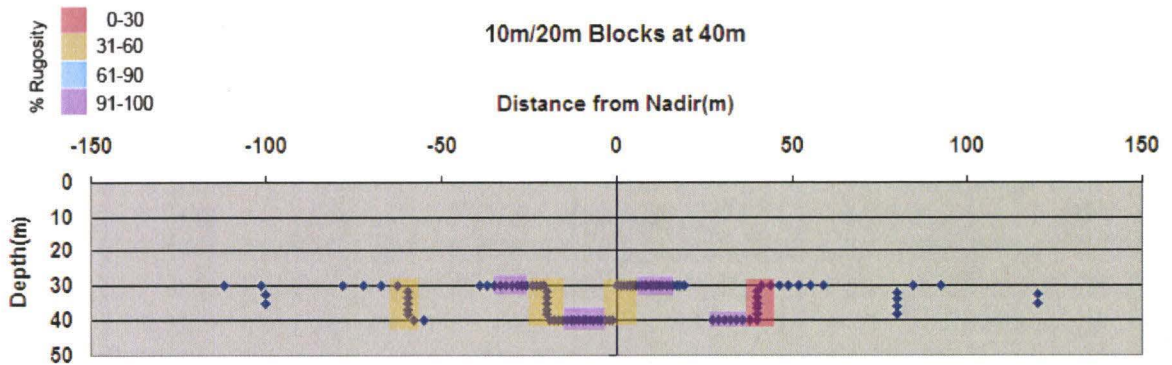
Figure 33: 10 m/20 m rectangles with rugosity values. This figure shows the sounding locations and the corresponding rugosity values as they would appear after being run through the rugosity algorithm. Rectangles represent 10 m binned data. Purple represents rugosity values correlating to a relatively smooth or flat surface. Red and Orange rectangles show areas that are nearly vertical and therefore correlating to low rugosity percents.

Curved Seafloor from 30m to 60m
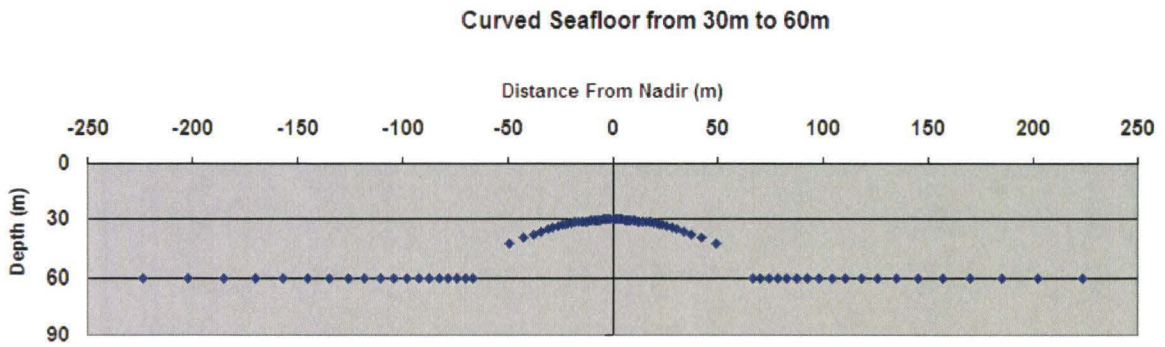
Figure 34: Plot of curved seafloor. This figure shows a curved seafloor (such as a hill) on a flat surface as it would appear after being ensonified by RESON 8101 multibeam sonar.

Curved Seafloor from 30m to 60m
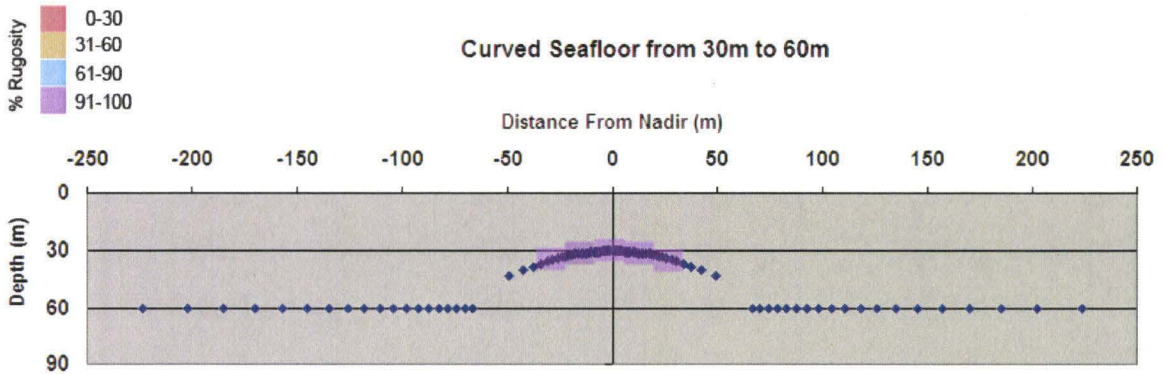
Figure 35: Curved seafloor with rugosity values as it would appear after being run through the rugosity algorithm. Rectangles represent 10 m binned data. Purple represents rugosity values correlating to a relatively smooth or flat surface. The rest of the ping did not have bins that passed the minimum sounding requirement due to the increased sounding spacing at depth.

The areas across the ping that were horizontal or that had a gradual slope returned rugosity values between 91 and 100 percent, and the areas across the ping that were nearly vertical returned values between 0 and 60 percent. The perfectly horizontal areas yielded rugosity values that were exactly 100 percent. The calculated rugosity values

63

were the same as the expected values for each bottom shape which showed that the rugosity algorithm worked as expected.

After testing the algorithm on different modeled surfaces we found that there are a few areas the algorithm could be improved. The main shortcoming of the algorithm is how it moves across a ping. The algorithm is designed to bin the data in even increments and discard bins that don't meet the minimum sounding requirement. However this often causes soundings to be discarded that could have yielded rugosity data had they been put in to their own bin. This can be seen in Figure 33where there are gaps in rugosity data because the bin encompassed soundings from both depths of 40 and 30 m. Had the algorithm been designed to slide across the ping one sounding at a time, until the minimum sounding requirement within a bin was fulfilled, then there may have been rugosity data across all the gapped sections. Therefore, in order to make the rugosity map representative of the densest rugosity data set possible, the algorithm should be reworked to bin on a sliding basis. This way the algorithm will try the most possible combinations of soundings, to fulfill the minimum sounding requirement, before discarding the data.

CHAPTER 5: RESULTS

5.1 Interpretation

The automated rugosity algorithm was applied to the Saipan multibeam data set and the data were processed to develop rugosity maps. Because the Garapan anchorage is a large area and the rugosity maps have such high resolution it is more useful to view individual sections of rugosity data to see the most fine scale rugosity information. Based on the seafloor model we showed that areas with perfectly flat morphologies returned automated rugosity values of 100% and vertical areas had rugosity values near 0%. Therefore, when looking at the rugosity data, perfectly flat areas and vertical areas are recognizable. However, since we determined that intermediate rugosity values are not representative of unique morphologies the intermediate rugosity data can only be used to compare different sections of the seafloor to determine the locations with the greatest rugosity which can be used to predict fish assemblages and species richness (Friedlander and Parish, 1998).

Figure 36 shows two locations where the rugosity algorithm has been applied to calculate the rugosity of the seafloor. The area 3 map shows that rugosity data can show the locations of rough features on the seafloor. Without ground truth data it is unknown whether these features correspond to coral reef colonies or rough bedrock. However, the light pink areas snaking around the rough blue sections can be interpreted as perfectly flat surfaces which are most likely sand channels in Saipan.

The area 3 map in Figure 36 shows that the seafloor in this location is consistently rough and doesn't have easily distinguishable rough features. Although we cannot infer

65

whether the seafloor surface is covered in coral or is simply rock, we can say that the

morphology is not perfectly flat and is therefore not a sand field.
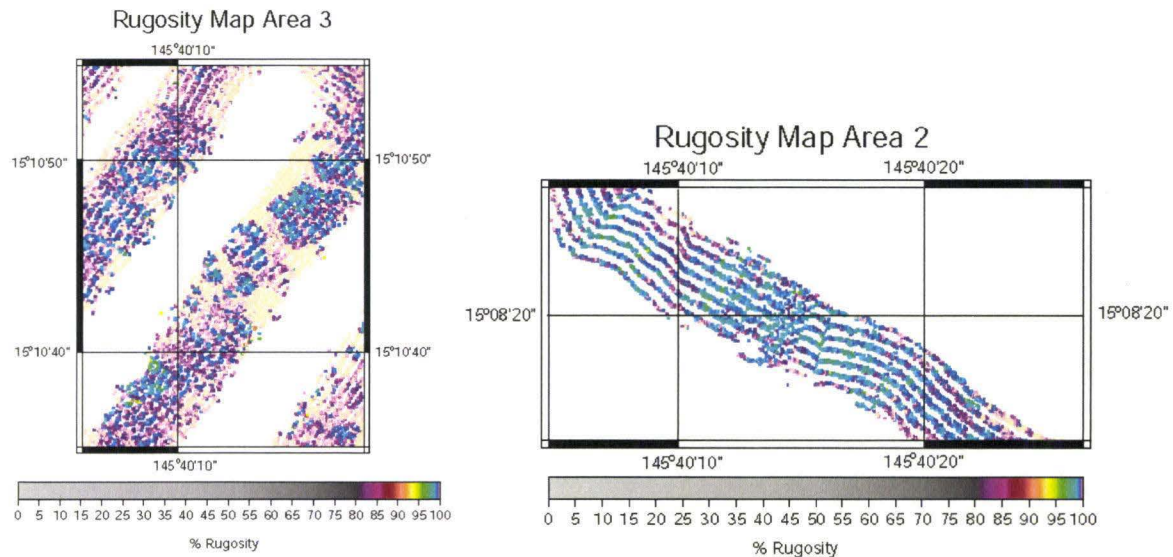
Figure 36: Rugosity of Area 2 and 3. This figure shows to sections of rugosity data from two separate areas within the Garapan Anchorage. Area 3 has distinguishable low rugosity (rougher) patches in aqua blue and green surrounded by channels of flat seafloor with rugosity values of 100% The light pink most likely represents sand fields since they have a flat morphology. The Area 2 rugosity map doesn't have distinguishable features within the swath but it is consistently showing a seafloor that is approximately 97% rugose which means the area is not a sand field.

Because we do not have ground truth data for 99.9% of the multibeam data set it

is necessary to see if there is correlation with other data sets. The sections of side-scan

data, multibeam data, and video classification data that correspond with areas 2 and 3

(Figure 36) are shown in the following figures. By comparing the rugosity data with

multibeam data, side-scan data, and the percentage of sand classifications from the towed

video data we can determine if there is a correlation with the seafloor morphology

(Figure 37). Comparing the rugosity data with the percentage of coral data would help

identify if there is a correlation between rugosity and benthic cover (Figure 38). Looking

66

at Figure 37, the low rugosity features on the rugosity map correlate with textural features expressed in the backscatter data. The similarity in shape between the rugosity and textural features is best seen along the data track that travels from the lower left corner to the upper right corner. The feature that shows up in all three maps is the mound in the SW corner or each map. Although the bathymetry data shows that this feature raises up off the sea floor over 25 m the rugosity data show that the fine scale roughness in this area is similar to other features along the track line. This demonstrates that the rugosity data are not overwhelmed by regional slope and the data are comparable across low and high relief seafloor surfaces. The sections of the rugosity map where areas of roughness do not correlate with textural features in the bathymetry or side-scan data show that the rugosity data are independent of large scale bathymetric features.
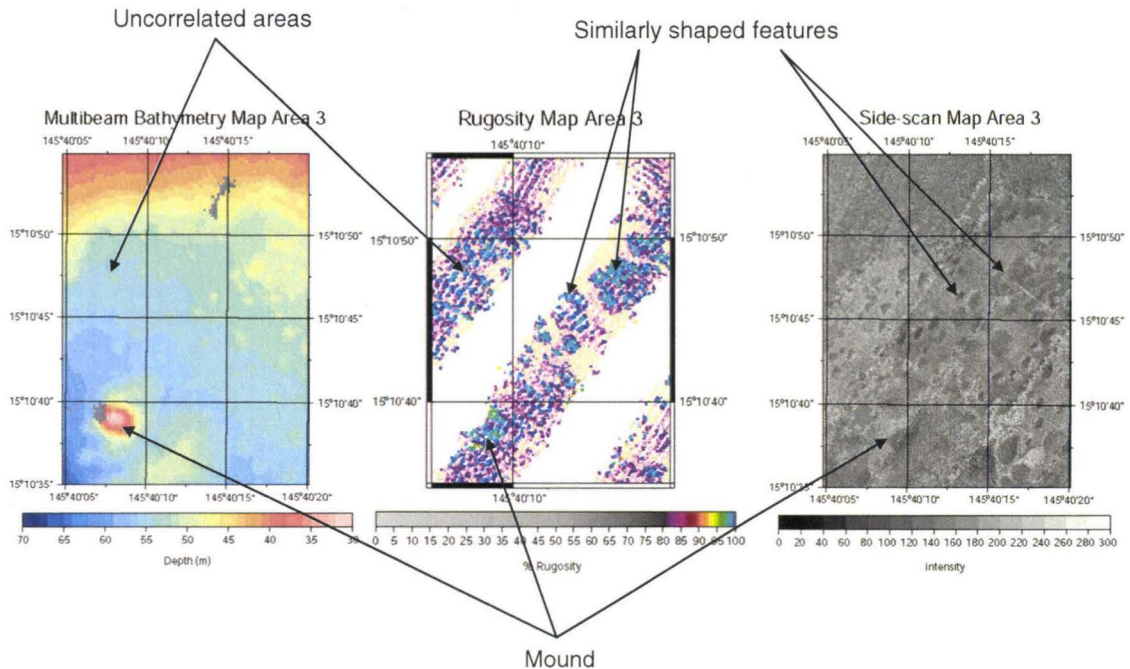
Figure 37: Area 3 comparison 1. This figure shows sections of multibeam bathymetry data and side-scan sonar data for comparison with the automated rugosity data from the same area. The bathymetry data are gridded at 5m, the side-scan data are gridded at 1 m and the rugosity data are binned at 15 m. The gray patches in the bathymetry map are areas where data were not collected. The black arrows point out areas of the rugosity map that correlate with the bathymetry and side-scan and have similar shapes. There is also an area pointed out where the bathymetry data doesn't correlate with the rugosity map.

When the rugosity data are compared with the towed video classification data there is not a strong correlation. This is because video classifications are only made every 20 m and there are not enough tow lines to give complete coverage over the seafloor. Therefore, sections of towed video data that intersect the rugosity data are limited. Another problem with comparing the data set is that the navigational uncertainty for the towed data is ±15 m and the bathymetry data that the rugosity data are based on has ±5 m of navigational uncertainty. Despite all that, there is a slight correlation between the rugosity data and the percent sand plot (Figure 38). The lowest and highest rugosity values intersect with the lowest and highest sand percent which is what we expected.

68

Also, the location shown in Figure 38 that was classified to have no coral corresponds

with a section of seafloor that has 100% rugosity. Because a rugosity value of 100%

indicates flat seafloor morphology we assume those areas to be sand fields. In this case

the video classification data confirms that the area with no coral is 100 % sand.
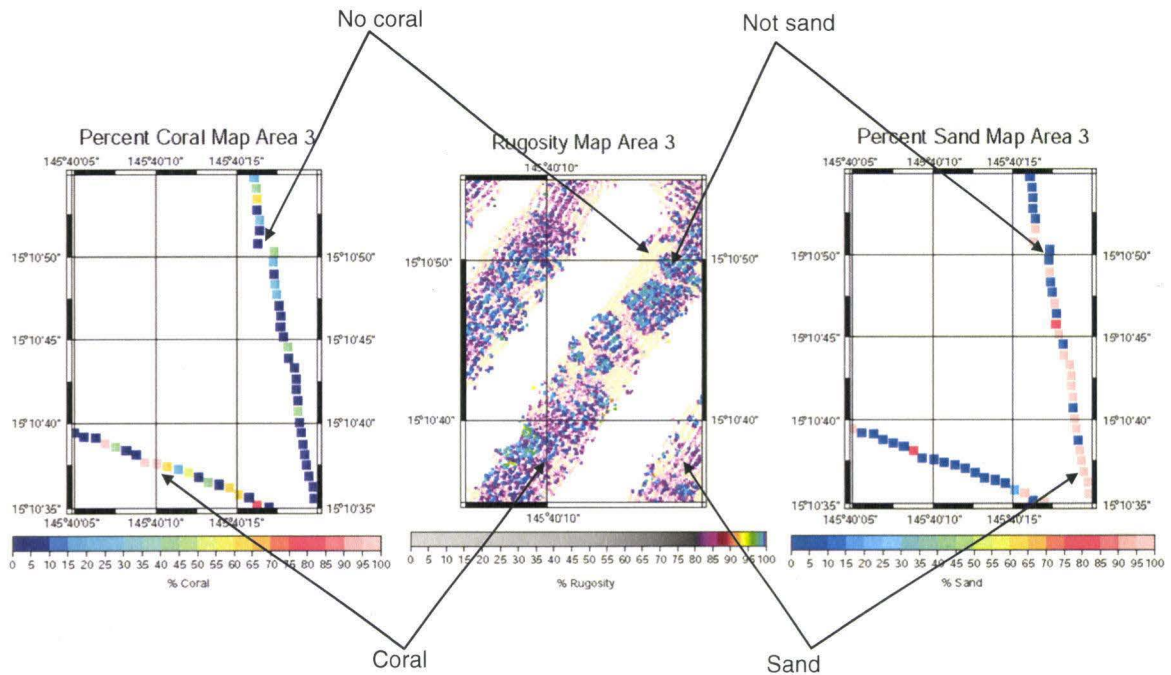
Figure 38: Area 3 comparison 2. This figure shows two towed video data sets from the same location for comparison with rugosity data. The rugosity map is binned at 15m, the video data are classified every 20 m. The black arrows point out sections of data that correlate with one another. The coral arrows show that an area classified to have 100% coral is located in an area with low rugosity values and no sand. This makes sense since we expect low rugosity areas to have more biological cover than high rugosity (or flat) areas.

Figure 39 shows another section of rugosity data and the corresponding

bathymetry and side-scan data that go with it. Because the backscatter and multibeam

bathymetry data do not show distinct textural or morphological features it is difficult to

correlate them to the rugosity data. There percent coral map shows that there is no coral

in this section. Unexpectedly, the percent sand map shows areas with high sand

69

percentages correlating with areas of increased roughness on the rugosity map (Figure 40). We expected these areas to have rugosity values closer to 100% since areas with 100% sand have flat morphologies.
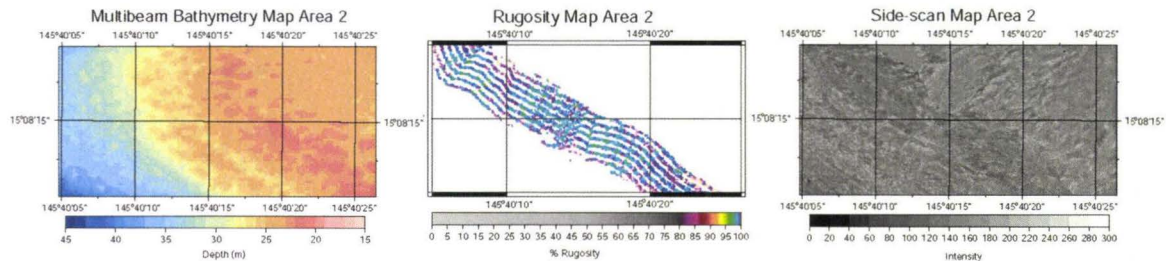
Figure 39: Area 2 comparison 1. This figure shows rugosity data binned at 15m (Rugosity Map), side-scan data gridded at 1m (Side-scan Map), bathymetry data gridded at 5m (Multibeam Bathymetry Map). Because the bathymetry and side-scan data do not have a unique shape or texture in this area it is difficult to tell if the two data sets correlate with the rugosity data.
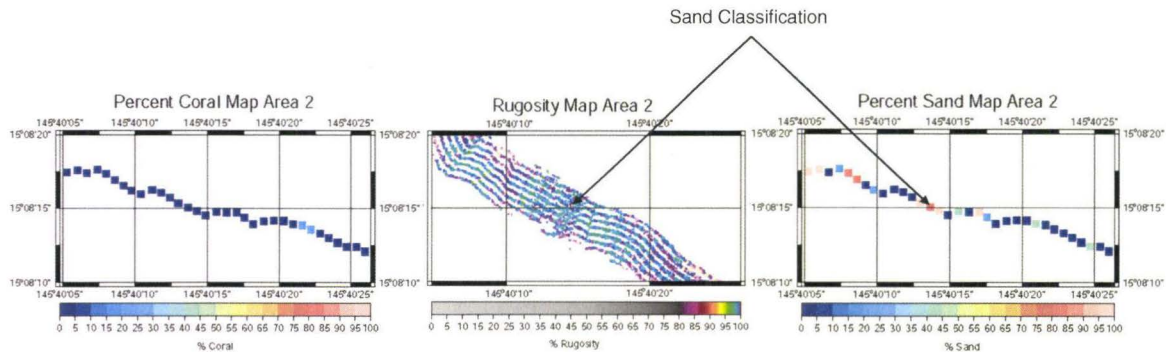
Figure 40: Area 2 comparison 2. This figure shows rugosity data binned at 15m (Rugosity Map), and video data showing percent coral (Percent Coral Map) and percent sand (Percent Sand Map) with classification spacing at 20m. The percent coral map is showing that there is 0% coral across the rugosity data swath. Because the rugosity data are showing a rough seafloor in this area we don't expect there to be much sand, but according to the percent sand map there are sections of 100% sand.

Comparing different data sets to the rugosity data has shown that the rugosity data often correlates with the bathymetry data, side-scan data, and the percentage of sand data. However, as Figure 40 shows, there are also areas where we would expect there to be no

sand based on the low rugosity values and yet the video data shows there to be 100%

sand at that point. Because we tested the rugosity algorithm on known seafloor surface

we know that it gives accurate rugosity values based on the data it is given. Therefore, we

assume that the video data and the rugosity data do not correlate perfectly due to

cumulative navigational uncertainty of ±20 m and the difference in spatial scales.

5.2 Correlations with Video Classification

Because side-scan data, bathymetry data and towed video data each have varying

spatial scales (from 1-20 m) and navigational uncertainty (from +-5-15 m), making

correlations to rugosity data is difficult, subjective, and time intensive. This is not

beneficial when developing policy or creating benthic habitat maps. Therefore, we want

to determine if the automated rugosity measurements can correlate to other data sets in a

quick, objective way. Since, video data are the most comprehensive ground truth

information collected in the Mariana Islands we want to understand how the rugosity

algorithm output correlates to the video classifications across the entire Garapan

Anchorage. To do this we took the latitude and longitude coordinates of each video data

point and found all the rugosity data within a set radius using the gmtselect program. The

search radius was set at 20 m to encompass the possible position error of the video

towfish as it was dragged behind the Carolinian. The error included ±13 m of horizontal

position uncertainty for the towfish and ±5 m horizontal accuracy for the multibeam data

(Rooney et al., 2005). Once all the surrounding rugosity data were found we plotted them

versus seafloor substrate type in order to determine if there was a correlation between

substrate type and rugosity (Figure 41).

71

Figure 41: Rugosity values vs. percent sand. This figure shows the rugosity values, binned at 15 m, which were within a 20 m radius from each sand video classification point. Because the data are so spread out the graph shows that there is not a direct correlation between the percent rugosity and the percentage of sand.

Because sand fields have a flat morphology we expected there to be a strong correlation between the percentage of sand in an area and rugosity. We expected that areas with 100% sand would correlate with rugosity values near 100%, since that signifies a flat morphology, and that areas with 0% sand would correlate with low rugosity values indicating a complex or near-vertical morphology. This was expected

72

because the manual rugosity values collected in Saipan show that there is a correlation between substrate type and rugosity. The sand bed rugosity measurement have the highest rugosity value at 98% and the pavement, which also has a relatively flat morphology, returns rugosity values around 76% (Table 2). However, Figure 38 shows that areas with 100% sand have a range of rugosity values from 7-100% and areas with 20 and 0% sand have a range of 0-100%. This means that there is not a direct correlation between rugosity and substrate type for this data set.

In order to determine if there is a correlation between the percentage of coral and rugosity we plotted the coral percent against the rugosity data within a 20 m radius. Because a coral reef has a complex and rough morphology we expected that the more coral an area had the rougher the seafloor would be which would correlate to low rugosity percents. However, as with the percent sand data, there does not appear be to a correlation between the percent coral and rugosity. In fact, Figure 42 shows that the more coral there is the higher rugosity values there are. This is the opposite of what we expected since manual rugosity measurements show that the reef habitats exhibited the lowest rugosity values.

Rugosity Values vs. Percent Coral

0 5 10 15 20 25 30 35 40 45 50 55 60 65 70 75 80 85 90 95 100
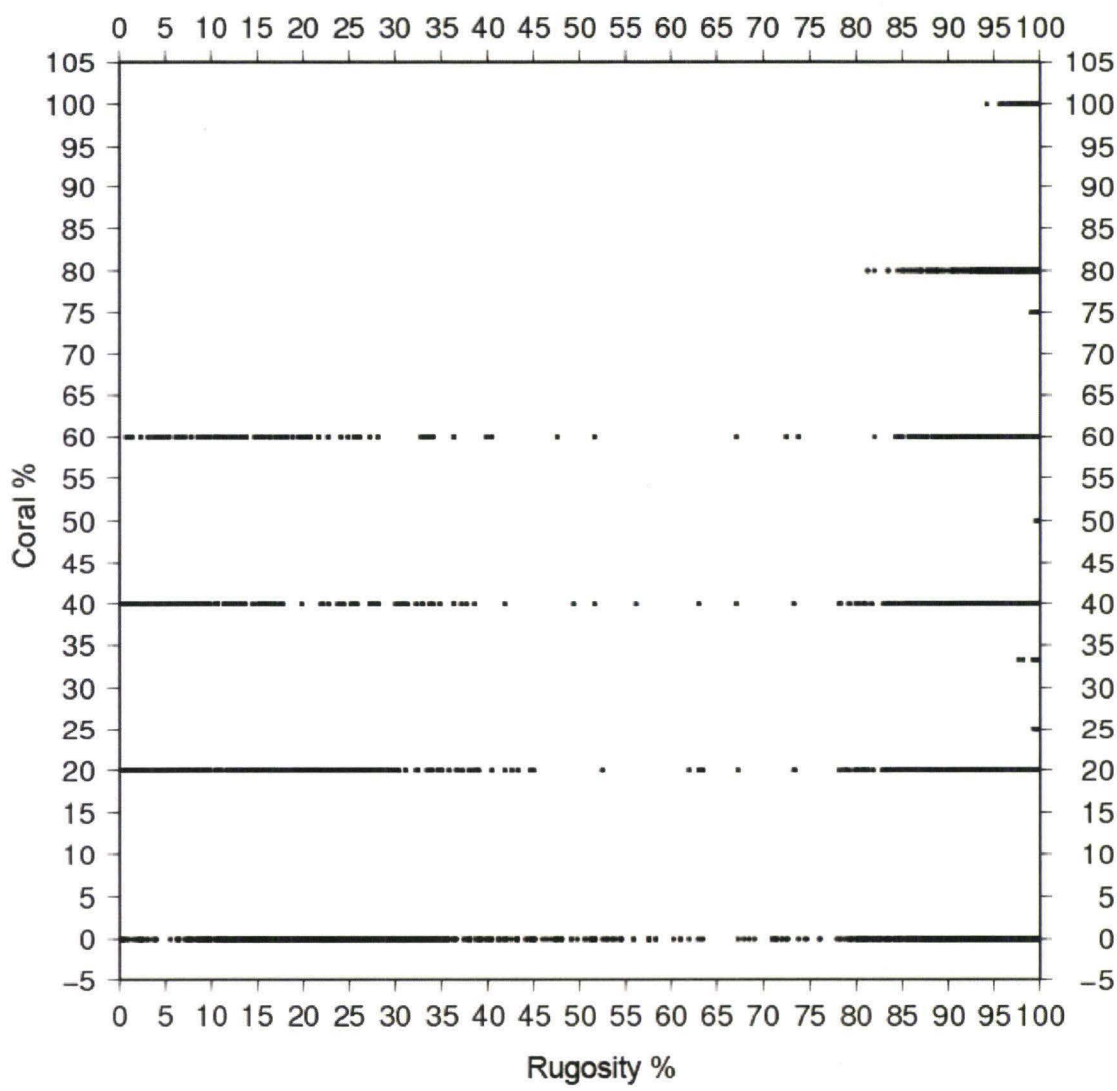
Figure 42: Rugosity values vs. percent coral. This figure shows the rugosity values, binned at 15 m, which were within a 20 m radius from each coral video classification point. Because the data are so spread out the graph shows that there is not a direct correlation between the percent rugosity and the percentage of coral.

Because Figures 41 and 42 each represent over 70,000 data points it is difficult to see a trend. To narrow down the data and determine if there is a correlation between the automated rugosity values and the percent sand and coral the rugosity data are separated

74

into sections based on percent and then processed to ascertain the mean and median

values (Figure 43).

Mean Values of Sand and Coral %
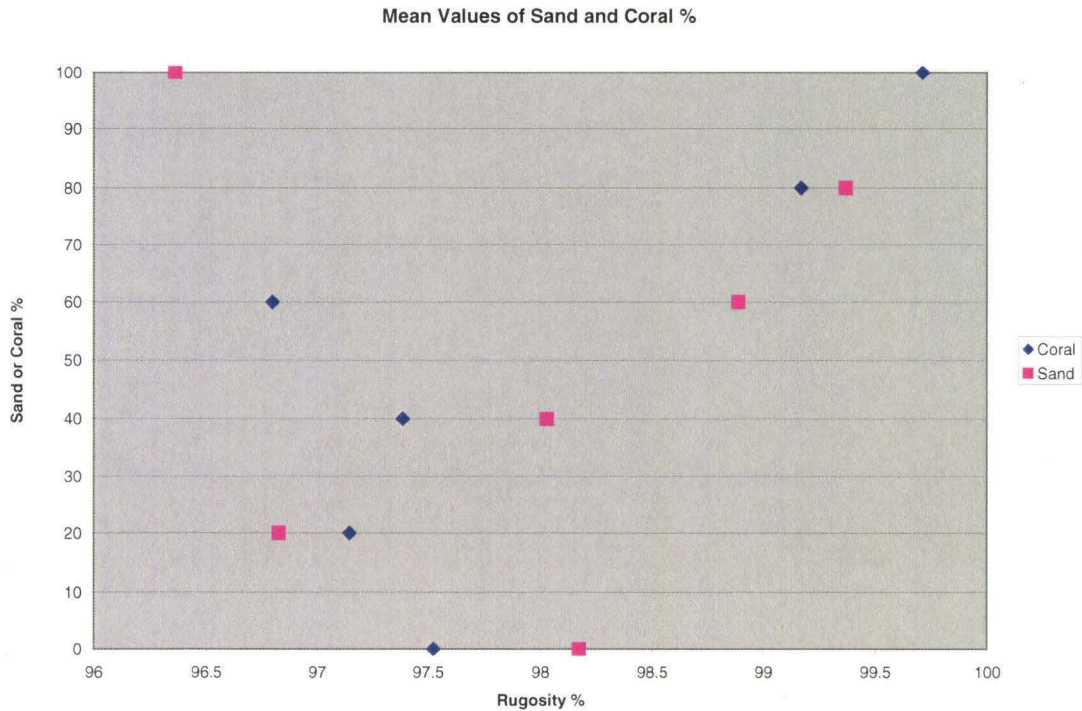
Figure 43: Mean values for percent coral and percent sand. This figure is based on the percent coral and percent sand from Figures 38 and 39 and plots the mean rugosity values from each row of percent coral and percent sand. By plotting the mean rugosity values the figure shows that there is a slight trend in the data. The percent sand increases with higher rugosity percents except at 0% and 100% sand. The percent coral does not have a strong trend but it also seems to increase with higher rugosity values except at 0% and 60% coral.

The intermediate mean values for percent sand show a trend towards higher

rugosity values as the sand percent increases. However at 100% sand the mean rugosity

value decreases to 96.4%. This is unexpected because areas with 100% sand are expected

to have flat morphologies and return rugosity values near 100%.

The percent coral mean values also show a trend towards higher rugosity values as the coral percent increases. The opposite was expected since areas of dense coral growth have the highest rugosity values of the areas measured manually.

5.3 Additional Video Error

Because video data interpretation is subjective and the quality of the data is not consistent, there may be significant error in the bottom classifications assigned which in turn affects our evaluation of the rugosity algorithm and its correlation with the towed video data. Some of the classification error was due to insufficient light in areas where the towfish was too high off the seafloor. This resulted in blurry or indistinguishable video data (Figure 44). Also, without sufficient lighting, species such as corals, hydrocorals, octocorals, and sponges could not be identified unless they had a distinctive morphology (Rooney et al., 2005). Also, because small coral colonies are not be easily identified, the percent coral estimates must be considered minimum estimates (Rooney et al., 2005).
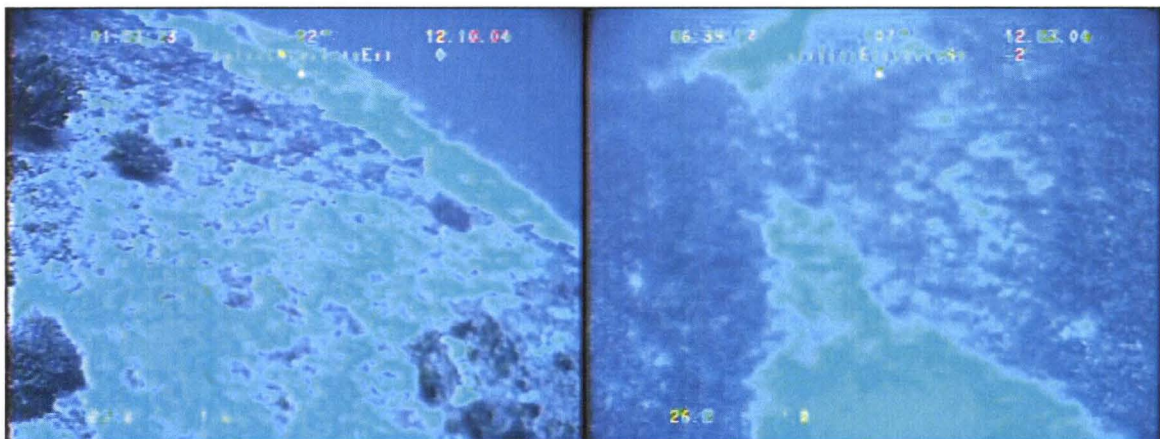
Figure 44: Towed video stills. The first frame shows slanted video data when the camera made contact with the seafloor and was rotated to the right. This frame also shows over exposed video in the lower part of the screen. This area appears to be sand when in fact there is very little sand present. The second frame represents the video data that was collected at too far from the seafloor making benthic cover impossible to classify.

76

Other classification errors were introduced because the towfish was not kept at a consistent altitude. Ideally, the camera was to be kept within a meter of the seafloor so that the benthic cover was easier to identify. However, because the bathymetry changed so rapidly the camera was often too high for substrate classification or so low that it made contact with the substrate. Depending on the altitude of the camera sled the width of video coverage could range between 0.5-10 m. This means that the classification results are not reproducible and are not readily comparable with other data sets. To illustrate this Figure 45 shows the same seafloor area from different altitudes. The first frame is classified as having 40% sand where the same area at a lower elevation is classified as 100% sand. Substrate classifications at low altitudes will yield higher resolution benthic classifications but they may not be representative of the surrounding area. Since the rugosity values that were compared with the video classification data were binned at 15m, they take into account terrain changes over much larger areas. Therefore, it is unlikely to see a strong correlation between automated rugosity values and video classifications.
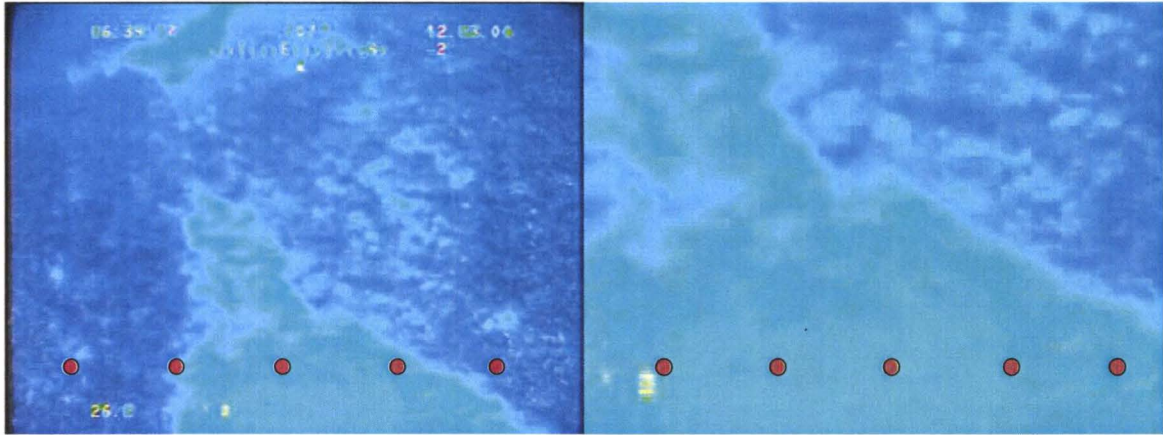
Figure 45: Video Classification at varying distances off seafloor. The red dots represent the classification points used to identify the substrate and living cover across a video frame. The second frame (right) is a zoomed in version of the first frame (left). If the camera were close to the sea floor this area would be classified as 100% sand. If the camera is further off the seafloor, as shown in frame 1, the bottom might only be classified as 40% sand.

5.4 Rugosity data compared with manual rugosity measurements

In order to determine if there is a correlation between the manual rugosity measurements and automated rugosity values we took the GPS locations of the dive sites (Figure 12) and found all the automated rugosity data within a 7 m radius circle or each location. We then averaged all the rugosity points within each circle and compared them against the average manual rugosity measurements from the same areas.

Dive site 3 is a flat sand field as evidenced by the video stills collected during the dive (Figure 46). Based on the rugosity formula, flat areas are expected to yield rugosity values near 100%. The average automated rugosity value for this area was 99.9% and corresponding manual rugosity measurement for dive site 3 was 98.0%. This example shows that the automated rugosity algorithm is applicable in flat areas.
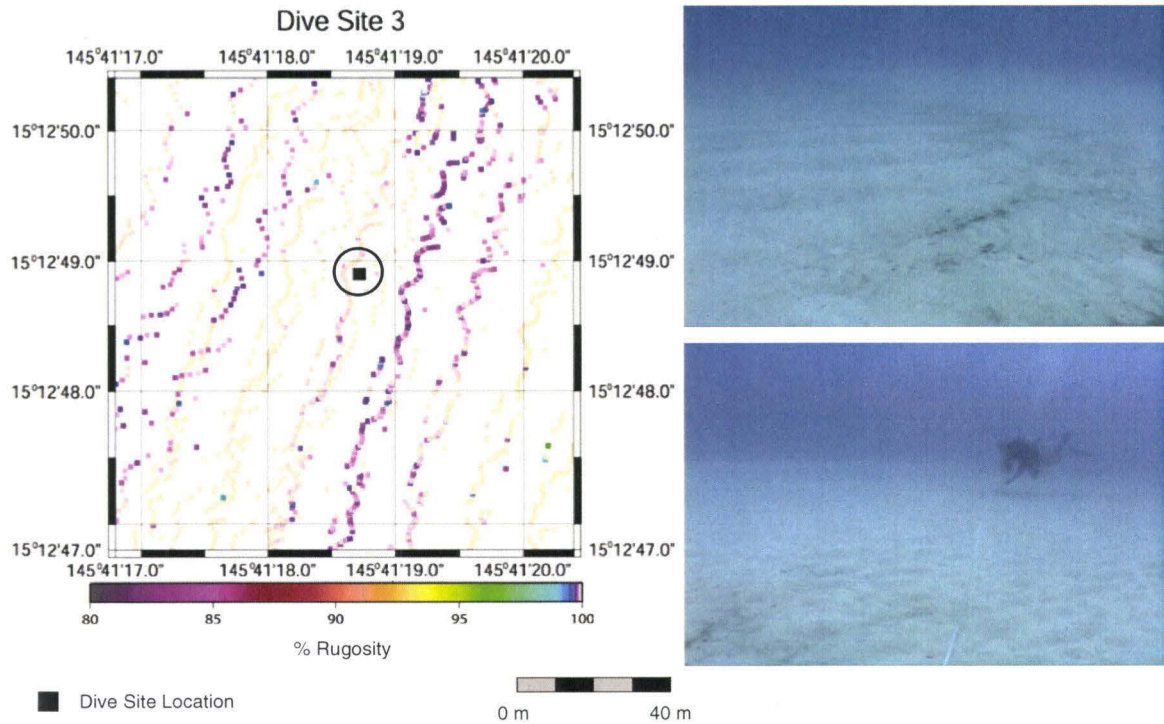
Figure 46: Rugosity map with dive site 3. Rugosity map showing the location of the dive site and the photographs taken there. The water depth at this location was 31 m. The manual rugosity measurements collected gave an average rugosity of 98.0%. The automated rugosity algorithm gives an average rugosity of 99.94% which was calculated by averaging together all the soundings located within a 7 m radius circle (black circle) centered on the dive site (black square).

The next location for comparison is dive site 6. This location has dense coral reef growth with some coral colonies larger than 0.5 m in diameter (Figure 47). The area is mostly hard substrate with some sand channels. The average automated rugosity value within 7 m of the dive site was 94.7%. This percentage is much higher than expected for an area with such a complex morphology, especially since the corresponding manual rugosity measurement was 55.6%. Although the automated rugosity value is higher than anticipated, it is lower than the automated rugosity value obtained from dive site 3 which means that the rugosity algorithm works and produced a rugosity value that indicates a rougher morphology.
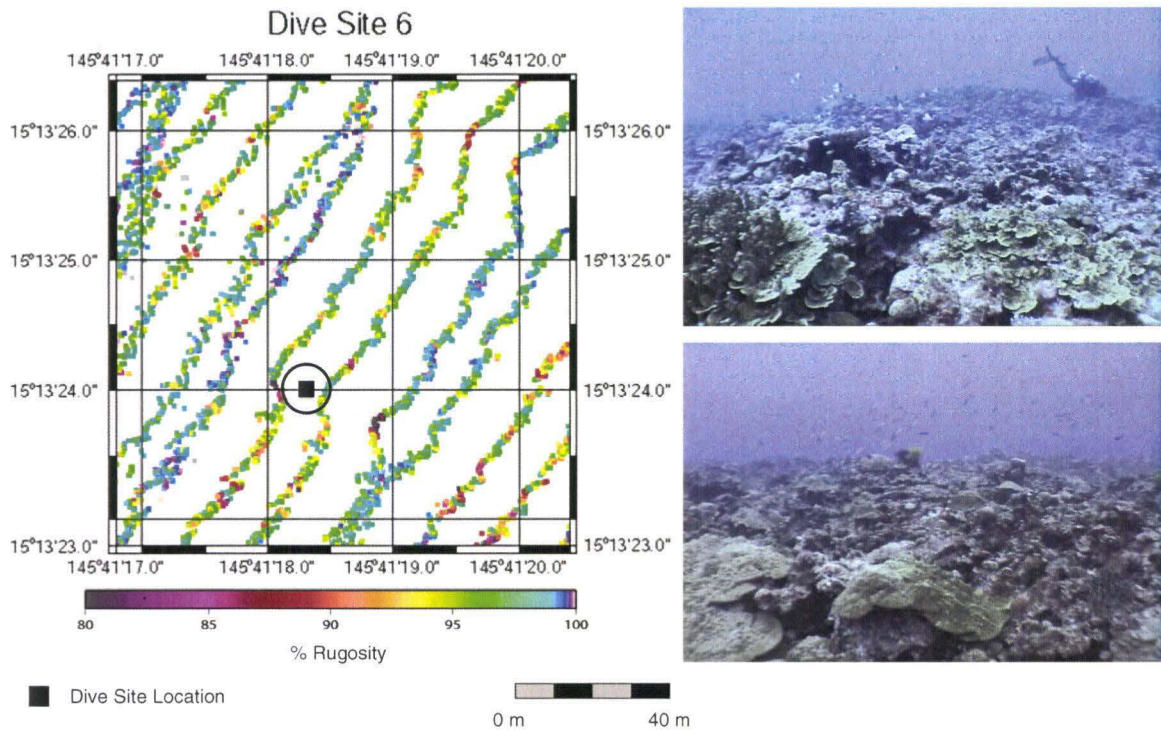
Figure 47: Rugosity map with dive site 6. Rugosity map showing the location of the dive site and the photographs taken there. The water depth at this site was 24 m. The manual rugosity measurements collected gave an average rugosity of 55.6%. The automated rugosity algorithm gives an average rugosity of 94.7% which was calculated by averaging together all the soundings located within a 7 m radius circle (black circle) centered on the dive site (black square).

Figure 48 is a graph showing the differences between the manual and automated rugosity values across four dive sites. The sand field showed the highest correlation between the manual and automated measurements. However the more convoluted the seafloor morphology is, the poorer the agreement between the two rugosity percentages.

The differences in the two rugosity values could be due to the spatial scales that the rugosity data were measured. The manual rugosity measurements were collected using a chain with a 0.012m link size where the automated rugosity measurements were created using a data set with varying resolution from .52m to 107m. Therefore it would be expected that the automated rugosity measurements would not be able to detect

80

morphological changes to the same degree, causing the seafloor to appear smoother than

it would using manual measurements.

Automated Rugosity vs. Manual Rugosity
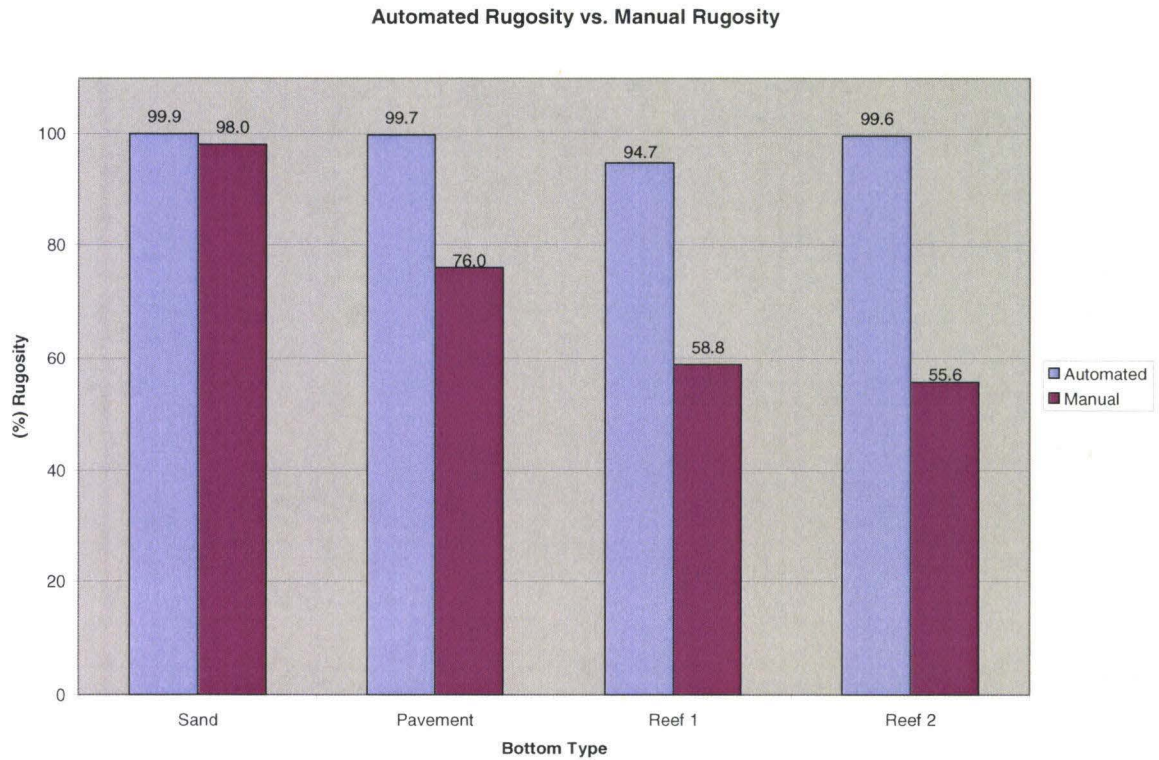
Figure 48: Manual vs. automated rugosity values. Graph showing the differences between the mean manual rugosity measurements and the mean of all automated rugosity measurements within a 7 m radius circle centered on each of the four dive sites. Although the automated rugosity values do decrease, indicating a rougher seafloor, where the manual rugosity measurements decrease, the range of returned rugosity values is not as great. This indicates that the two methods are measuring different scales of rugosity.

CHAPTER 6: DISCUSSION OF RESULTS

6.1 How useful is the rugosity algorithm?

When applied to known seafloor shapes, the rugosity algorithm responded as expected and returned low rugosity values on areas with highly variable bathymetry or near vertical surfaces (Figures 24 and 33). It also returned high rugosity values on smooth or flat seafloor surfaces. When the rugosity data were compared to towed video data there were correlations between 100% sand video classifications and 100% rugosity values indicating a flat morphology (Figure 37). The correlation between rugosity and the percentage of coral was not as strong but in Figure 38 and 40 the areas identified as having 100% coral correlated with areas of lower rugosity values. Also, we demonstrated that the rugosity data were independent of bathymetry since slope was removed from each bin. This means that the rugosity data can be compared across the entire data set regardless of relief. Overall, determining how rugosity correlates is time consuming and is not necessarily accurate because of the differences in position error of the towfish and also the different classification scales.

In order to determine if there was a correlation between the percentage of sand and coral with rugosity we compared the data across the entire Saipan data set. We found that there was not a strong correlation between the percentage of sand and automated rugosity values. This was unexpected since the forward model showed that areas with flat morphologies should correspond to high rugosity values. When we compared the percentage of coral and rugosity we again found that there was not a strong correlation. In fact, the data showed that the more coral an area had the higher the corresponding rugosity value. We determined that the inconsistent spatial scale of the video

classifications coupled with the navigational uncertainty of both data sets contributed to the unexpected results.

When the automated rugosity values were compared with manual dive data there was a correlation between the rugosity values in areas with a flat morphology. However, as the seafloor morphology became more complex the manual and automated rugosity values were no longer close. Although the automated rugosity values decreased with a rougher seafloor, the values did not represent as rough a surface as was expected by the forward model or the manual rugosity measurements. We determined that the automated rugosity data returned higher rugosity values than the manual rugosity measurements because of the spatial scale at which the seafloor was sampled. The manual rugosity measurements were collected continuously using a chain with half inch links where the automated rugosity data points were collected every .5 m to 50 m depending on the water depth and distance from nadir. Therefore the manual rugosity data were sampled on a much smaller scale which allowed rugosity to be measured at a finer scale.

6.2 Bin size and sounding requirements in depth

We determined that for a bin size of 10 m, and a minimum sounding requirement of 3, information can only be obtained to a depth of 180 m of depth before there are no bins that pass the minimum requirement. Therefore, a minimum sounding requirement of 5-7 better describes the seafloor roughness. However if we require there to be at least 5-7 soundings in a bin rugosity data can only be obtained between 80 m (requirement of 7) and 100 m (requirement of 5). Therefore the rugosity equation may only be useful at shallow depths. However if the rugosity algorithm was applied to towed sonar data,

which is colleted close to the sea floor at deeper depths, rugosity information would no longer be depth limited and would be available at over a wider range.

The rugosity algorithm can be adjusted to accommodate the sonar data set being used. For instance, if the beam spacing of a sonar system are spaced closer together than the RESON 8101 then the minimum sounding requirement for a bin could be increased to increase the overall accuracy of the rugosity data. The bin size can also be adjusted to get the highest resolution rugosity data. For the RESON 8101 multibeam sonar a bin size of 15 m appeared to work best because it provides both high resolution rugosity data and good coverage of the seafloor without leaving large gaps between the swaths. If the swaths of bathymetry data overlapped more the bin size could be decreased without leaving large gaps in the rugosity data set.

6.3 Conclusions

We determined that the resolution of the RESON 8101 multibeam sonar is not fine enough to resolve the small scale rugosity of coral head or possibly a reef. This means that benthic habitat maps cannot be based on sonar data alone. Other interpreted data sources are needed, including rugosity. Also, it was determined that the automated rugosity measurements are not directly comparable to manual measurements. This is because multibeam data are collected on the scale of several meters and manual measurements are collected at 0.012 m size, or the size of the chain links. In order to compare manual rugosity measurements with automated rugosity data the density of the bathymetry data would need to increase. This requires the sonar system to have beams spaced closer together than $1.5°$.

In order to better asses the accuracy of the rugosity algorithm, more manual rugosity measurements need to be collected at varying spatial scales consistent with the sounding spacing at depth. Also, the rugosity algorithm should be run on higher resolution data sets to get an understanding of the classification capabilities of rugosity data. In order to get higher resolution rugosity information towed sonar or autonomous underwater vehicle (AUV) systems should be used. This way the altitude from the sea floor can be controlled which would give greater and higher resolution coverage at deeper depths so that obtaining rugosity information is not depth limited.

APPENDIX A

Look up table of sounding spacing.

(A) Angle	Tan(Radians(A))	Depth (m) 20	20	30	30	40	40	60	60	80	80	100	100
1.5	0.0261859	0.52		0.79		1.05		1.57		2.09		2.62	
3	0.0524078	1.05	0.52	1.57	0.79	2.1	1.05	3.14	1.57	4.19	2.1	5.24	2.62
4.5	0.0787017	1.57	0.53	2.36	0.79	3.15	1.05	4.72	1.58	6.3	2.1	7.87	2.63
6	0.1051042	2.1	0.53	3.15	0.79	4.2	1.06	6.31	1.58	8.41	2.11	10.5	2.64
7.5	0.1316525	2.63	0.53	3.95	0.8	5.27	1.06	7.9	1.59	10.5	2.12	13.2	2.65
9	0.1583844	3.17	0.53	4.75	0.8	6.34	1.07	9.5	1.6	12.7	2.14	15.8	2.67
10.5	0.185339	3.71	0.54	5.56	0.81	7.41	1.08	11.1	1.62	14.8	2.16	18.5	2.7
12	0.2125566	4.25	0.54	6.38	0.82	8.5	1.09	12.8	1.63	17	2.18	21.3	2.72
13.5	0.2400788	4.8	0.55	7.2	0.83	9.6	1.1	14.4	1.65	19.2	2.2	24	2.75
15	0.2679492	5.36	0.56	8.04	0.84	10.7	1.11	16.1	1.67	21.4	2.23	26.8	2.79
16.5	0.2962135	5.92	0.57	8.89	0.85	11.8	1.13	17.8	1.7	23.7	2.26	29.6	2.83
18	0.3249197	6.5	0.57	9.75	0.86	13	1.15	19.5	1.72	26	2.3	32.5	2.87
19.5	0.3541186	7.08	0.58	10.6	0.88	14.2	1.17	21.2	1.75	28.3	2.34	35.4	2.92
21	0.383864	7.68	0.59	11.5	0.89	15.4	1.19	23	1.78	30.7	2.38	38.4	2.97
22.5	0.4142136	8.28	0.61	12.4	0.91	16.6	1.21	24.9	1.82	33.1	2.43	41.4	3.03
24	0.4452287	8.9	0.62	13.4	0.93	17.8	1.24	26.7	1.86	35.6	2.48	44.5	3.1
25.5	0.4769755	9.54	0.63	14.3	0.95	19.1	1.27	28.6	1.9	38.2	2.54	47.7	3.17
27	0.5095254	10.2	0.65	15.3	0.98	20.4	1.3	30.6	1.95	40.8	2.6	51	3.25
28.5	0.5429557	10.9	0.67	16.3	1	21.7	1.34	32.6	2.01	43.4	2.67	54.3	3.34
30	0.5773503	11.5	0.69	17.3	1.03	23.1	1.38	34.6	2.06	46.2	2.75	57.7	3.44
31.5	0.6128008	12.3	0.71	18.4	1.06	24.5	1.42	36.8	2.13	49	2.84	61.3	3.55
33	0.6494076	13	0.73	19.5	1.1	26	1.46	39	2.2	52	2.93	64.9	3.66
34.5	0.687281	13.7	0.76	20.6	1.14	27.5	1.51	41.2	2.27	55	3.03	68.7	3.79
36	0.7265425	14.5	0.79	21.8	1.18	29.1	1.57	43.6	2.36	58.1	3.14	72.7	3.93
37.5	0.767327	15.3	0.82	23	1.22	30.7	1.63	46	2.45	61.4	3.26	76.7	4.08
39	0.809784	16.2	0.85	24.3	1.27	32.4	1.7	48.6	2.55	64.8	3.4	81	4.25
40.5	0.8540807	17.1	0.89	25.6	1.33	34.2	1.77	51.2	2.66	68.3	3.54	85.4	4.43
42	0.900404	18	0.93	27	1.39	36	1.85	54	2.78	72	3.71	90	4.63
43.5	0.9489646	19	0.97	28.5	1.46	38	1.94	56.9	2.91	75.9	3.88	94.9	4.86
45	1	20	1.02	30	1.53	40	2.04	60	3.06	80	4.08	100	5.1
46.5	1.0537801	21.1	1.08	31.6	1.61	42.2	2.15	63.2	3.23	84.3	4.3	105	5.38
48	1.1106125	22.2	1.14	33.3	1.7	44.4	2.27	66.6	3.41	88.8	4.55	111	5.68
49.5	1.1708496	23.4	1.2	35.1	1.81	46.8	2.41	70.3	3.61	93.7	4.82	117	6.02
51	1.2348972	24.7	1.28	37	1.92	49.4	2.56	74.1	3.84	98.8	5.12	123	6.4
52.5	1.3032254	26.1	1.37	39.1	2.05	52.1	2.73	78.2	4.1	104	5.47	130	6.83
54	1.3763819	27.5	1.46	41.3	2.19	55.1	2.93	82.6	4.39	110	5.85	138	7.32
55.5	1.455009	29.1	1.57	43.7	2.36	58.2	3.15	87.3	4.72	116	6.29	146	7.86
57	1.539865	30.8	1.7	46.2	2.55	61.6	3.39	92.4	5.09	123	6.79	154	8.49
58.5	1.6318517	32.6	1.84	49	2.76	65.3	3.68	97.9	5.52	131	7.36	163	9.2
60	1.7320508	34.6	2	52	3.01	69.3	4.01	104	6.01	139	8.02	173	10
61.5	1.8417709	36.8	2.19	55.3	3.29	73.7	4.39	111	6.58	147	8.78	184	11
63	1.9626105	39.3	2.42	58.9	3.63	78.5	4.83	118	7.25	157	9.67	196	12.1
64.5	2.0965436	41.9	2.68	62.9	4.02	83.9	5.36	126	8.04	168	10.7	210	13.4
66	2.2460368	44.9	2.99	67.4	4.48	89.8	5.98	135	8.97	180	12	225	14.9
67.5	2.4142136	48.3	3.36	72.4	5.05	96.6	6.73	145	10.1	193	13.5	241	16.8
69	2.6050891	52.1	3.82	78.2	5.73	104	7.64	156	11.5	208	15.3	261	19.1
70.5	2.8239129	56.5	4.38	84.7	6.56	113	8.75	169	13.1	226	17.5	282	21.9
72	3.0776835	61.6	5.08	92.3	7.61	123	10.2	185	15.2	246	20.3	308	25.4
73.5	3.3759434	67.5	5.97	101	8.95	135	11.9	203	17.9	270	23.9	338	29.8
75	3.7320508	74.6	7.12	112	10.7	149	14.2	224	21.4	299	28.5	373	35.6

(A) Angle	Tan(Radians(A))	Depth (m) 120	120	140	140	160	160	180	180	200	200	220	220
1.5	0.026186	3.14		3.67		4.19		4.71		5.24		5.76	
3	0.052408	6.29	3.15	7.34	3.67	8.39	4.2	9.43	4.72	10.5	5.24	11.5	5.77
4.5	0.078702	9.44	3.16	11	3.68	12.6	4.21	14.2	4.73	15.7	5.26	17.3	5.78
6	0.105104	12.6	3.17	14.7	3.7	16.8	4.22	18.9	4.75	21	5.28	23.1	5.81
7.5	0.131652	15.8	3.19	18.4	3.72	21.1	4.25	23.7	4.78	26.3	5.31	29	5.84
9	0.158384	19	3.21	22.2	3.74	25.3	4.28	28.5	4.81	31.7	5.35	34.8	5.88
10.5	0.185339	22.2	3.23	25.9	3.77	29.7	4.31	33.4	4.85	37.1	5.39	40.8	5.93
12	0.212557	25.5	3.27	29.8	3.81	34	4.35	38.3	4.9	42.5	5.44	46.8	5.99
13.5	0.240079	28.8	3.3	33.6	3.85	38.4	4.4	43.2	4.95	48	5.5	52.8	6.05
15	0.267949	32.2	3.34	37.5	3.9	42.9	4.46	48.2	5.02	53.6	5.57	58.9	6.13
16.5	0.296213	35.5	3.39	41.5	3.96	47.4	4.52	53.3	5.09	59.2	5.65	65.2	6.22
18	0.32492	39	3.44	45.5	4.02	52	4.59	58.5	5.17	65	5.74	71.5	6.32
19.5	0.354119	42.5	3.5	49.6	4.09	56.7	4.67	63.7	5.26	70.8	5.84	77.9	6.42
21	0.383864	46.1	3.57	53.7	4.16	61.4	4.76	69.1	5.35	76.8	5.95	84.5	6.54
22.5	0.414214	49.7	3.64	58	4.25	66.3	4.86	74.6	5.46	82.8	6.07	91.1	6.68
24	0.445229	53.4	3.72	62.3	4.34	71.2	4.96	80.1	5.58	89	6.2	98	6.82
25.5	0.476976	57.2	3.81	66.8	4.44	76.3	5.08	85.9	5.71	95.4	6.35	105	6.98
27	0.509525	61.1	3.91	71.3	4.56	81.5	5.21	91.7	5.86	102	6.51	112	7.16
28.5	0.542956	65.2	4.01	76	4.68	86.9	5.35	97.7	6.02	109	6.69	119	7.35
30	0.57735	69.3	4.13	80.8	4.82	92.4	5.5	104	6.19	115	6.88	127	7.57
31.5	0.612801	73.5	4.25	85.8	4.96	98	5.67	110	6.38	123	7.09	135	7.8
33	0.649408	77.9	4.39	90.9	5.12	104	5.86	117	6.59	130	7.32	143	8.05
34.5	0.687281	82.5	4.54	96.2	5.3	110	6.06	124	6.82	137	7.57	151	8.33
36	0.726543	87.2	4.71	102	5.5	116	6.28	131	7.07	145	7.85	160	8.64
37.5	0.767327	92.1	4.89	107	5.71	123	6.53	138	7.34	153	8.16	169	8.97
39	0.809784	97.2	5.09	113	5.94	130	6.79	146	7.64	162	8.49	178	9.34
40.5	0.854081	102	5.32	120	6.2	137	7.09	154	7.97	171	8.86	188	9.75
42	0.900404	108	5.56	126	6.49	144	7.41	162	8.34	180	9.26	198	10.2
43.5	0.948965	114	5.83	133	6.8	152	7.77	171	8.74	190	9.71	209	10.7
45	1	120	6.12	140	7.14	160	8.17	180	9.19	200	10.2	220	11.2
46.5	1.05378	126	6.45	148	7.53	169	8.6	190	9.68	211	10.8	232	11.8
48	1.110613	133	6.82	155	7.96	178	9.09	200	10.2	222	11.4	244	12.5
49.5	1.17085	141	7.23	164	8.43	187	9.64	211	10.8	234	12	258	13.3
51	1.234897	148	7.69	173	8.97	198	10.2	222	11.5	247	12.8	272	14.1
52.5	1.303225	156	8.2	182	9.57	209	10.9	235	12.3	261	13.7	287	15
54	1.376382	165	8.78	193	10.2	220	11.7	248	13.2	275	14.6	303	16.1
55.5	1.455009	175	9.44	204	11	233	12.6	262	14.2	291	15.7	320	17.3
57	1.539865	185	10.2	216	11.9	246	13.6	277	15.3	308	17	339	18.7
58.5	1.631852	196	11	228	12.9	261	14.7	294	16.6	326	18.4	359	20.2
60	1.732051	208	12	242	14	277	16	312	18	346	20	381	22
61.5	1.841771	221	13.2	258	15.4	295	17.6	332	19.7	368	21.9	405	24.1
63	1.962611	236	14.5	275	16.9	314	19.3	353	21.8	393	24.2	432	26.6
64.5	2.096544	252	16.1	294	18.8	335	21.4	377	24.1	419	26.8	461	29.5
66	2.246037	270	17.9	314	20.9	359	23.9	404	26.9	449	29.9	494	32.9
67.5	2.414214	290	20.2	338	23.5	386	26.9	435	30.3	483	33.6	531	37
69	2.605089	313	22.9	365	26.7	417	30.5	469	34.4	521	38.2	573	42
70.5	2.823913	339	26.3	395	30.6	452	35	508	39.4	565	43.8	621	48.1
72	3.077684	369	30.5	431	35.5	492	40.6	554	45.7	616	50.8	677	55.8
73.5	3.375943	405	35.8	473	41.8	540	47.7	608	53.7	675	59.7	743	65.6
75	3.732051	448	42.7	522	49.9	597	57	672	64.1	746	71.2	821	78.3

Table 3: This table calculates the spacing of soundings across a ping. The green column is the angle of the beam from nadir or zero degrees. The yellow column is the angle converted from degrees to radians. The blue columns are the distance in meters from nadir. The purple column subtracts the distances to find the spacing in meters between individual soundings in the across track direction.

Rugosity Algorithm:

```
#! /bin/csh -f
# Program : trend1-09-15-06.csh
# Date : September 15, 2006
# By : Erin Diurba
# /home/kii1a/bruce/rugosity
# trend1-09-15-06.csh - Takes pink data in the "PN, X, Y, Lat. Lon." form
# and runs it through trend 1d to remove slope from data set.
# Last edited 9-15-06
# USAGE: trend1-09-15-06.csh ahmba03234.d09.xz
# EXAMPLE: trend1-09-15-06.csh  ahmba03234.d09.xz
#Set up variables to work with
set infile      = $1
#Renames the outfile using the beginning of the infile and adding a .xyr
set inf         = $infile:r
set outfile     = $inf.bin-$bin.xyr
#This is where the across track bin width is set
set bin         = 15
#Removes files with same name if they already exist.
if (-f $outfile) \rm $outfile
if (-f binfile) \rm binfile
if (-f pingfile) \rm pingfile
#Setting up additional variables
set ping        = `cat $infile | head -1 | awk '{print $1}'`
set lastping    = ` cat $infile | tail -1 | awk '{print $1}' `
#Factor is the number we multiply the bin size by (noisedist) to get a distance between adjacent soundings
#that would not exist in cleaned data. These data can then be discarded.
set factor      = 1
#Radius gives the number of attempts the program will complete before moving on to the next data point.
#This is necessary for groups of erroneous points because the program is designed to keep looking for a
#distance that is not greater than the set "Factor". So without a catch, the program would skip over whole
#pings of useable data.
set radius      = 2
set noisedist   = ` echo $bin $factor | awk '{printf "%8.3f\n", $1/$2}' `
#R is the longitude and latitude limits of our data.
set R           = -120/120/40/50
#These variables determine the number of lines in a file
set totallist   = ` wc -l $infile | awk '{printf "%d\n", $1}' `
#This variable subtracts one from the totallist so the program knows how many times to loop through.
set totallistend = ` echo $totallist | awk '{printf "%d\n", $1-1}' `
set begintotlist = 0
#*********************************************************************************
#This is the beginning of the "loopping" loop. This portion sets then re-sets variables each time the
#program completes a ping.
loopping:
 #This removes the "binfile" if it already exists.
 if (-f binfile) \rm binfile
 #This statement looks at the original data file and creates a new file called "pingfile" that is used so that
 #the original data is not compromised.
 gawk '{if ($1==target) print $0}'  target=$ping $infile >! pingfile
 #Sets the variable to the first x value (furthest left) in the pingfile
```

```
set x0            = `cat pingfile | head -1 | awk '{printf "%8.3f\n", $2}'`
#Sets the variable to the last x value (furthest right) in the pingfile
set xLast         = `cat pingfile | tail -1 | awk '{printf "%8.3f\n", $2}'`
#Counts the number of soundings in a pingfile
set nsounds       = `cat pingfile | wc -l`
set nsoundsend    = ` echo $nsounds| awk '{printf "%d\n", $1-1}' `
#Re-sets variables to zero.
set soundings     = 0
set usounds2      = 0
#This is a counter that increases by "nsounds" each time through the loop
set begintotlist  = `echo $begintotlist $nsounds | awk '{printf "%d\n", $1+$2}'`
#Sets variables
set count2        = 1
set count3        = 1
set count4        = 1
set badcount      = 0
#This looks at the "pingfile" and determines the first x value which is where the program will start
#binning.
set sstart        = ` cat pingfile | awk '{if(NR==rec)printf "%8.6f\n", $2}' rec=$count3 `
#This variable takes the first x value and adds on the distance of the set bin value so that the program has
#a stopping point as well as a beginning point.
set binmax        = ` echo $sstart $bin | awk '{printf "%8.6f\n", $1+$2}' `
#*******************************************************************************
#This starts the "binner" loop which is where the program moves across the ping and bins the data
binner:
#This checks to see if the program has used enough soundings (usounds) to have reached the end
#(nsoundsend). If it has reached the end then the program goes to the end of the scrip and finishes.
#Otherwise the script continues through another loop.
if ($usounds2 >= $nsoundsend) goto done
#This variable is set to the number x value that corresponds with the current value of "count2".
set s1x           = ` cat pingfile | awk '{if(NR==rec)printf "%8.3f\n", $2}' rec=$count2 `
#*******************************************************************************
#This starts the "skip" loop. Before the data are binned the data are checked for erroneous points that
#are then removed.
skip:
#Sets "z" to the number z value that corresponds with the current value of "count4"
set z             = ` cat pingfile | awk '{if(NR==rec)printf "%8.3f\n", $3}' rec=$count4 `
#Sets "z" to the number latitude and longitude values that correspond with the current value of "count4".
set lat           = ` cat pingfile | awk '{if(NR==rec)printf "%8.6f\n", $5}' rec=$count4 `
set lon           = ` cat pingfile | awk '{if(NR==rec)printf "%8.6f\n", $4}' rec=$count4 `
#Increases the counters "count4 and count2" by 1 or 1 time through the loop.
set count4        = ` echo $count4  | awk '{print $1 + 1}' `
set count2        = ` echo $count2  | awk '{print $1 + 1}' `
#This variable is set to the number x value that corresponds with the current value of "count2"
set s2x           = ` cat pingfile | awk '{if(NR==rec)printf "%8.6f\n", $2}' rec=$count2 `
#Finds the difference between the first x value (when count=1) and next x value (when count=2)
set xdif          = ` echo $s1x $s2x | awk '{printf "%8.6f\n", $2-$1}' `
#Takes the absolute value of the difference "xdif"
set xdifabs       = ` echo $xdif | awk '{printf "%8.6f\n", sqrt($1^2)}' `
#The next two lines set up check questions.
#If the first x value is less than oe equal to "binmax" print "y" or yes else print no or "n"
set check         = ` echo $s1x $binmax | awk '{if($1 <= $2) print "y"; else print "n"}' `
#If the absolute value of the "xdif" is greater than the "noisedist"  print "yes" else print "no"
set check2        = ` echo $xdifabs $noisedist | awk '{if($1>$2) print "yes"; else print "no"}' `
# This begins and if, then, else, statement
```

90

```
#This set of code is followed if the x value is less than or equal to the "binmax"
if ($check == y) then
                #This section removes the erroneous data if the distance between soundings is greater than the
                #pre-set "noisedist"
                if ($check2 == yes) then
                    #This moves the counter forward even though the bad sounding will not be used
                    set usounds2 = ` echo $usounds2 | awk '{print $1 + 1}'`
                    #This moves the "badcount" counter up 1 so that the program know how many tries it has
                    #completed to find a sounding whose distance is less than the set "noisedist".
                    set badcount     = ` echo $badcount  | awk '{print $1 + 1}'`
                        #If the counter goes over the number of tries allowed, the program goes back to "binner"
                        # and re-sets the "badcount" counter at zero.
                        if ($badcount > $radius) then
                          set badcount = 0
                          goto binner
                        endif
                    #If the number of used soundings reaches the end then go to "done"
                    if ($usounds2 >= $nsoundsend) goto done
                            goto skip
                else
                    #If the program hasn't used enough soundings then the information for the current sounding is
                    #added to the information in the "binfile" and the program loops back to "binner".
                    echo $ping $s1x $z $lat $lon,| awk '{printf "%8.0f %8.3f %8.3f %8.6f %8.6f\n", $1, $2, $3, $4,
                        $5}' >> binfile
                goto binner
                endif
        endif
    endif
#The next lines re-set all the variables.
set soundings    = ` wc -l binfile | awk '{print $1}'`
set usounds2 = ` echo $soundings $usounds2 | awk '{print $1+$2}'`
set soundlon1      = 0
set soundlat1      = 0
set soundlon2      = 0
set soundlat2      = 0
set latstart       = 0
set lonstart       = 0
set lattot         = 0
set lontot         = 0
set lonavg         = 0
set latavg         = 0
set soundrun       = 0
set soundrise      = 0
set soundAsqB      = 0
set soundC         = 0
set soundCtot      = 0
set rugosity       = 0
    #The next if else statement makes sure that the bins meet the sounding requirement which is listed here
    #as 5. If there are not enough soundings in the bin than the program goes back to "binner".
    if ($soundings<5) then
        #The binmax is increased by the width of the next bin.
        set binmax  = ` echo $binmax $bin | awk '{print $1+$2}'`
        if (-f binfile) \rm binfile
        #The "count" counters have 1 subtracted from them so that this middle step doesn't get counted
        #twice.
```

91

```
        set count2      = ` echo $count2 | awk '{print $1 - 1}' `
        set count4      = ` echo $count4 | awk '{print $1 - 1}' `
        goto binner
#If there are enough soundings in the bin than the program can proceed on to remove slope and calculate
#rugosity within the bin.
else if ($soundings>4) then
        set count2      = ` echo $count2 | awk '{print $1 - 1}' `
        set count4      = ` echo $count4 | awk '{print $1 - 1}' `
        #To remove the trend the x and z data are extracted and put in a new file called "trendfile".
        cat binfile | awk '{print $2, $3}' >! trendfile
        #Using GMT's trend1d the slope of the data is determined. Then an output file is created with the x
        #position and residual values.
        trend1d -Fxr -N2 trendfile >! trendoutfile
        cat trendoutfile | awk '{print $0}'
        #To find the short length, or linear distance, of the rugosity equation the length of the line between the
        #beginning "XTrendBeg" and end "XTrendEnd" points using the x distances.
        set XTrendBeg   = ` cat trendfile | head -1 | awk '{printf "%8.3f\n", $1}' `
        set XTrendEnd   = ` cat trendfile | tail -1 | awk '{printf "%8.3f\n", $1}' `
        set C           = ` echo $XTrendEnd $XTrendBeg | awk '{printf "%8.3f\n", $1-$2}' `
        set Cabs        = ` echo $C | awk '{printf "%8.3f\n", sqrt($1^2)}' `
        echo "XTrendBeg XTrendEnd Cabs: " $XTrendBeg $XTrendEnd $Cabs
        #Now the residuals need to be added up.
        #A counter is started to make sure that every sounding in a bin is used.
        set count       = 1
        #Variables are set up to equal the first values in the bin.
        set xbeg        = ` cat trendoutfile | awk '{if(NR==rec)printf "%8.5f\n", $1}' rec=$count `
        set sound1x     = ` cat trendoutfile | awk '{if(NR==rec)printf "%8.5f\n", $1}' rec=$count `
        set sound1z     = ` cat trendoutfile | awk '{if(NR==rec)printf "%8.5f\n", $2}' rec=$count `
        set soundlon1   = ` cat binfile | awk '{if(NR==rec)printf "%8.6f\n", $4}' rec=$count `
        set soundlat1   = ` cat binfile | awk '{if(NR==rec)printf "%8.6f\n", $5}' rec=$count `
        #These two lines add up the latitude and longitude values.
        set lattot      = ` echo $lattot $soundlat1 | awk '{printf "%8.6f\n", $1+$2}' `
        set lontot      = ` echo $lontot $soundlon1 | awk '{printf "%8.6f\n", $1+$2}' `
        #*******************************************************************************************
        #This starts the "counter" loop.
        counter:
          if ($count<$soundings) then
            #This increases the "count" counter up one so that we can move to the next sounding in the bin.
            set count       = ` echo $count | awk '{print $1 + 1}'
            #These variables are set up to represent the next variables in the bin.
            set xend        = ` cat trendoutfile | awk '{if(NR==rec)printf "%8.5f\n", $1}' rec=$count `
            set sound2x     = ` cat trendoutfile | awk '{if(NR==rec)printf "%8.5f\n", $1}' rec=$count `
            set sound2z     = ` cat trendoutfile | awk '{if(NR==rec)printf "%8.5f\n", $2}' rec=$count `
            set soundlon2   = ` cat binfile | awk '{if(NR==rec)printf "%8.6f\n", $4}' rec=$count `
            set soundlat2   = ` cat binfile | awk '{if(NR==rec)printf "%8.6f\n", $5}' rec=$count `
            #Again, the next two lines add up the latitude and longitude values.
            set lattot      = ` echo $lattot $soundlat2 | awk '{printf "%8.6f\n", $1+$2}' `
            set lontot      = ` echo $lontot $soundlon2 | awk '{printf "%8.6f\n", $1+$2}' `
            #These two lines subtract the second x or z value from the first x or z value to find the rise and run.
            set soundrun    = ` echo $sound1x $sound2x | awk '{printf "%8.5f\n", $1-$2}' `
            set soundrise   = ` echo $sound1z $sound2z | awk '{printf "%8.5f\n", $1-$2}' `
            #These two lines use the Pythagorean Theorem to find the C distance between the first and second
            #(or second and third, third and fourth, etc.) soundings.
            set soundAsqB = ` echo $soundrise $soundrun | awk '{printf "%12.5f\n", ($1^2)+($2^2)}' `
            set soundC      = ` echo $soundAsqB | awk '{printf "%12.7f\n", sqrt($1)}' `
```

92

```
                    #This line adds up all the hypotenuse values to get the overall distance between soundings within a
                    #bin.
                    set soundCtot   = ` echo $soundCtot $soundC | awk '{printf "%12.7f\n", $1+$2}' `
                    #The variables are reset here.
                    set soundC      = 0
                    set soundAsqB   = 0
                    set soundrise   = 0
                    set soundrun    = 0
                    set sound1x     = $sound2x
                    set sound1z     = $sound2z
                    set sound2z     = 0
                    set soundlon1   = $soundlon2
                    set soundlat1   = $soundlat2
                    goto counter
                  endif
              #These two lines find the average of all the latitude and longitude values in a bin and find the average
              #value for each so that the rugosity can be plotted.
              set latavg      = ` echo $lattot $soundings | awk '{printf "%8.6f\n", $1/$2}' `
              set lonavg      = ` echo $lontot $soundings | awk '{printf "%8.6f\n", $1/$2}' `
              set xdif        = ` echo $xend $xbeg | awk '{printf "%12.7f\n", $1-$2}' `
              #Rugosity is calculated here by taking the distance between the first and last residual value in a bin
              #and dividing that by the total of the residual values.
              set rugosity    = ` echo $Cabs $soundCtot | awk '{printf "%12.7f\n", ($1/$2)*100}' `
              echo "rugosity:" $rugosity
              #This step saves the information necessary to plot the rugosity values to a file called "$outfile".
              echo $latavg $lonavg $rugosity | awk '{printf "%8.6f %8.6f %8.6f\n", $1, $2, $3}' >> $outfile
            endif
          else
            echo "Something crazy happened in the binning loop"
          endif
        set binmax = ` echo $binmax $bin | awk '{print $1+$2}' `
        if (-f binfile) \rm binfile
        goto binner
        #**********************************************************************************************
        #This starts the "done" loop.
        done:
          echo "Moving On"
          #If the running counter "begintotlist" equals or exceeds the value from "totallist" than the program says
          #it is done and goes to "end"
          if ($begintotlist >= $totallist) then
            echo "DONE"
            goto end
          endif
          #Otherwise the program adds 1 to the "ping" counter and goes back to "looping".
          set ping = ` echo $ping | awk '{print $1 + 1}' `
          echo $ping
          goto loopping
        endif
        #**********************************************************************************************
        #The end of the loop has been reached meaning that the data file has been completed.
        end:
```

93

REFERENCES

Andrefouet, S., Kramer, P., Torres-Pulliza, D., Joyce, K.E., Hochberg, E.J., Garza-Perez, R., Mumby, P.J., Riegl, B., Yamano, H., White, W.H., Zubia, M., Brock, J.C., Phinn, S.R., Naseer, A., Hatcher, B.G. and Muller-Karger, F.E., 2003. Multi-site evaluation of IKONOS data for classification of tropical coral reef environments. Remote Sensing of Environment, 88: 128-143.

Ardon, J., 2002. A GIS recipe for determining benthic complexity: an indicator of species richness. In: J. Breman (Editor), Marine Geography: GIS for the Oceans and Seas. ESRI Press, Redlands, pp. 169-175.

Birkeland, C., 1997. Life and Death of Coral Reefs. Chapman and Hall, New York, 536 pp.

Bryant, D., Burke, L., McManus, J. and Spalding, M., 1998. Reefs at risk: A map-based indicator of threats to the world's coral reefs. World Resources Institute, Washington, 60 pp.

Carruth, R.L., 2003. Ground-water resources of Saipan Commonwealth of the Northern Mariana Islands. Water-Resources Investigations Report 03-4178, U.S. Geological Survey.

Cloud, P.E., Schmidt, R.G. and Burke, H.W., 1956. Part 1. General geology. USGS Professional Paper 280-A,

Cloud, P.E., Schmidt, R.G. and Burke, H.W., 1959. Part 4. Submarine topography and shoal water ecology. USGS Professional Paper 280-K,

Collins, W.T. and Galloway, J.L., 1998. Seabed classification and multibeam bathymetry: tools for multidisciplinary mapping. Sea Technology, 39(9): 45-49.

Coral Reef Task Force, 2004. United States Government, http://www.coralreef.gov/library/pdf/blueprnt.pdf

Cutter Jr., G.R., Y. Rzhanov, and L.A. Mayer, 2003. Automated segmentation of seafloor bathymetry from multibeam echosounder data using Local Fourier Histogram Texture features. J. Exp. Mar. Biol. Ecol. , 285-286: 355-370.

Federal Emergency Management Agency 2005. Commonwealth of the Northern Mariana Islands Map, http://www.fema.gov/news/event.fema?id=3304.

Friedlander, A.M. and Parish, J.D., 1998. Habitat characteristics affecting fish assemblages on a Hawaiian coral reef. J. Exp. Mar. Biol. Ecol., 244: 1-30.

Frost, N.J., Burrows, M.T., Johnson, M.P., Hanley, M.E. and Hawkins, S.J., 2005. Measuring surface complexity in ecological studies. Limnol. Oceanogr. Methods, 3: 203-210.

Gardner, J., Field, M.E., Lee, H. and Edwards, B.E., 1991. Ground-truthing 6.5-kHz side scan sonographs: What are we really imaging? Journal of Geophysical Research, 96: 5955-5974.

Goff, J.A., Olson, H.C. and Duncan, C.S., 2000. Correlation of side-scan backscatter intensity with grain-size distribution of shelf sediments, New Jersey Margin. Geo-Marine Letters, 20: 43-49.

Hobson, R.D., 1972. Surface roughness in topography: Quantitative approach. In: R.J. Chorley (Editor), Spatial Analysis in Geomorphology. Methuen & Co., London, pp. 221-245.

Hoegh-Guldberg, O., 1999. Climate change, coral bleaching and the future of the world's coral reefs. Marine and Freshwater Research, 50: 839-866.

Holden, H. and Ledrew, E., 1999. Hyperspectral identification of coral reef features. International Journal of Remote Sensing, 20: 2545-2563.

Houk, P., 2001. State of the reef report for saipan island, commonwealth of the northern mariana islands, Division of Environmental Quality, Saipan,

Hughes Clarke, J.E., L.A. Mayer and D.E. Wells 1996. Shallow-water imaging multibeam sonar: A new tool for investigating seafloor processes in the coastal zone and on the Continental Shelf. Marine Geophysical Researchers, 18: 607-629.

Jenness, J., Jenness Enterprises, 2003. Grid surface areas: surface area and ratios from elevation grids, http://www.jennessent.com/arcview/arcview_extensions.htm.

Kuffner, I.B., Brock, J.C., Grober-Dunsmore, R., Bonito, V.E., Hickey, T.D. and Wright, C.W., 2007. Relationships between reef fish communities and remotely sensed rugosity measurements in Biscayne National Park, Flordia, USA. Environ Biol Fish, 78: 71-82.

L-3 Communication, 2000. Multibeam Sonar: Theory of Operation, L-3 Communications SeaBeam Instruments, East Walpole.

Luckhurst, B.E. and Luckhurst, K., 1978. Analysis of the influence of substrate variables on coral reef fish communities. Marine Biology, 49: 317-323.

Malinverno, A., Edwards, M.H. and Ryan, W.B., 1990. Processing of SeaMARC swath sonar data. Journal of Oceanic Engineering, 15: 14-23.

McCormick, M.I., 1994. Comparison of field methods for measuring surface topography and their associations with a tropical reef fish assemblage. Marine Ecology Progress Series, 112: 87-96.

Mumby, P.J. and Edwards, A.J., 2002. Mapping marine environments with IKONOS imagery: enhanced spatial resolution can deliver greater thematic accuracy. Remote Sensing of Environment, 82: 248-257.

Mumby, P.J., Green, E.P., Edwards, A.J. and Clark, C.D., 1997. Coral reef habitat-mapping: How much detail can remote sensing provide? Marine Biology, 130(2): 193-201.

Naval Intelligence Division, 1945. Pacific Islands, Volume IV: Western Pacific (New Guinea and Islands Northward), Geographical Handbook Series. Her Majesty's Stationary Office, London.

Ninio, R., Delean, K., Osborne, H. and Sweatman, H., 2003. Estimating cover of benthic organisms from underwater video images: Variability associated with multiple observers. Marine Ecology Progress Series, 265: 107-116.

NOAA, 2006. Coral Reef Information System http://www.coris.noaa.gov/.

RESON, 2005. SeaBat 8101 Multibeam Echosounder, http://www.reson.com/graphics/design/Spec%20sheets/SeaBat/8101%20-%20US.pdf.

Rooney, J., Parke, M., Lundblad, E., Chojnacki, J., Holst, S., Miller, J. and Laughlin, J., 2005. Characterization of benthic habitat for Saipan Anchorage Commonwealth of the Northern Mariana Islands Coral Reef Ecosystem Division, Honolulu,

The World Fact Book, 2002. Oceania Map, https://www.cia.gov/cia/publications/factbook/reference_maps/oceania.html.

Verbree, E. and vanOosterom, P., 2006. Better surface representations by Delaunay Tetrahedronized Irregular Networks, ESRI GIS and Mapping Software, http://www.esri.com.

Weier, J., Earth Observatory, 2001. Mapping the decline of coral reefs, http://earthobservatory.nasa.gov/Study/Coral.

Wessel, P., 2006. GMT – The Generic Mapping Tools. http://gmt.soest.hawaii.edu/

Zhou, F., Feng, J. and Shi, Q., 2001. Texture feature based on local Fourier transform. IEEE, 2: 610-613.